Bacterial Bio-factories for the Production of Valuable Chemicals

Doctor of Philosophy (PhD)

Stylianos Grigoriou

Thesis to be submitted to University of Nottingham in partial fulfilment of requirements for the degree of PhD

University of Nottingham

School of Chemistry, University of Nottingham, University Park, NG7 2RD

September 2019

Abstract

This thesis focuses on the development of novel enzymatic approaches for chiral amine synthesis utilizing amine transaminases (ATAs) and 'smart' amine donors. Different strategies were combined for the expansion of the existing biocatalytic toolbox, paving the way towards green alternatives for the enantioselective production of valuable chemicals.

In the first chapter, the wider application of the 'smart' amine donors is presented. Initially, a panel of 400 ketones/aldehydes was screened, using *o*-xylylenediamine as the amine donor, with a commercially available ATA. The colored precipitate was used as a positive indicator, to reveal a pattern for the carbonyl tolerance of the ATA. Subsequently, the commercial value of the corresponding chiral amines was evaluated with the assistance of the industrial partner Key Organics. The viable substrates were thoroughly investigated with different 'smart' diamine donors, in an effort to reduce the production costs. 1,5-Diaminopentane (cadaverine) was the most effective donor and was used for the preparation of five ketones on preparative scale, from which three became commercially available through Key Organics.

In the second chapter, the development of a novel whole-cell system, mediating ATA reaction in a self-sufficient manner, is presented. A selection of (*S*)- and (*R*)-selective ATAs were screened against 'smart' amine donors utilizing a panel of carbonyl-containing compounds. Five (*S*)-selective ATAs were identified and transformed in *Corynebacterium glutamicum* cells, which have been engineered to produce cadaverine and 1,4-diaminobutane (putrescine). Due to endogenous side-reactions and complications with expression, three ATAs were successfully expressed and utilized for the whole-cell transamination of a model ketone substrate. New strains with enhanced ATA production were developed and the reaction conditions were optimized to afford an enantiomerically pure (>99%) (*S*)-pyrroline with 42% isolated yield.

Acknowledgements

I would first like to thank my supervisor Dr. Elaine O'Reilly for providing me with the opportunity to undertake my PhD and work on this exciting project. I am grateful for her supervision and guidance over these past four years, as well as her support in my career development. Also, I would like to thank my co-supervisors Dr. Phil Hill and Prof. John King for sharing their knowledge and helping me overcome difficulties associated with my project. Special thanks to two wonderful post-docs, Dr. Evelina Kulcinskaja and Dr. Frederik Walter, who were being patient with me and assisted in my transition to biotechnology.

This work would not have been possible without the unconditional support of my family; Mum and Dad thank you! You mean the world to me. Thank you to all my friends, old and new ones, for supporting me through my PhD and making the past four years enjoyable. To all my colleagues and friends in C19 and B27; it's been amazing working with you guys.

Finally, I would like to thank the University of Nottingham and the School of Chemistry, for providing me a well-equipped and stimulating work environment where I undertook my PhD. I thank he graduate school for funding one of the international conferences I attended; the BBSRC and EPSRC for providing me with a scholarship; our collaborators, Prof. Volker F. Wendisch and his group from the University of Bielefeld, Germany, for providing us with the engineered strains. Special thanks to Pierre Kugler for assisting me during my visit to Prof. Wendisch labs. Finally, to Prof. Uwe Bornscheuer and his group from the University of Greifswald, Germany, and Prof. Nicholas Turner and his group from the University of Manchester, UK, for providing us with the ATAs essential to my project.

Abbreviations

(*S*)-PEA	(*S*)-Phenylethylamine
3HMU	*Silicibacter pomeroyi* ω-TA
3I5T	*Rhodobacter sphaeroides KD131* ω-TA
Ac_2O	Acetic anhydride
ACE	Angiotensin-converting enzyme
ADH	Alcohol dehydrogenase
AldDH	Aldehyde dehydrogenases
ALS	Acetolactate synthase
AspFum	*Aspergillus fumigatus* ω-TA
AspOry	*Aspergillus oryzae* ω-TA
AspTA	Aspartate transaminase
ATA	Amine transaminase
BCAT	Branched chain aminotransferase
BHIS	Brain heart infusion sorbitol
BLAST	Basic Local Alignment Search Tool
Cal-B	Lipase B from *Candida antarctica*
ChrVio	*Chromobacterium violaceum* ω-TA
DCM	Dichloromethane
DKR	Dynamic kinetic resolution
ee	Enantiomeric excess
EtOAc	Ethylacetate
FDA	Food and Drug Administration
FDH	Formate dehydrogenase

GABA	*gamma*-aminobutyric acid
GC-FID	Gas chromatography-flame ionization detector
GFP	Green Fluorescence Protein
HCl	Hydrochloride
HEPES	4-(2-Hydroxyethyl)piperazine-1-ethanesulfonic acid
HEWT	*Halomonas elongate* ω-TA
HMG-CoA	Hydroxymethylglutaryl-CoA
HTP	High-throughput
IPA	Isopropylamine
IPTG	Isopropyl β-D-1-thiogalactopyranoside
IRED	Imine reductases
LB	Luria-Bertani
ldcC	Lysine decarboxylase
LDH	Lactate dehydrogenase
L-glu	L-glutamate
L-Tle	L-*tert*-leucine
MycVan	*Mycobacterium vanbaalenii* ω-TA
NeoFis	*Neosartoria fischeri* ω-TA
NADH	Nicotinamide adenine dinucleotide
PcATA	*Pseudomonas chlororaphis subsp. Aureofaceins* ω-TA
PDC	Pyruvate decarboxylase
PfATA	*Pseudomonas fluorescens* ω-TA
PLP	Pyridoxal-5'-phosphate
PMP	Pyridoxamine phosphate

PpATA	*Pseudomonas putida* ω-TA
RBS	Ribosomal binding site
SDS-PAGE	sodium dodecyl sulfate-polyacrylamide gel electrophoresis
SpeC	Ornithine decarboxylase
TA	Transaminase
TEA	Triethylamine
THF	Tetrahydrofuran
TLC	Thin layer chromatography
VibFlu	*Vibrio fluvialis* ω-TA
WCP	Wet cell pellets
WT	Wild type
α-TA	α-Transaminase
ω-TA	ω-Transaminase

Table of contents

Abstract i

Acknowledgements iii

Abbreviations iv

1. Introduction 1

1.1 Chirality and its importance 1

1.2 Chiral Amines 4

1.3 Synthetic approaches for the production of chiral amines 5

1.3.1 Traditional chemical approaches 5

1.3.2 Biocatalytic alternatives 6

1.4 Transaminases 16

1.4.1 General characteristics 16

1.4.2 Active site and mechanism of ω-TAs 17

1.4.3 Applications and challenges 21

1.5 Overall aims and objections 28

2: Application of smart amine donors for the production and commercialization of chiral amines 29

2.1 Introduction 29

2.2 Aims and Objectives 30

2.3 Substrate screen of ATA256 30

2.4 Asymmetric amine synthesis using compounds **1** and **8** 35

2.5 Conclusion 41

2.6 Experimental 42

2.6.1 General Methods and Materials 42

2.6.2 High-throughput screening 43

2.6.3 Analytical scale biotransformations of ketones 1-9 with ATA 256 and cadaverine 43

2.6.4 GC Method 44

2.6.5 Measurement of conversion 44

2.6.6 Analytical scale biotransformations of ketone 1 and 8 with ATA256 and cadaverine using various co-solvents 45

2.6.7 Preparative scale biotransformations of compounds 10, 17 46

2.6.8 Standard procedure for derivatizing free amines with Mosher's Acid Chloride 47

3. Development of a self-sufficient whole-cell biocatalyst for chiral amine synthesis 50
3.1 Introduction 50
3.2 Aims and objectives 52
3.3 Identification of ATAs accepting the smart amine donors 53
3.3.1 Investigation of the carbonyl substrate of 3HMU 56
3.3.2 Transamination with bacterial supply of 'smart' amine donor 58
3.4 Expression of 3HMU in *C. glutamicum* strains 59
3.4.1 Investigation of expression system 62
3.4.2 Investigation of toxicity and rare codons 64
3.5 Identification of a putrescine ATA from *Halomonas elongata* 66
3.5.1 Substrate scope of HEWT 66
3.5.2 Expression of HEWT in *C. glutamicum* strains 67
3.6 Investigation of three additional putrescine ATAs 74
3.6.1 Elucidation of substrate scope 74
3.6.2 expression of putrescine ATAs in *C. glutamicum* strains 78
3.6.3 Optimization of *in vivo* Whole cell biotransformations 86
3.7 Conclusion and future work 89
3.8 Experimental 90
3.8.1 Sterile conditions 91
3.8.2 Media and agar preparation 91
3.8.3 Preparation of chemo- and electro- competent cells 92
3.8.4 Transformation protocols 93
3.8.5 Polymerase-chain reaction (PCR) mixing protocol 95
3.8.6 Plasmid isolation 95
3.8.7 Agarose Gel Electrophoresis 95
3.8.8 Expression of recombinant protein 96
3.8.9 Protein purification 97
3.8.10 Protein determination and SDS-PAGE analysis 98
3.8.11 Acetophenone assay 98
3.8.12 Colony based solid-phase ATA assay 99
3.8.13 Analytical scale biotransformations 99
3.8.14 Preparative scale biotransformation of **27** 100
4: Overall conclusion and future work 102
A. Appendix 106

A.1 Supplementary material to 'Application of smart amine donors for the production and commercialization of chiral amines' 106
A.2 Supplementary material to 'development of self-sufficient whole-cell biocatalyst for chiral amine synthesis' 107
A.2.1 Activity measurement through acetophenone assay 107
A.2.2 Estimation of the amount of HEWT (mg) in clarified extract 109
A.2.3 Statistical analysis 110
A.2.4 Supplementary data 126
A.2.4 Polymerase Chain Reaction (PCR) conditions 135
A.2.5 Gas Chromatography (GC) traces 138
References 143

1. Introduction

1.1 Chirality and its importance

Our world is surrounded by chiral entities, ranging from our left and right hands to complicated macromolecular protein complexes and drug molecules. An abundance of chiral molecules exist in nature, including amino acids and sugars. To better understand this concept, chemists define chirality as a pair of molecules that exists as two non-superimposable mirror images, for example where a carbon atom has four different substituents as shown in Figure 1.1.[1] The two enantiomers are chemically equivalent but have a different orientation of atoms in space, around the stereogenic carbon center.[1]

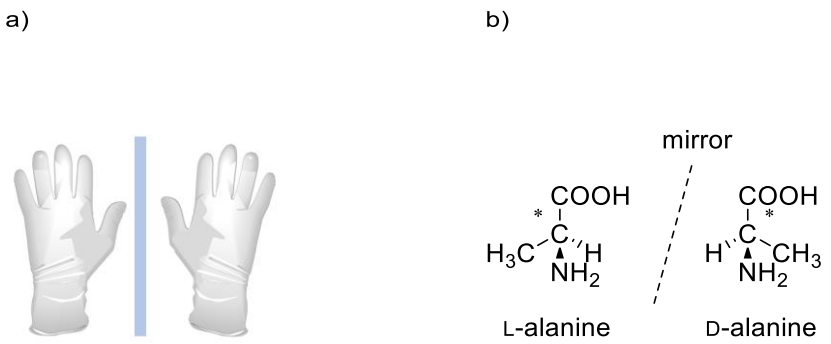

***Figure 1.1**. a) A pair of hands as chiral objects, b) L- and D-alanine as an example of a chiral molecule.*

The importance of chirality was highlighted in 2001, when the Nobel Prize in Chemistry was awarded to three scientists, for the development of catalysts applied in the production of enantiomerically pure drugs and chemicals.[2][3] More than half of the drugs available on the market contain one or more chiral centers (Figure 1.2).[3–6] A landmark example of a chiral drug is Lipitor (Figure 1.2a), an antilipemic agent that inhibits the hydroxymethylglutaryl-CoA (HMG-CoA) reductase.[131] Lipitor was

developed by Pfizer as a cholesterol lowering medication and has been prescribed to more than 29 million patients, generating more than 200 billion U.S. dollars since 2003, when it was first introduced to the market.

In recent years, a number of reviews have shown the connection between biological activity and chirality.[3] An example of a drug molecule would be Propoxyphene (Figure 1.2b), where the two enantiomers display different activity. The (*D*)-enantiomer was introduced in the market as an analgesic, whereas the (*L*)-enantiomer was identified to exert antitussive properties.[7] Other characteristic examples include, (-) menthol, which is responsible for the minty odor (Figure 1.2c)[8,9] and the (-)-(*Z*)-β-Santalol, which exhibits the sandalwood oil odor, while the (+)- enantiomer is odorless (Figure 1.2d).[8–12] Altogether, this showcases the broad spectrum of chiral products in the market.[10–16]

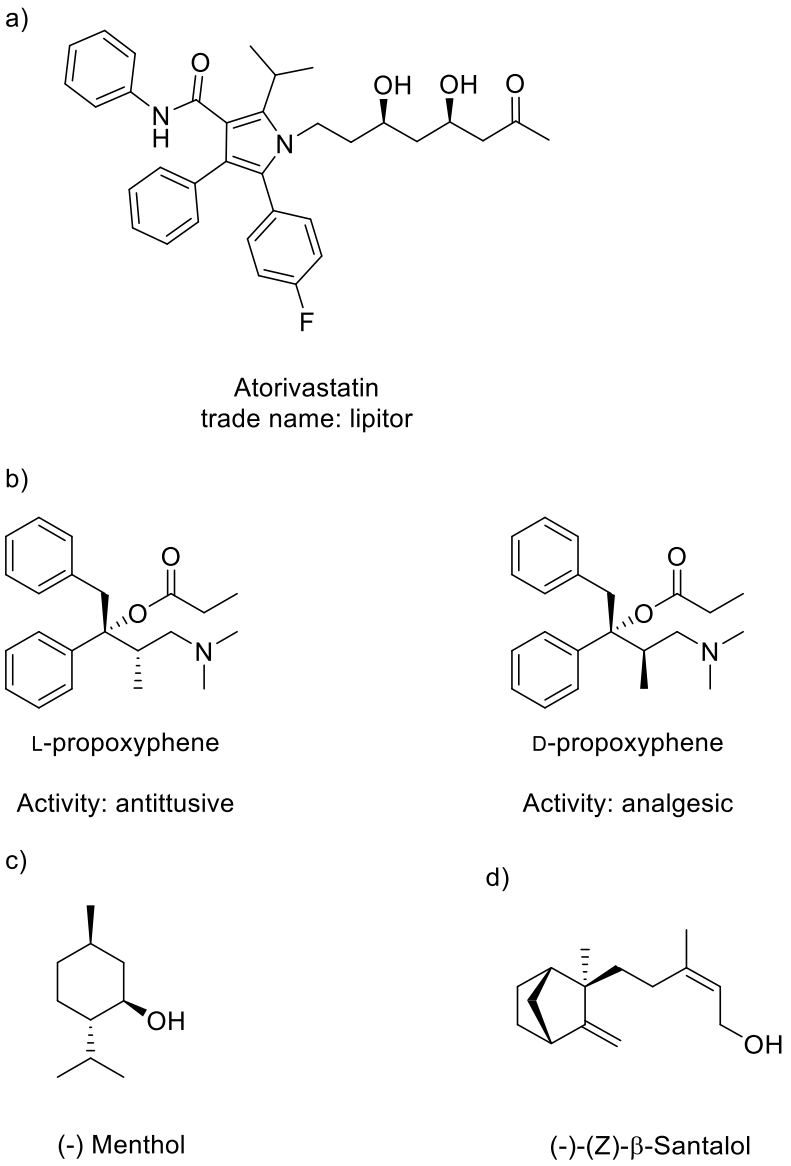

***Figure 1.2**. Examples of chiral compounds in medicine, fragrances and flavours. a) Lipitor, b) propoxyphene,* [7] *c) (-) menthol,*[8,9] *and d) (-)-(Z)-β-Santalol.*[8–12]

It is now obvious that different enantiomers have different properties, which led to the US Food and Drug Administration (FDA) to request manufacturers to isolate and fully characterize individual isomers in racemic mixtures. The decision to commercialize a drug as a racemic mixture or in enantiomerically pure form is based on production cost and clinical significance of each enantiomer. Therefore, the development of

novel methodologies enabling access to chiral molecules became one of the key research areas.[3]

1.2 Chiral Amines

Chiral amines play a crucial role in organic chemistry, as they exist in numerous ligands and auxiliaries[17–24] as well as in natural products and drug molecules.[15,25,26] Therefore, their synthesis is appealing to both industry and the academic community. Ligand 8-((2*R*,5*R*)-2,5-dimethylpyrrolidin-1-yl)quinolone is an example of how the chirality of the amine plays an important role in the palladium-catalyzed synthesis of polyketones (Figure 1.3a). M. R. Axet *et al*. 2009 demonstrated that both the activity of the catalyst, as well as the stereoselectivity of the reaction, were dependent on the ligand fragment containing the sp^2 nitrogen atom.[24] Another example is the antihypertensive drug Enalaprilat (Figure 1.3b), the first dicarboxylate containing angiotensin-converting enzyme (ACE) inhibitor.[27] During the structure-based design, the chiral amine moiety (shown in blue) is shown to form H-bonds with a histidine residue in the active site of ACE, contributing to the increased affinity of the drug to the target protein.[27,28]

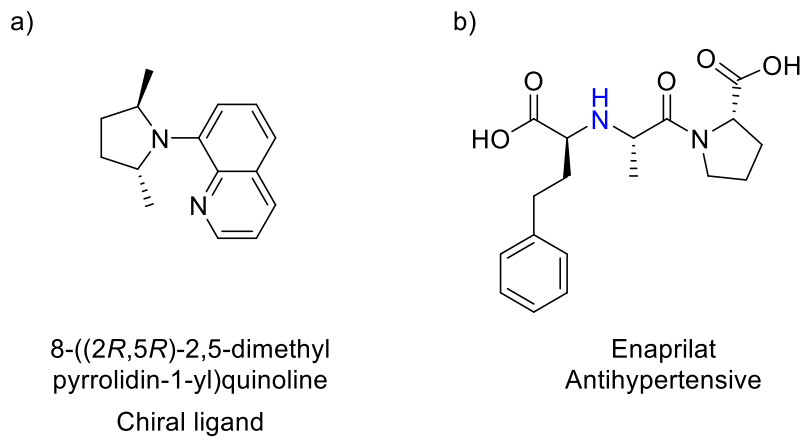

***Figure 1.3**. Selected examples of a chiral a) ligand[24] and b) drug molecule.*[27]

1.3 Synthetic approaches for the production of chiral amines

1.3.1 Traditional chemical approaches

In 2010, a book thoroughly describing the past and present chemical pathways in the synthesis of chiral amines (Scheme 1.1) was published.[17] Hydrogenation of an imine or an enamine in the presence of a metal complexes and/or chiral phosphorous complexes is described.[29–36] Work on one-pot conversion of ketones to chiral amines *via* reductive amination, where a ketone and a reducing agent coexist, is also presented.[37–39] Other methods include hydroamination, which is the addition of an N-H bond across an sp^2 or sp hybridized C-C bond of alkenes, alkynes, and dienes, employs metal complexes and represents a facile approach for the production of enantiomerically pure amines in high yield.[40–43] Finally, metal complexes can be utilized for the direct amination of sp^3 compounds in both an inter- or intramolecular way. [44–46]

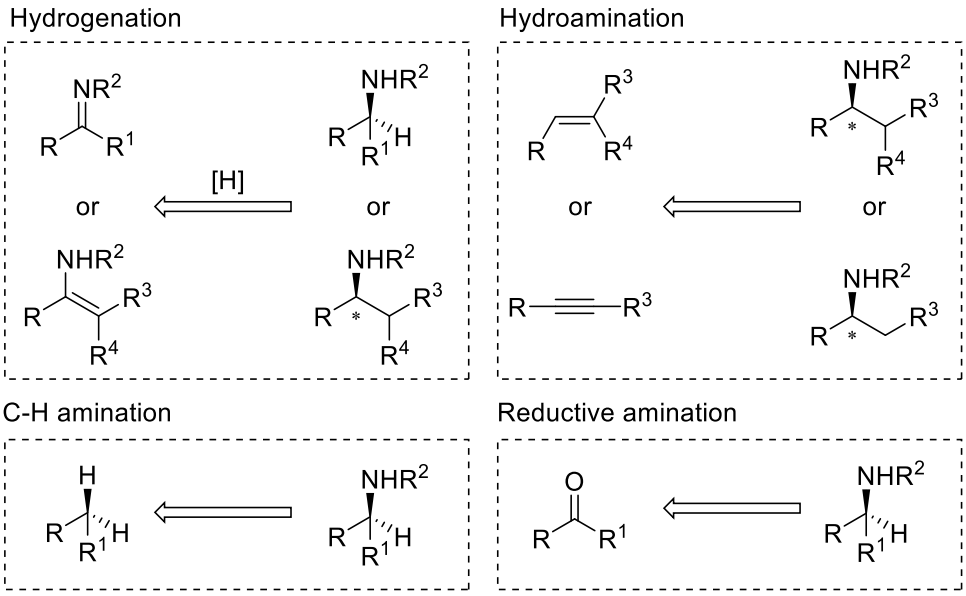

***Scheme 1.1**. Selected examples of methods used in organic chemistry for the production of chiral amines.*[17]

These traditional approaches in organic chemistry have been well studied and are widely used in both industry and academia, offering high atom economy (e.g. in hydrogenation) and in most cases high enantioselectivity, avoiding the costly chiral separation of a mixture of enantiomers.[29–36] However, they often suffer from requiring expensive organocatalysts, toxic precious metals, organic solvents, harsh reaction conditions and high pressure reactors,[17] which add to the total cost and the impact on the environment. As the chemical industry begins to move away from traditional chemical synthesis, this provides the opportunity for the development of 'green' and sustainable chiral amine synthesis. [47]

1.3.2 Biocatalytic alternatives

1.3.2.1 Cell-free enzyme catalysis

Biocatalysis has been highlighted as a green and sustainable alternative to traditional chemistry for a number of reasons.[48, 50-52] Enzymes are active in water, neutral pH and relevantly low temperatures, which altogether

constitute important features in the field of green chemistry.[48] These macromolecules can selectively react with their substrates and afford optically pure compounds in one step, without the need of protecting groups. Lastly, biocatalysts are biodegradable and can be easily produced (up to 1 g protein per liter of culture)[49] from commonly used bacterial hosts (e.g. *Escherichia coli*), utilizing inexpensive growth media, .[50–52]

A variety of different enzyme classes are described in the literature for the kinetic resolution of chiral amines. The resolution of racemic mixtures can be accomplished *via* selective acetylation or oxidation of a single enantiomer from lipases or monoamine oxidases, respectively, afford enantiomerically pure amines with 50% theoretical yield. Also, amine transaminases (ATA) and amine dehydrogenases selectively convert one of the enantiomers to the corresponding ketone utilizing pyruvate (for example) or NAD^+, respectively (Figure 1.4). Among others,[50,52] a recent review from the O'Reilly group reports some of the applications of these biocatalysts in the formation of drug molecules and key intermediates.[51]

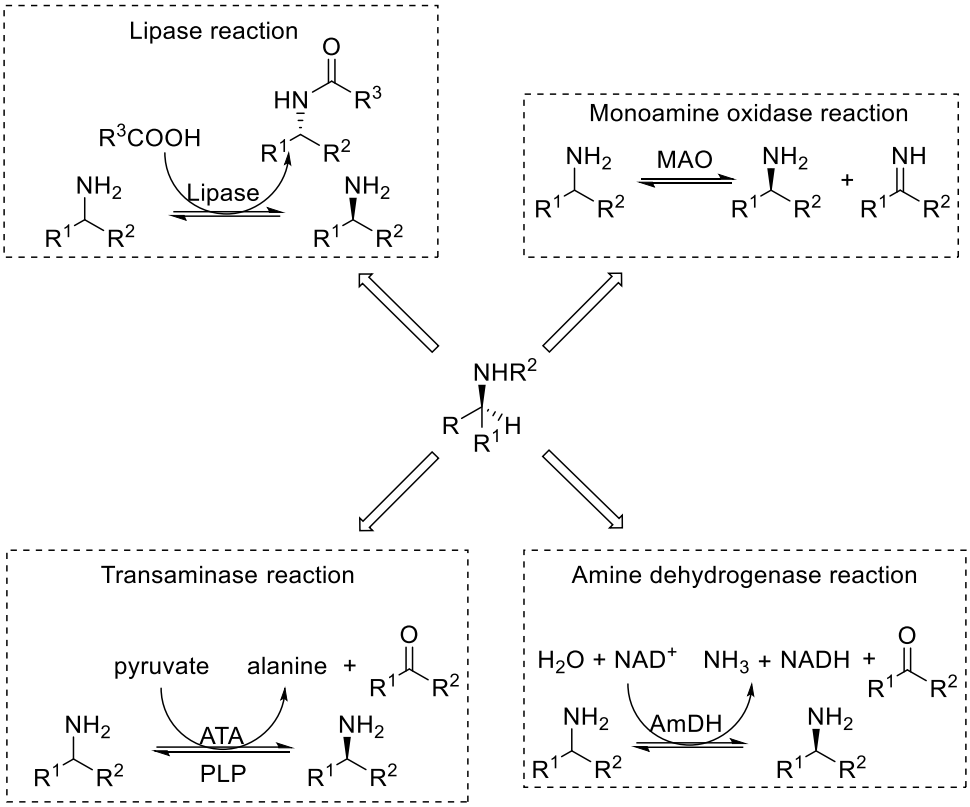

***Figure 1.4**. Selected examples of enzymes employed in the kinetic resolution of amines.*[51,53–58]

A landmark example of an industrial-scale application of a biocatalyst, consists of the use of a leucine dehydrogenase, for the production of the non-natural amino acid L-*tert*-leucine (L-Tle) on a tonne-scale. Bommarius *et al*. 1995 showed that leucine dehydrogenase can convert trimethylpyruvate and ammonium formate to L-Tle on a tonne-scale when combined with a secondary biocatalytic system. The latter is employed for the regeneration of the expensive co-factor nicotinamide adenine dinucleotide (NADH) from NAD^+ and formate utilizing a formate dehydrogenase (FDH), as shown in Scheme 1.2.[59] The biocatalytic production of L-Tle has great potential in the agrochemical and pharmaceutical industry, as L-Tle is a key building block for many biologically active compounds, such as HIV protease inhibitors[13] and pesticides.[59]

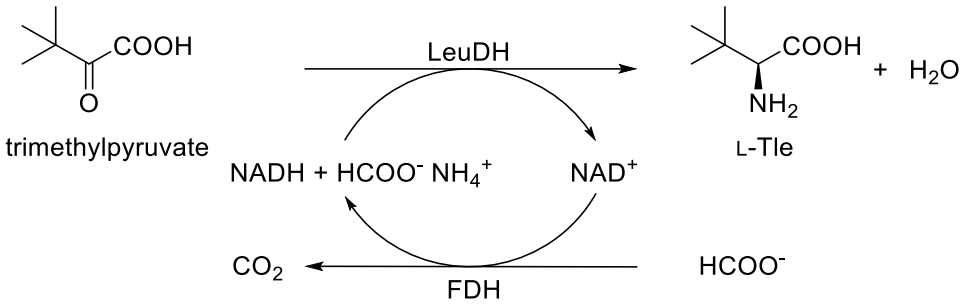

***Scheme 1.2**. Production of L-tert-leucine from ammonium formate and trimethylpyruvate via a coupled enzymatic system.* [59]

The most commonly used biocatalyst in both industry and academia is the lipase class. In particular, lipase B from *Candida antarctica* (Cal-B) has been used by BASF to resolve racemic mixtures of various amines on a multi-tonne scale by combining the enantioselective acetylation of alkyl and aryl alkyl amines.[50] In the first step, only one of the two enantiomers reacts with the acetylating agent in the presence of Cal-B, allowing the isolation of the unreacted enantiomer. Subsequent hydrolysis of the acetylated compound affords the second enantiomer in optically pure form, as shown for the example of (*R*)-1-phenylethylamine in Scheme 1.3. [50,56]

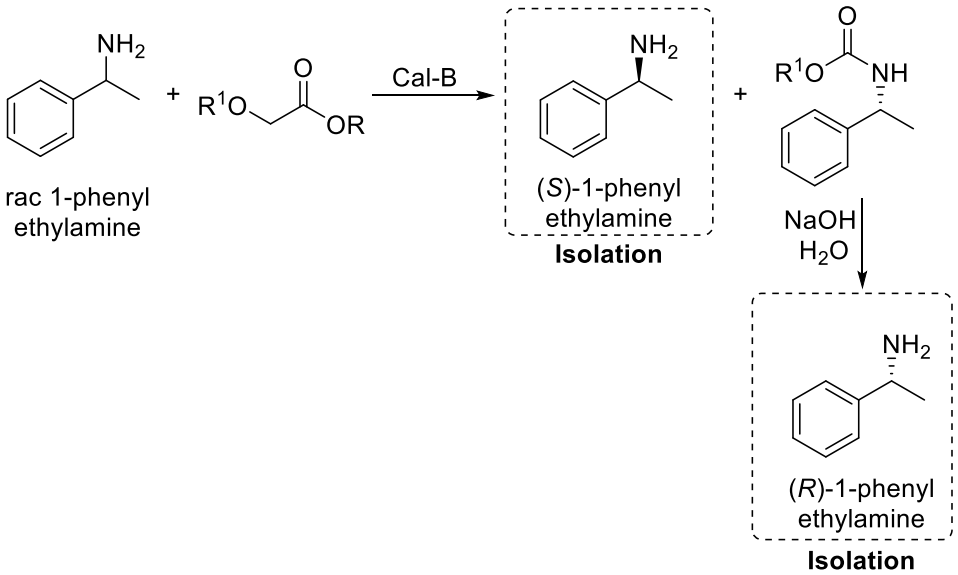

***Scheme 1.3**. A selected example of CAL-B in the production of chiral amines from BASF.*[50]

The ω-transaminases class of enzymes have also been shown to be valuable catalysts for the synthesis of chiral amines. These versatile biocatalysts can be employed in the deracemization amines or used for the asymmetric synthesis of chiral amines, starting from the corresponding ketone substrate. A collaborative project between Merck and Codexis, highlighted the use of a heavily engineered transaminase (TA) for the synthesis of the antidiabetic drug Sitagliptin on an industrial scale.[61] The traditional route includes enamine formation, followed by rhodium-catalyzed asymmetric hydrogenation under high pressure to afford sitagliptin with 97% emamtiomeric excess (ee). Subsequent recrystallization is required for increased ee values. This pathway was replaced from a single biocatalytic step utilizing a heavily engineered (*R*)-selective ω-transaminase and isopropylamine (IPA), shown in Scheme 1.4. In this work, two rounds of mutations were carried in order to fit the prositagliptin ketone in the active site of the transaminase and also increase its activity. Eleven more rounds were required to create a variant that meets the manufacturing process requirements. This variant tolerates high concentrations of both substrates as well as the co-solvent DMSO, and maintains its activity at elevated

temperatures (>40˚C). The manufacturers benefited by introducing a transaminase step in their synthetic pathway, as they were able to increase their overall yield (by 10-13%) and productivity (by 53%), avoid the use of metal catalyst and reduce their total waste (by 19%) and expenses, as the high-pressure hydrogenation equipment was replaced by a multipurpose vessel.[61]

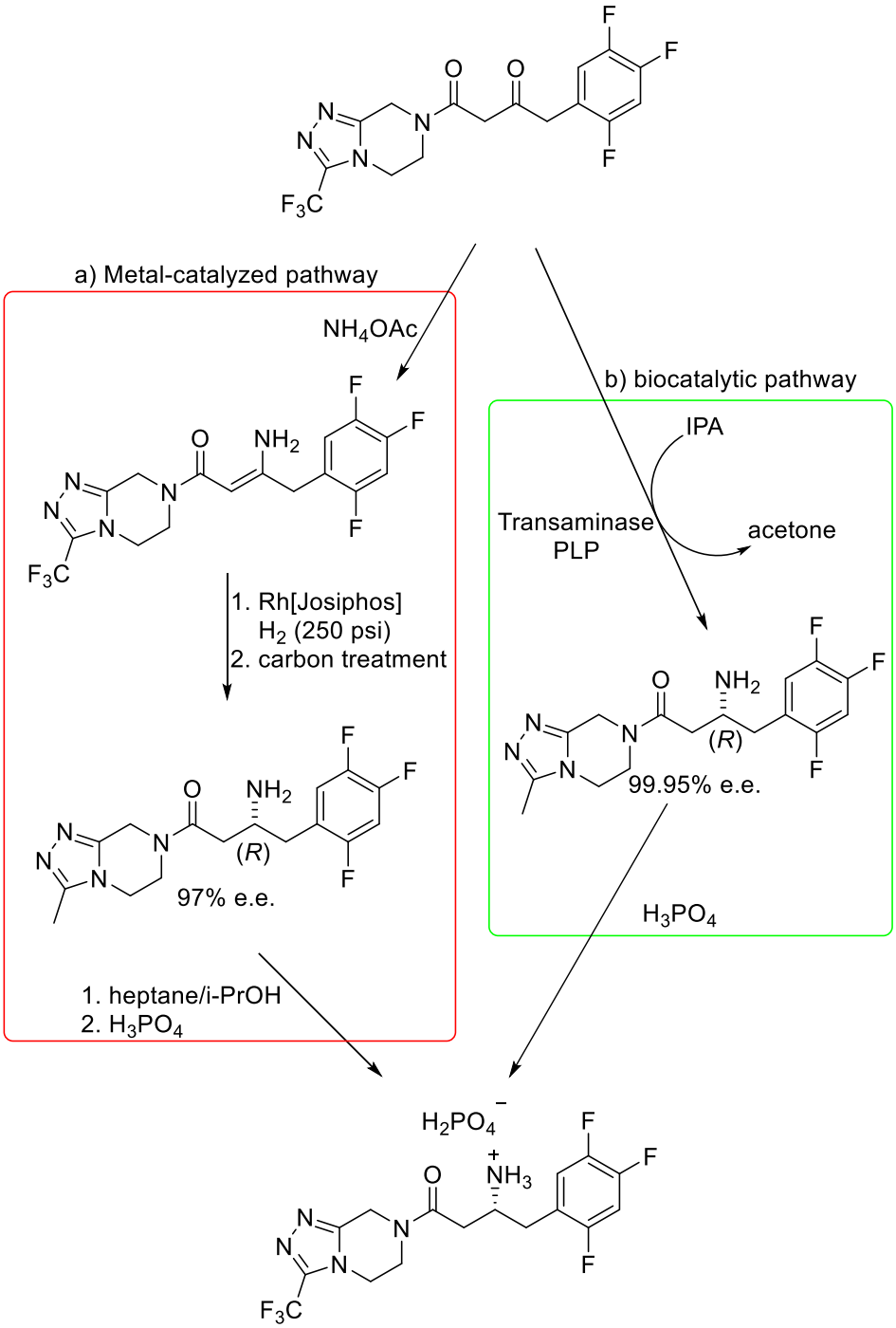

***Scheme 1.4**. a) The traditional and b) the biocatalytic route for the synthesis of sitagliptin.*[61]

1.3.2.2 Whole cell biocatalysis

The rapid progress in synthetic biology enabled the development of efficient whole-cell systems, expanding the biocatalytic toolbox.[62] Metabolic engineering enables scientists to selectively silence, activate or

introduce specific genes in bacterial and fungal strains, leading to pathways tailored to fit a purpose. This paved the way for the sustainable production of fine chemicals[63–72] and amino acids,[73–75] *via* fermentation. Bacterial strains can also be engineered for the expression of recombinant proteins utilizing a plasmid DNA. As mentioned in 1.3.2.1, this enables the production of biocatalysts from inexpensive carbon and nitrogen sources, such as glucose and ammonium ions.[76] Tedious and costly processes of cell lysis and protein purification can be avoided through direct use of whole cells.[77] The advantages are more obvious in industrial processes, where a biocatalytic step is initially tested utilizing purified enzymes, but is subsequently replaced with whole-cell systems (when viable), in order to reduce the upstream cost of the total synthesis.[78]

Cells in stationary phase, which are still metabolically active but have stopped dividing,[79–83] as well as growing cells[84,85] can be utilized for whole cell biocatalysis.[62,68,86,87] The membrane of the cell acts as a barrier that separates and protects the intracellular environment from external factors, enhancing protein stability and regulating the internal pH.[76,88,89] This has great application in unstable proteins, such as P450 monooxygenase, which are difficult to isolate in active form.[90] Co-factors, such as NAD(P)H, are naturally produced and recycled from the metabolism of the host cell. Many proteins, such as imine reductases (IREDs), utilize such co-factors and thus whole cells provide an attractive cost-effective alternative to cell-free biocatalysis. [80,90,91] Leipold *et al*. 2013, described the use of *E. coli* BL21 overexpressing (*S*)-IRED from *Streptomyces* sp. GF3546 for the conversion of a range of cyclic imines. 1-Methyl-3,4-dihydroisoquinoline was successfully converted to its corresponding chiral amine on a 200 mg scale with 87% isolated yield and >98% enantiomeric excess (ee) (Scheme 1.5).[80]

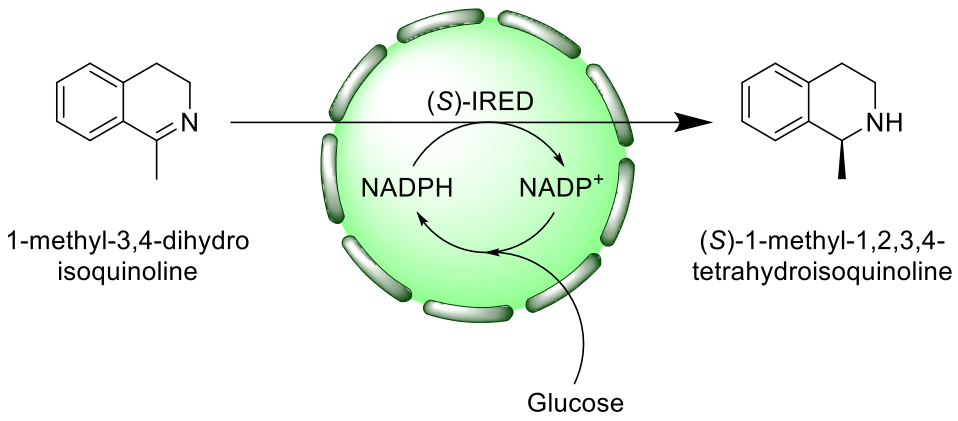

***Scheme 1.5**. Conversion of 1-methyl-3,4-dihydroisoquinoline to (S)-1-methyl-1,2,3,4-tetrahydroisoquinoline from E. coli overexpressing (S)-IRED.*[80]

In the above example higher concentrations led to poor conversion, which can be attributed to the poor mass transfer through the cell membrane.[76,77] This limitation can be addressed by increasing the permeability of the membrane with detergents. [76,77,92–94] Enhanced productivity has also been reported with overexpression of membrane transporters[76,77,95–100] or expression of the biocatalyst on the surface of the host cell.[77,101,102] An interesting alternative employs biphasic systems, where one phase (usually aqueous) provides the protective environment of the biocatalyst and the second phase (organic, ionic liquid or polymer based aqueous media) is the substrate and/or product pool.[103–105] Shin *et al.* 1997, utilized whole cells *Bacillus thuringiensis* JS64 in a biphasic system to resolve 500 mM rac-*a*-phenylethylamine and isolate (*S*)-phenylethylamine. In this study, the biocompatibility and the extracting capacity of the organic solvent were examined, and cyclohexanone was selected as the organic phase. The introduction of a biphasic system drastically reduced product inhibition of the TA leading to nine-fold improvement (Scheme 1.6).[103]

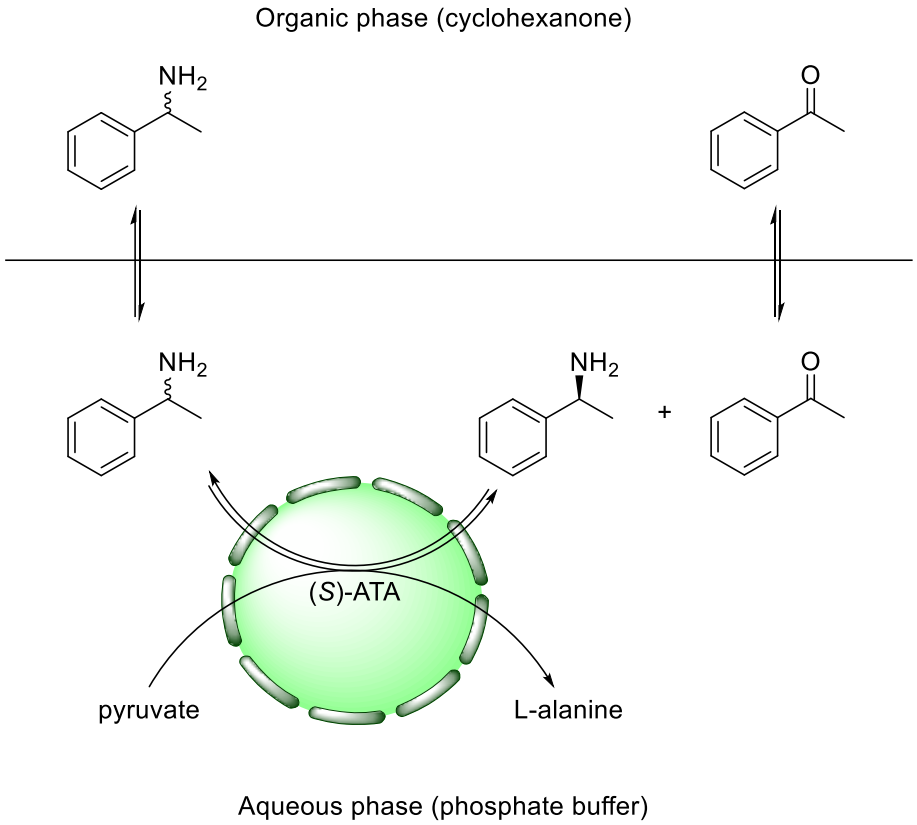

***Scheme 1.6**. Kinetic resolution of rac-a-phenylethylamine utilizing whole cells in water-cyclohexanone biphasic system.*[103]

The capability to build bio-cascades in a single organism is one of the most prominent advantages of whole-cell systems.[77,106] Both bacteria and yeasts can be engineered to co-express multiple enzymes, creating a biocatalytic workhorse capable of multi-step reactions.[106] The enzymes co-expressed are in close proximity inside the cell, thus ensuring high efficiency reaction cascade.[77] Both *et al.* 2015, reported a stereoselective C-H amination of 4-substituted ethylbenzenes *via* a whole cell multienzymatic cascade. *E. coli* cells overexpressing a P450 monoxygenase, *R*- and *S*-alcohol dehydrogenases and an *ω*-ATA were employed for the production of chiral amines with conversions up to 26% and >99% ee (Scheme 1.7). Firstly, a hydroxyl group was introduced on the aliphatic chain *via* a P450 monoxygenase step. The racemate of the alcohol formed was subsequently oxidized to the corresponding ketone from a pair of (*S*) and (*R*)-selective alcohol dehydrogenases (ADHs). Lastly, the ketone

product was converted to the corresponding chiral amine *via* an (*R*)-selective ω-ATA.[81]

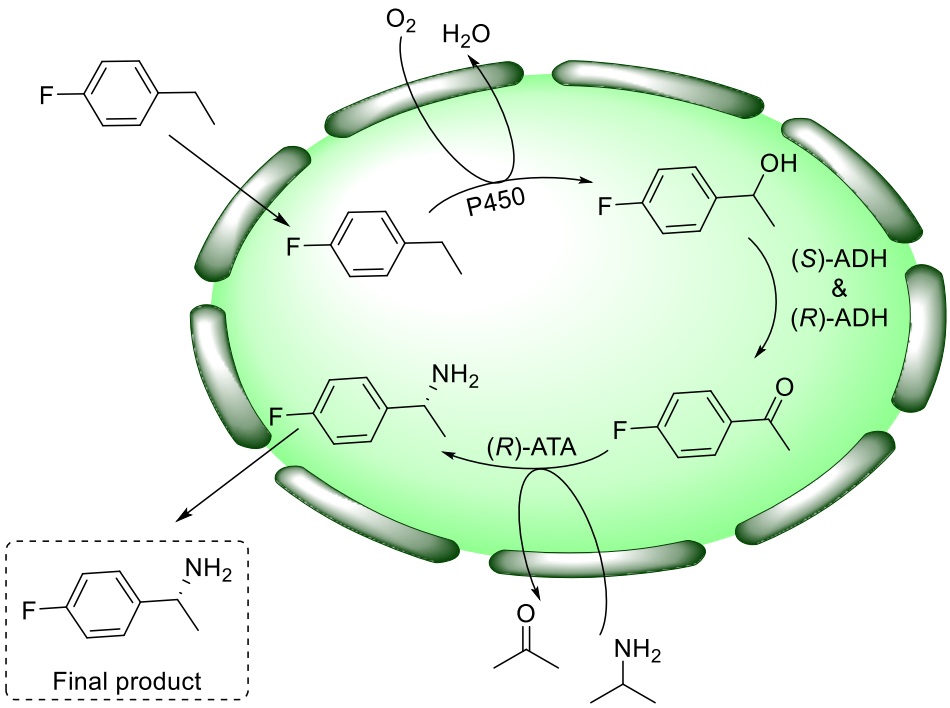

***Scheme 1.7**. Multi-enzymatic cascade in E. coli host for the stereoselective C-H amination of 4-fluorophenylbenzene.*[81]

1.4 Transaminases

1.4.1 General characteristics

TAs utilize pyridoxal-5'-phosphate (PLP) co-factor and catalyze the transfer of an amino group, from a suitable donor, to a carbonyl acceptor. This reaction (Scheme 1.8) exists in equilibrium.[107]

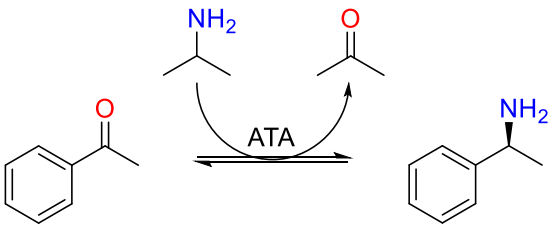

***Scheme 1.8**. The conversion of acetophenone to S-methylbenzylamine is illustrated as an example of a transaminase reaction.*

All PLP-dependent enzymes are categorized based on the architecture of their active site in relevance to their co-factor, and TAs belong to fold type I and IV.[108–113] A more biocatalytically relevant classification groups TAs based on their substrate recognition. As shown in Figure 1.5, there are two distinct groups: the α-transaminases (α-TAs), which catalyze the conversion of α-amino acids to α-keto acids and vice-versa, and the ω-transaminases (ω-TAs), which accept substrates with the carbonyl or amino group distant from α-position.[107] Interestingly, ω-TAs include a group of TAs that can convert amines lacking a carboxyl group and are named amine transaminases (ATAs).[107,114,115]

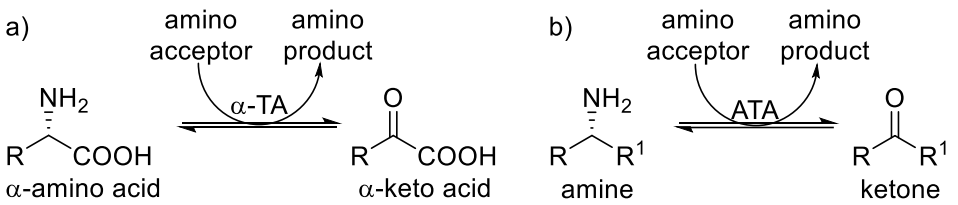

***Figure 1.5**. General reaction schemes of a) α-TA and b) ATA.* [107]

ω-TAs have a wide range of applications due to their versatile nature, thus appealing to the research community.[116] There has been extensive research, including mechanistic studies and resolving crystal structures, which altogether contribute to a greater understanding and application of these biocatalysts.[114]

1.4.2 Active site and mechanism of ω-TAs

It has been reported that ω-TAs are generally homodimers or homotetramers,[108] and each monomer comprises of a large domain, which is conservatively centered by seven-stranded parallel β sheets, and a smaller discontinuous domain.[117] The active site resides between those domains and forms multiple interactions with the PLP in a relatively conserved way. The phosphate group, pyridine nitrogen and phenolic oxygen of the PLP form H-bonds with both hydrophilic residues and water

molecules, as shown in Figure 1.6 for the gamma-aminobutyric acid (GABA)-TA from *E. coli*.[108]

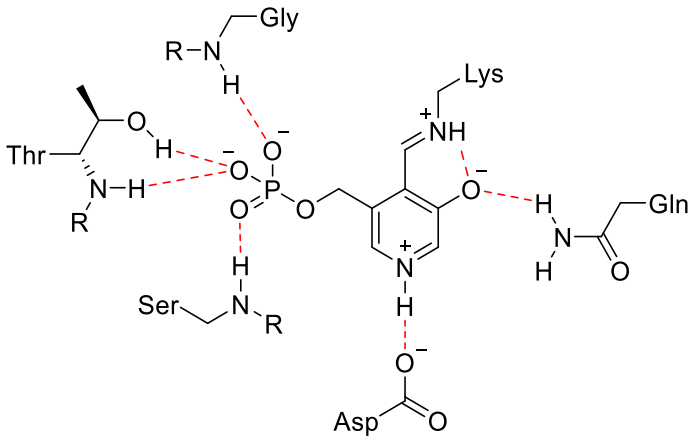

***Figure 1.6**. The interactions of the co-factor PLP with some key residues from the active site of GABA-TA are shown as a representative example. H-bonds are shown in red.* [108]

The PLP co-factor is a 4-formyl-5-hydroxy-6-methylpyridin-3-yl-methyl dihydrogen phosphate. The basic nature of the nitrogen group of the pyridine ring in combination with the acidity of the phenol group stabilizes an ionic tautomeric form of the PLP (Scheme 1.9), which actively contributes to the enzymatic reaction. [118]

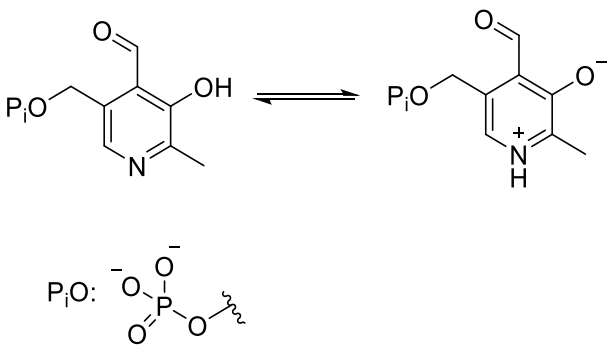

***Scheme 1.9**. Tautomeric forms of PLP.*

The formyl group of the PLP plays a crucial role in the transaminase mechanism, forming Schiff base intermediates with amines (Scheme 1.10). Firstly, it reacts with the amino group of a lysine residue in the active site to form an internal aldimine (step 1). The amino group of the amine donor displaces the lysine residue forming an external aldimine (step 2), which is stabilized by multiple non-covalent interactions. Subsequent hydrolysis leads to the formation of a ketone and pyridoxamine phosphate (PMP), completing the first half of the TA reaction (step 3).[118,119] The second half (steps 4 and 5) follows the same route in a reverse way.[119]

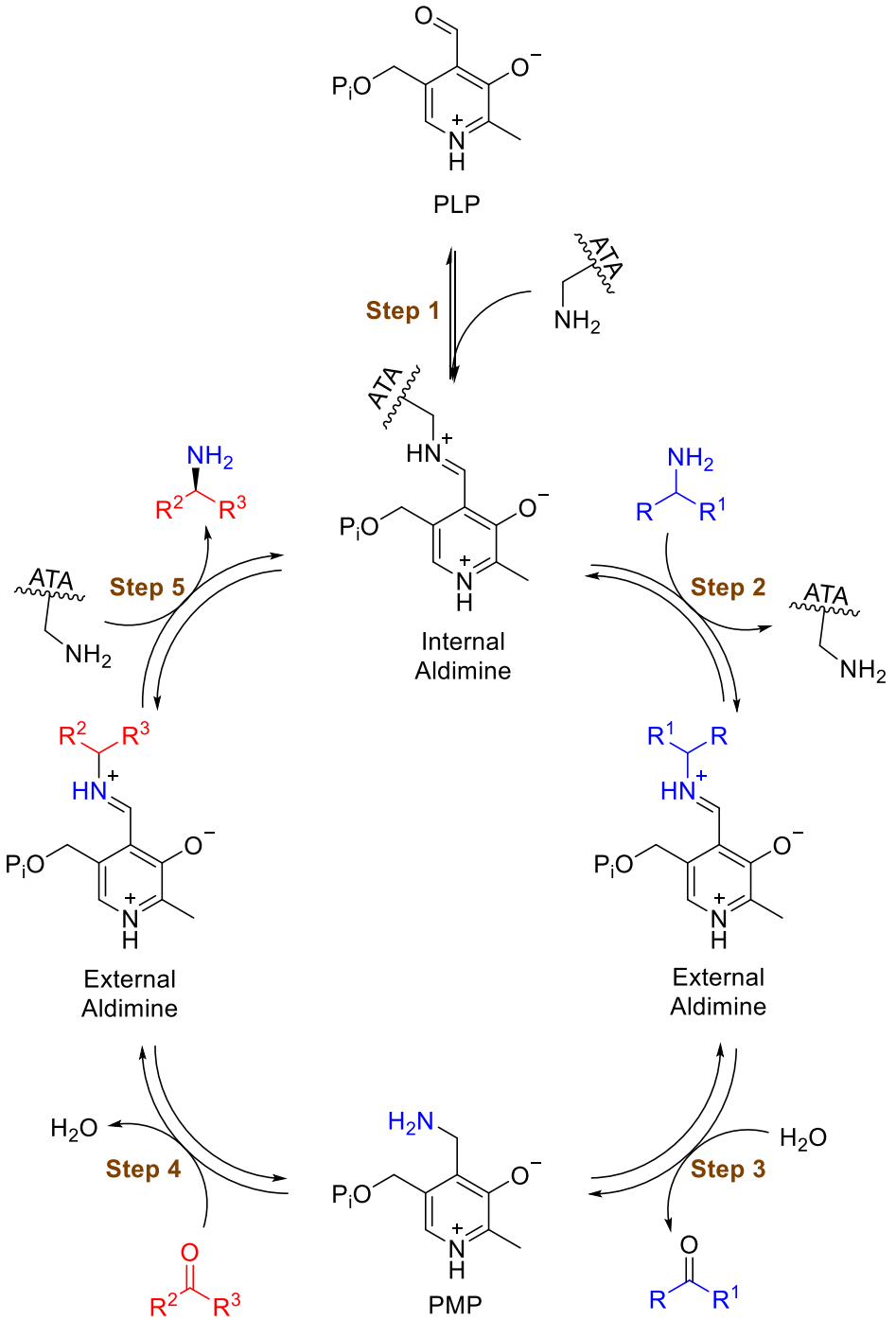

***Scheme 1.10**. A proposed mechanism of an ATA reaction*.[119]

The stereoselectivity is decided during step **4**, which is more thoroughly described in Scheme 1.11. The free electron pair of the amino group (shown in blue) of PMP attacks the electrophilic carbon of the ketone (shown in red) to afford an intermediate amino-alcohol. Subsequent proton transfer from the amino to the hydroxyl group, leads to an imine and release of a

water molecule. Intramolecular proton transfer is mediated by a key lysine residue in the active site, and is directed by the small and large pocket of the active site as well as the size of the R^2 and R^3 groups. The imine formed is then released as a chiral amine, during step **5** described in Scheme 1.10.

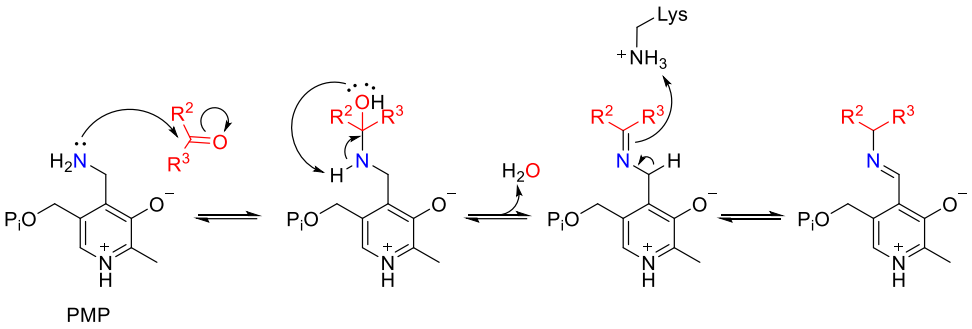

***Scheme 1.11**. A detailed description of step **4**, which defines the stereoselectivity in the TA reaction.*

1.4.3 Applications and challenges

There are three distinct pathways for the production of enantiomerically pure amines utilizing TAs; a) kinetic resolution, b) deracemization and c) asymmetric synthesis (Scheme 1.12).[120]

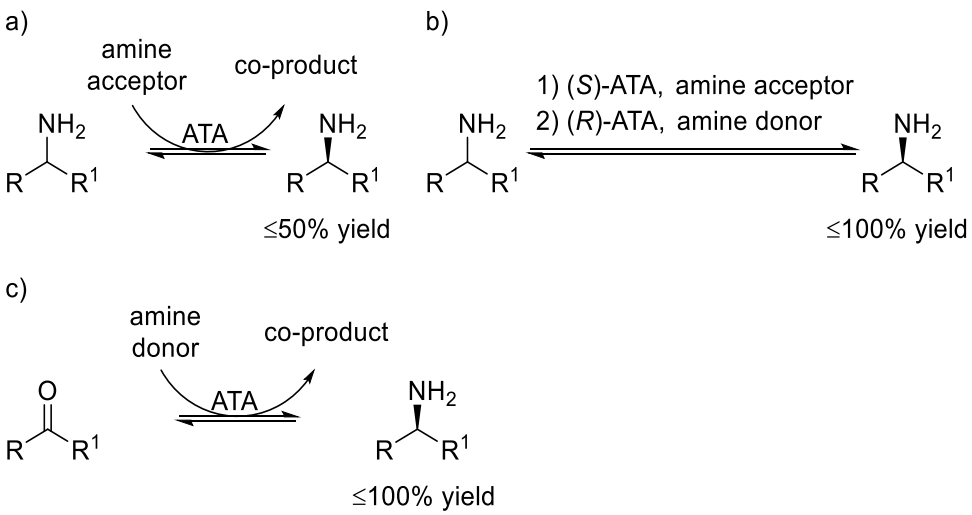

***Scheme 1.12**. Chiral amine synthesis utilizing ATA via a) kinetic resolution, b) deracemization or c) asymmetric synthesis.[120]*

a) Kinetic resolution

In kinetic resolution, racemic mixtures of amines can be turned into optically pure amines with a theoretical yield of 50%. However, ketones present in the reaction solution inhibit the ATA hence prohibiting its use in higher concentrations.[121–123] In order to overcome this limitation, researchers either utilize a biphasic system or engineer the TA to tolerate higher concentrations of the ketone substrate. Kim *et al*. 2005 successfully engineered the ω-TA from *Vibrio fluvialis* JS17 to tolerate aliphatic ketones. The new mutant was able to resolve up to 150 mM 2-aminoheptane to (*R*)-2-aminoheptane with 50% conversion and >99 ee (Scheme 1.13).[123]

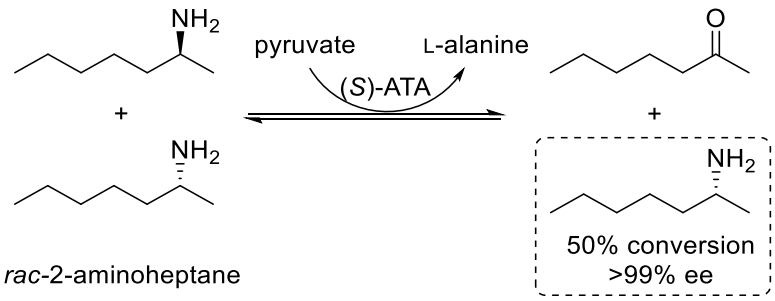

***Scheme 1.13**. Conversion of 2-aminoheptane to (R)-2-aminoheptane with kinetic resolution.*[123]

b) Deracemization

There are two possible approaches for deracemization, both with 100% theoretical yield.

I) Dynamic kinetic resolution (DKR) is similar to kinetic resolution with the difference that the two enantiomers of the starting material exist in equilibrium.[124] In 2009, Kroutil and co-workers were the first to report DKR with ω-TAs for the production of (*R*)- and (*S*)-4-phenylpyrrolidin-2-one with >99% conversion and up to 65% ee, shown in Scheme 1.14a.[124]

II) A two-step one-pot process employs two ATAs of opposite enantioselectivity, stoichiometric amount of pyruvate, D- and L-alanine and a ketone substrate for the production of optically pure amines.[14,125] Koszelewski *et al*. 2009, have described the synthesis of (*R*)- and (*S*)-mexiletine in enantiomerically pure form, utilizing ω-TAs of opposite stereoselectivity (Scheme 1.14b).[120,125] As shown in Scheme 1.14b, mexiletine is initially deracemized from an (*R*)-ATA in the presence of pyruvate, to afford D-alanine, (*S*)-mexiletine and its corresponding ketone. The reaction is driven forward from a D-amino acid oxidase (D-AAO), which converts D-alanine to pyruvate in the presence of water and molecular oxygen. During a second transaminase step, an (*S*)-ATA converts the intermediate ketone to (*S*)-mexiletine in the presence of L-alanine.

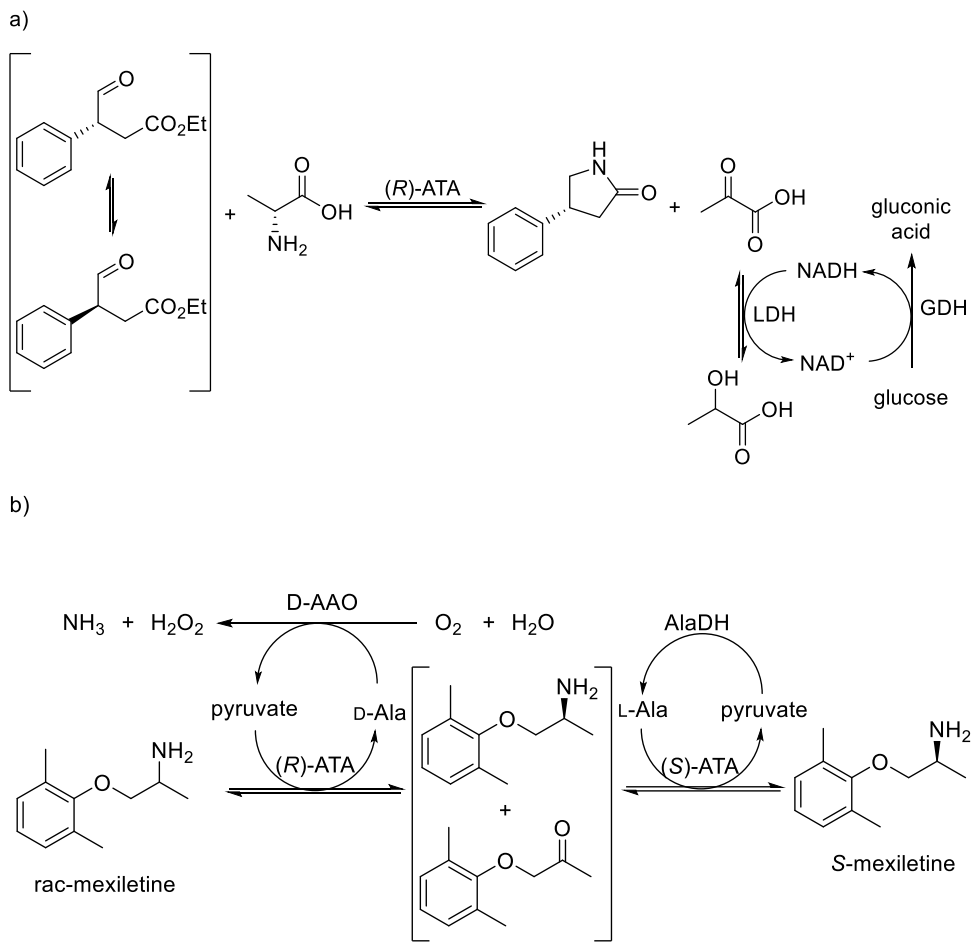

***Scheme 1.14**. a) An ATA mediated DKP for the synthesis of (R)-4-phenylpyrrlidin-2-one with 65% ee,*[124] *b) Deracemization of mexiletine in a two-step one-pot method.*[125]

c) Asymmetric synthesis

In asymmetric synthesis the amino group of the amine donor is transferred to a prochiral ketone affording an optically pure amine with a theoretical yield of 100%. However, the unfavorable thermodynamic equilibrium as well as the inhibitory effect of the ketone by-product have hampered the widespread application of this approach.[120] In order to overcome these challenges, researchers came up with the concept of by-product removal, which diminishes the inhibition of the enzyme and drives the equilibrium forward.

In industry, IPA is employed as the amine donor coupled with the *in situ* evaporation of the co-product (acetone), shown in Scheme 1.15a.[61] However, IPA is poorly accepted by most ATAs thus requiring higher concentrations or protein engineering to achieve greater conversions.

In academic laboratories, L-alanine is commonly used as an amine donor with a coupled enzymatic system for the elimination of the co-product (pyruvate), shown in Scheme 1.15b. Lactate dehydrogenase (LDH) is employed for the conversion of pyruvate to lactate. Stoichiometric amounts of NADH used are recycled from the degradation of glucose from glucose dehydrogenase.[16,126] Alternatively, pyruvate can be decarboxylated by pyruvate decarboxylase (PDC), which does not require expensive NAD(P)H co-factors.[16,127] Lastly, acetolactate synthase (ALS) is employed to produce acetolactate from two molecules of pyruvate. [128] This co-product spontaneously decomposes to 3-hydroxybutan-2-one (also known as acetoin) and CO_2.[129]

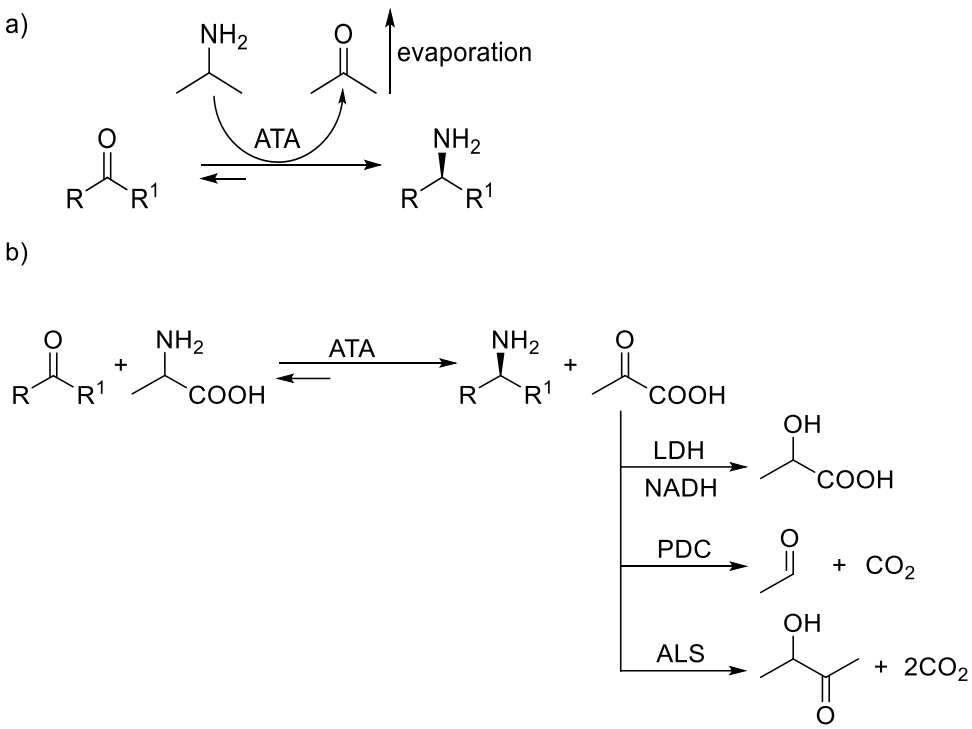

***Scheme 1.15**. The reaction equilibrium of an ATA reaction is displaced by utilizing either a) IPA as an amine donor and subsequently evaporating the acetone formed or b) L-alanine coupled with an enzymatic system for the elimination of pyruvate.*

Required protein engineering or coupled enzymatic systems, utilizing NAD(P)H co-factor, increase the total cost of an ATA reaction. Recently, a novel process utilizing diamines as 'smart' amine donors was developed.[130] In 2013, O'Reilly and co-workers identified o-xylylenediamine as the first 'smart' amine donor, which led to complete conversion of a series of ketone substrates with only 1-1.5 equivalent. The aldehyde by-product undergoes intramolecular cyclization affording the corresponding imine, which spontaneously tautomerizes to the more stable aromatic isoindole. Subsequent polymerization affords a colored precipitate that effectively drives the equilibrium forward (Scheme 1.16).[130]

In this study, O'Reilly and coworkers used a commercial ATA for the conversion of the model ketone substrate (4-fluorophenyl)acetone with

the diamine and compared it to IPA and L-alanine. The latter gave poor results despite the use of up to 100 equivalents. The introduction of a pyruvate removal system slightly increased the conversion to 21%, which still remains modest when compared to the >99% conversion achieved with 1-1.5 equivalents of o-xylylendiamine (Scheme 1.16). In this reaction, a coloured precipitate is formed as a co-product (not characterized), which is removed *via* centrifugation. [130]

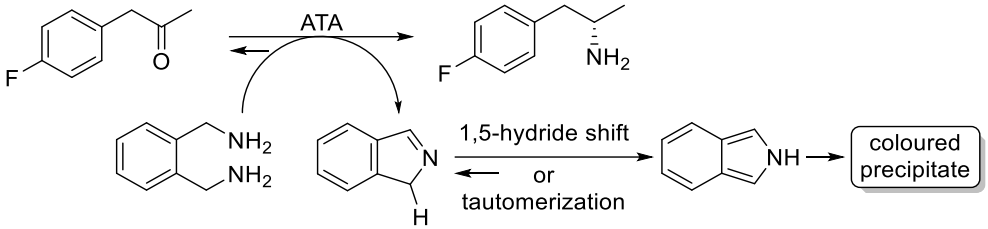

***Scheme 1.16**. A selected example of an ATA reaction utilizing o-xylylenediamine as amine donor.*[130]

In a more recent study from the O'Reilly group, cadaverine (or 1,5-diaminopentane, 1,5-DAP) was identified as a 'smart' amine donor with a commercial ATA. This diamine is driving the equilibrium of an ATA reaction in a similar way.[131] The amino-aldehyde by-product formed, spontaneous cyclizes and trimerizes in a pH-dependent fashion, as shown in Scheme 1.17.[131]

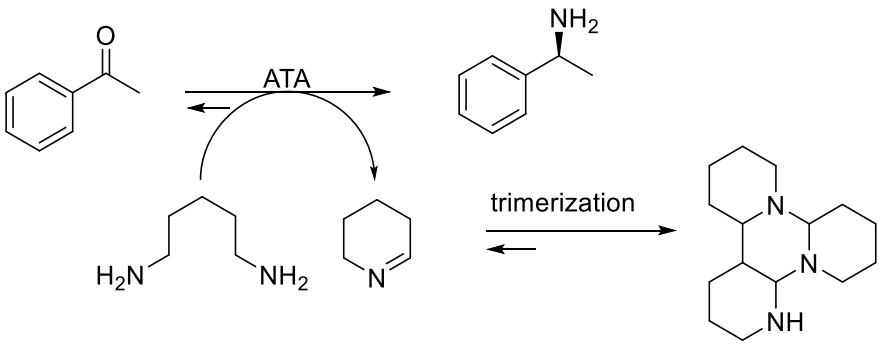

***Scheme 1.17**. A selected example of an ATA reaction utilizing cadaverine as amine donor.*[131]

The use of *o*-xylylendiamine and cadaverine as amine donors paved the way towards the development of the novel approach of 'smart' amine donors, as a cost-effective mean to overcome the challenging ATA equilibrium.

1.5 Overall aims and objections

The overall aim of this thesis is the development of new methodologies for the asymmetric synthesis of chiral amines from transaminases utilizing 'smart' amine donors. More specifically, this work aims to:

- Understand the potential of these donors in high-throughput screen and scale-up applications
- Explore whole-cell system alternatives for improved performance of ATA reactions

2: Application of smart amine donors for the production and commercialization of chiral amines

The research described in this chapter has been published: A. Gomm[+], S. Grigoriou[+], C. Peel, J. Ryan, N. Mujtaba, T. Clarke, E. Kulcinskaja, E. O'Reilly *Eur. J. Org. Chem.* **2018**, *2018*, 5282-5284.

[+]: Shared first author

2.1 Introduction

'Smart' amine donors were only recently discovered, and their potential has yet to be fully explored. Green *et al.* 2014, reported *o*-xylylenediamine as a possible candidate for a high-throughput (HTP) colorimetric screening method to detect desired ATA activity. The colored precipitate, formed as a co-product following transamination (see section: 1.4.3), can be exploited to explore the carbonyl substrate scope of ATA enzymes. Importantly, it can be successfully employed on a small scale (100-200 uL), thus reducing the total costs. However, this screen is not quantitative due to the strong background of the black precipitate.[130] In 2017, Guo and Berglund described different HTS for ATAs,[132] including the use of 2-(4-nitrophenyl)ethan-1-amine[133] or alanine[134] as alternatives to *o*-xylylenediamine screen. The former is not well accepted by ATAs, affording low conversions and is limited to aldehyde substrates,[133] while the latter requires a coupled enzymatic system and a pH indicator dye that increases the operating cost.[134] An essential requirement to all screens is the acceptance of the amine donor from the ATA, which was taken advantage in the study presented herein.

Of particular interest to our group are the 'smart' amine donors and ATAs that accept those donors. Information extracted from the *o*-xylylenediamine screen is unique, because it is directly linked to 'smart'

amine donors and reveals the ketone/aldehyde substrates that are transaminated in the presence of such donors.

2.2 Aims and Objectives

The aim of this chapter is the development of a facile route for chiral amine synthesis utilizing commercially available transaminases in combination with 'smart' amine donors. More specifically, this work aims to:

- Explore the potential of an *o*-xylylenediamine high-throughput screen
- Investigate inexpensive 'smart' amine donor alternatives
- Produce and commercialize valuable chemicals

2.3 Substrate screen of ATA256

Commercially available ATA256 from Codexis was used in this work. This ATA has been heavily engineered to tolerate higher temperatures and DMSO concentration.[135,136] In past and recent years, the research community has employed this ATA for the production of chiral amines.[137,138] Recently reports demonstrated that ATA256 accepts *o*-xylylendiamine[130] and cadaverine,[131] and hence was selected as a good starting point to expand the application of 'smart' amine donors. The carbonyl substrate scope of ATA256 was explored by screening a library of 400 compounds, which were kindly provided by Key Organics. The library contained both aldehydes and ketones with diverse structures including aliphatic, aromatic, polyaromatic and cyclic scaffolds and a wide range of functional group substitutions.[139] The initial colorimetric HTS utilizing *o*-xylylenediamine was carried out in 96-well plates. The formation of a dark precipitate was observed after 1 and 24 hours allowing the qualitative determination of ATA activity, as shown for a representable example in Figure 2.1. Wells of light green colour correspond to unreacted ketone/aldehyde substrates, whereas fading dark orange is linked to negligible formation of black precipitate, thus indicating poor conversions

(<1%). All dark wells indicate precipitation and thus treated as positive results. This screen is extremely sensitive but not quantitative, as both 5% and 90% conversions would give the same colour. However, it can be used at an early stage, as described herein, to rapidly identify potential substrates and reduce the numbers of subsequent biotransformations.

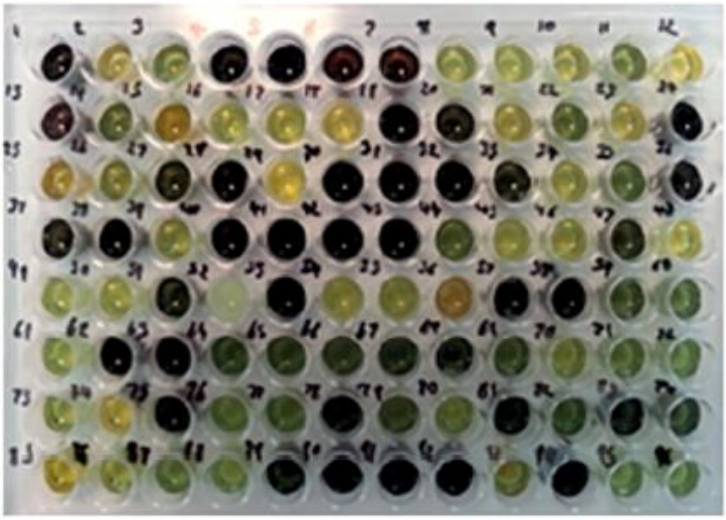

This screen was conducted by our then master student Nafees Mujtaba and is presented herein solely for clarity purpose.

Figure 2.1. *Representative 96-well plate showing the application of the o-xylylenediamine screen with ATA256, for the identification of ketones and aldehyde substrates. Pictures after 24h.*

Analysis of the compounds that gave an intense coloured read-out revealed a trend in the substrate specificity of the ATA256. As illustrated in figure 2.2, the molecular weight and calculated volume were compared.[140] The results revealed a preference towards small molecules (up to 200 Da), which can be attributed to the nature of the active site of the transaminase.[108] The inevitable increase of volume that comes with higher molecular weight, potentially lead to compounds that are unable to fit into the active site pocket of the enzyme, thus explaining the loss of activity observed for larger molecules.

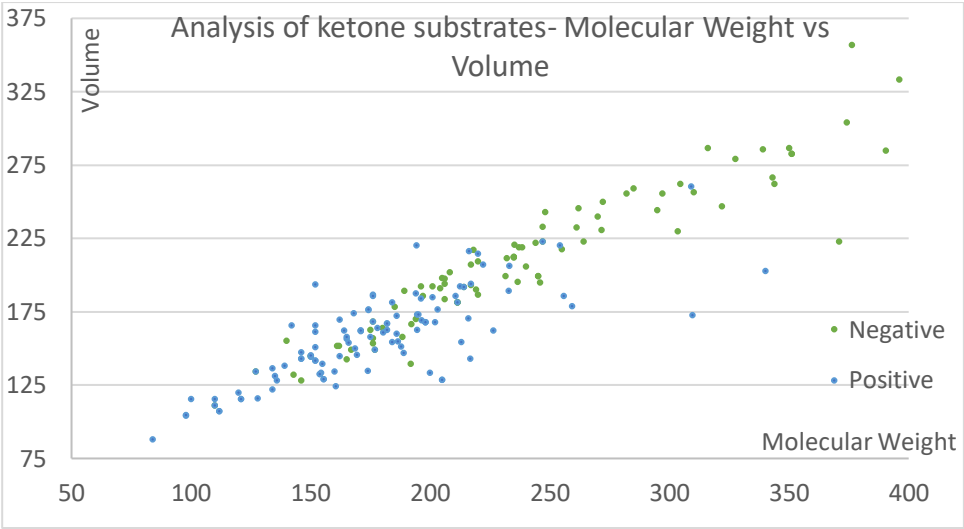

***Figure 2.2**. Plot of molecular weight vs calculated volume of carbonyl-substrates. The blue dots correspond to compounds that afforded a colored precipitate, while for the green dots no precipitate was observed.*

Some compounds of small molecular weight and volume gave negative response (Figure 2.3). These molecules either consist of bulky substitutes (such as cyclopropane) on both sides of the carbonyl group, which restrict their access to the active site,[108] or contain functional groups that complicate the ATA reaction. For example, trifluoromethylketones have been reported to inhibit enzymes, such as lipases, by forming a stable intermediate through covalent bonding with key residues in the active site.[141]

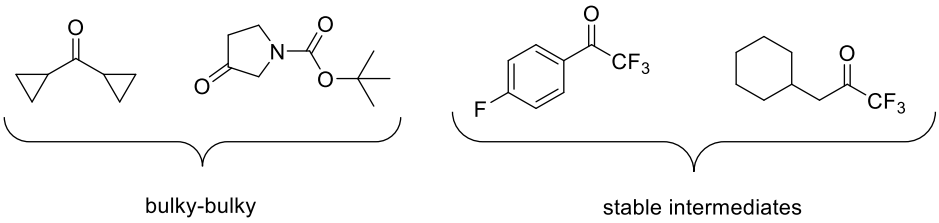

Figure 2.3. *Examples of small molecules with negative response*

Owing to the rapid results of the screen, the number of potential substrates was halved (204 out of 400 gave positive result). After consulting Key Organics, the upscaling of the biocatalytic reaction of 13 compounds was further investigated, based on the commercial interest of the corresponding amine. Some of the products were either not commercially available, were extremely expensive or required complicated traditional chemical synthesis.[142–149]

In an effort to reduce the downstream cost for preparative scale reactions, the 'smart' amine donor *o*-xylylenediamine was replaced with cadaverine, which drives the equilibrium forward in a similar way (see section 1.4.3).[131] Analytical scale biotransformations were conducted on the selected 13 compounds utilizing 1 or 3 equiv. of cadaverine and the conversion was measured *via* GC-FID (see section 2.6.5). For comparison, the well-established amine donor IPA was tested under the same reaction conditions. As shown in Figure 2.4, cadaverine outperformed IPA in almost every experiment. Significantly, only 3 equiv. of cadaverine were required to achieve 98% conversion of the challenging ketone **1** to the corresponding chiral amine. On the other hand, IPA afforded a moderate conversion of 70% under the same conditions. Poor performance of compounds **3**, **4**, **5**, **7** and **9** with both donors is indicative of complications due to the electronic effects of functional groups adjacent to the carbonyl moiety. Despite the promising results demonstrated for compound **6**, preliminary tests showed

complications with downstream purification procedures, as the product was degrading during purification.

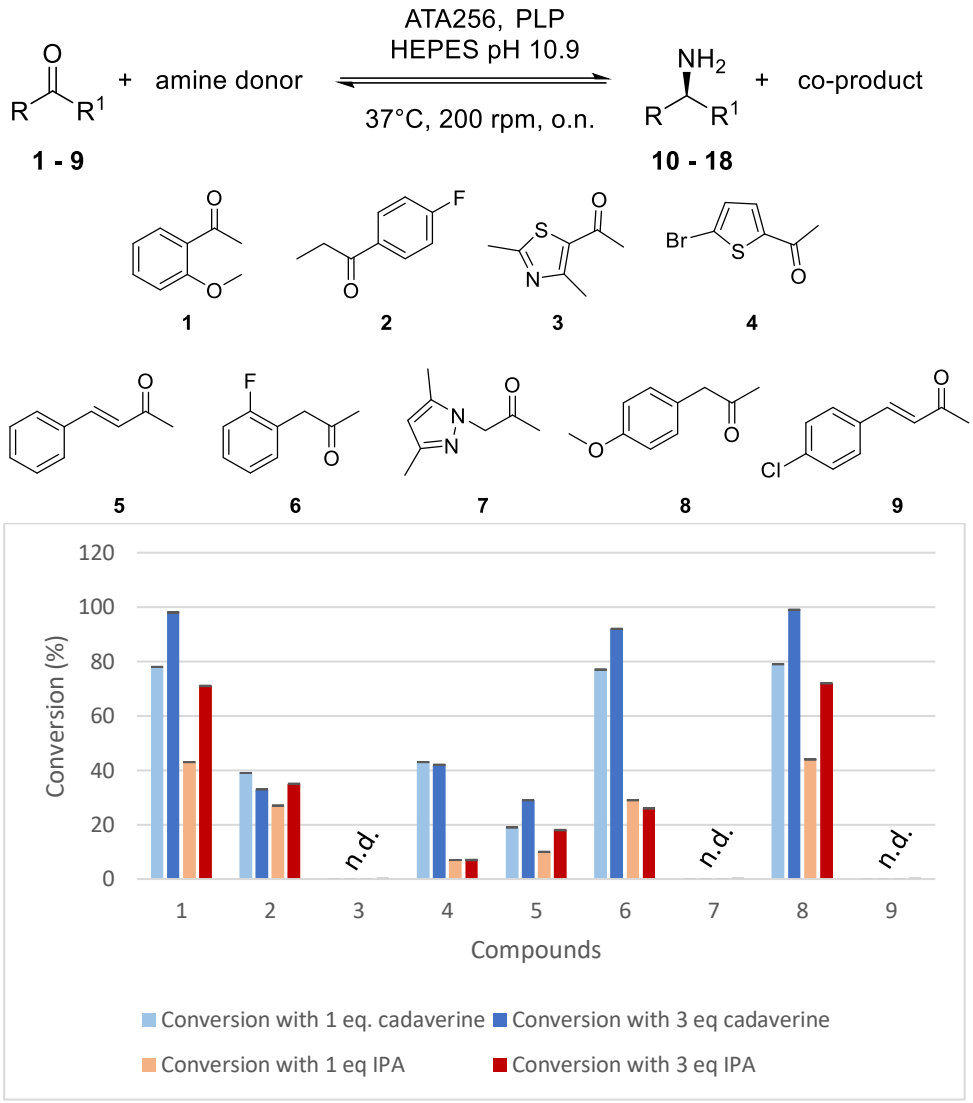

***Figure 2.4**. Conversions (n=3, std <1%) of compounds **1**-**9** (20 mM) to their corresponding amines, utilizing 1 or 3 equiv. amine donor, cadaverine (light and dark blue, respectively) or IPA (beige and red, respectively), ATA256 (2.5 mg/mL) and PLP (1 mM) on analytical scale. Conversions were measured as described in section 2.6.5.*

Altogether, these findings contributed to selecting cadaverine as the sacrificial amine donor for the transamination of ketones **1** and **8** on a preparative scale.

2.4 Asymmetric amine synthesis using compounds 1 and 8

Solvent DMSO could complicate downstream purification procedures on a preparative scale and hence an alternative solvent was sought to replace it. Initially, different co-solvents were tested, to identify a suitable alternative. The majority of the solvents afforded similar conversions to DMSO for all ketones. A significant drop of 20% was observed for acetonitrile and THF with compound **10**, whereas 10% loss was reported when DMF or PEG was utilized. The two most promising co-solvents were methanol and ethanol, which gave similar conversions to DMSO (Table 2.1). On the contrary, acetone gave poor results indicating severe inhibition of the ATA.

***Table 2.1**. Conversions (n=3, std <1%) of compounds **1** and **8** (20 mM added as 10% from a 200 mM stock dissolved in the co-solvent tested) into the corresponding amine using ATA256 (2.5 mg/mL), PLP (1 mM) and 1,5-DAP (3 eq) at 30°C, 200 rpm for 48h. Conversions were measured as described in section 2.6.5.*

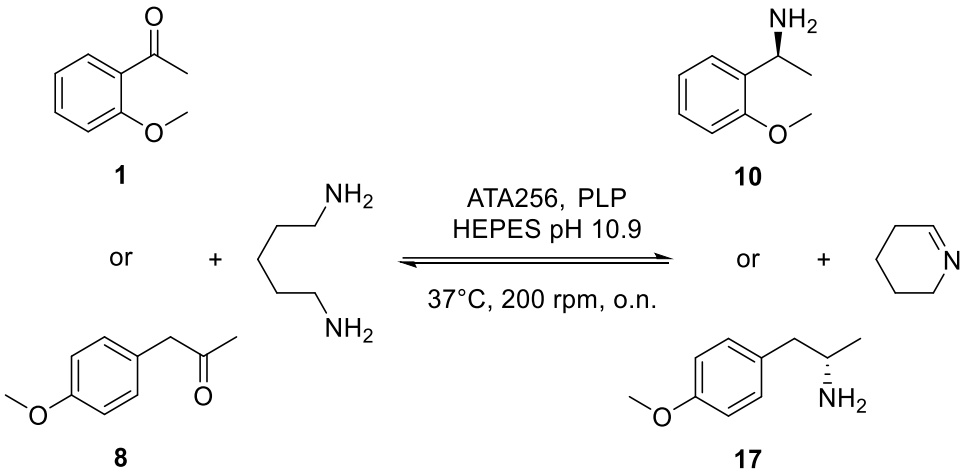

Solvent	Conversion of ketone	
	1	**8**
DMSO	>99%	75%
Methanol	>99%	81%
Ethanol	>99%	79%
Acetonitrile	97%	76%
THF	>99	78%
DMF	96%	41%
Acetone	10%	n.d.
PEG	>99%	77%

Subsequently, experiments were carried out to identify the maximum substrate concentration tolerated by ATA256 maintaining high conversions. ATA256 could tolerate concentrations as high as 100 mM with little to no

impact on the conversion of ketone **8** (Table 2.2). High concentrations of ketone **1** inhibited ATA256, as the conversion dropped sharply from 98% to 60%, when increasing from 20 mM to 50 mM of ketone and reached as low as 30%, when 100 mM of ketone **1** were used (Table 2.2).

***Table 2.2**. Conversions (n=3, std <1%) of different concentrations of compounds **1** and **8** to the corresponding amine using ATA256 (2.5 mg/m), PLP (1 mM) and 1,5-DAP (3 eq) 30°C, 200 rpm for 48h. Conversions were measured as described in section 2.6.5.*

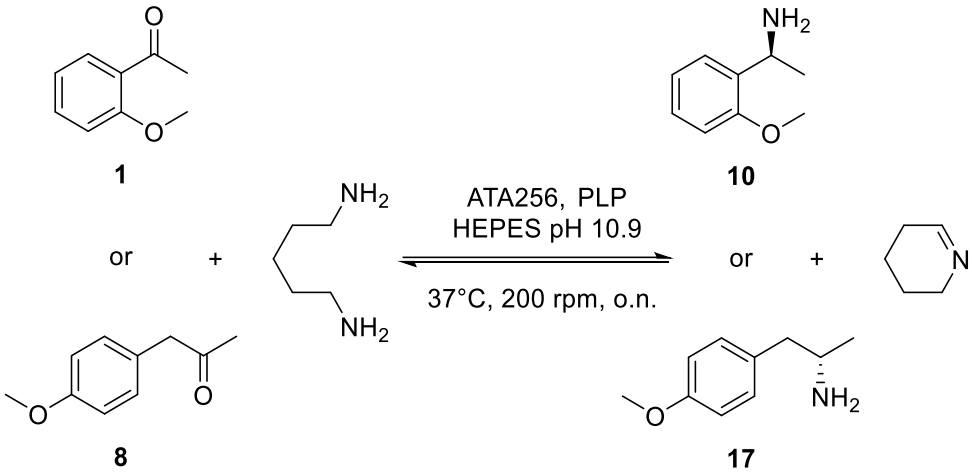

Ketone	Conversion at ketone conc.		
	20 mM	50 mM	100 mM
1	98%	61%	30%
8	99%	99%	96%

Preparative biotransformations were carried out utilizing ATA256 (2.5 mg/mL) rehydrated in 4-(2-hydroxyethyl)piperazine-1-ethanesulfonic acid (HEPES) buffer (pH 10.9).[131] The unusually high pH has been previously shown to contribute to higher conversions with cadaverine. As previously mentioned (see section 1.4.3), transamination of cadaverine affords a co-product, which trimerizes in a pH dependent way. The trimer was reported

stable in higher pHs (10.9), thus driving the equilibrium forward. Preliminary results on preparative scale showed a significant decrease in conversion (60%) of compound **8** with methanol as solvent. Complete conversion was observed when this was replaced with DMSO, but only moderate isolated yield (49%) was observed. The purification step with column chromatography was compromised due to the presence of DMSO. Reaction of compound **1** was scaled-up to a concentration of 20 mM with 10% methanol as co-solvent leading to complete conversion and 70% isolated yields (Table 2.3). Conversions of all biotransformations were analyzed *via* GC-FID equipped with a chiral column. The purity of the products, determined by LC-MS, met the required standards and therefore were made commercially available through Key Organics.

Table 2.3*. Conversions (n=3, std <1%) and yields of scale-ups of compounds* ***1*** *and* ***8****. Conversion were measured as described in section 2.6.5.*

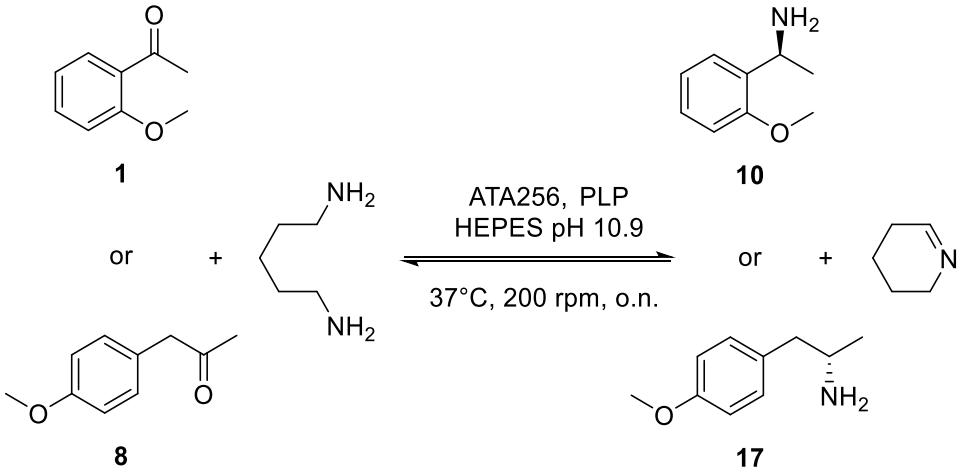

Ketone	Operating concentration	Conversion	Yield
1	20 mM	98%	70%
8 + MeOH	100 mM	60%	N/A
8 + DMSO	100 mM	96%	49%

N/A: Not Available

As already mentioned, these products (**10**, **17**) were either not commercially available, were too expensive or were difficult to synthesize

using traditional chemical routes, thus an approach was required to verify the stereoselectivity retrospectively. Hoye *et al.* 2007, have reported a delicate method for the determination of absolute configuration by analyzing the Mosher esters,[150] which can also be applied to Mosher amides for this case. Relevant Mosher amides were synthesized by reacting the chiral amines (**10, 17**) with both the (*S*)- and (*R*)-enantiomers of the Mosher acid chlorides in dichloromethane (DCM) overnight (Scheme 2.1).

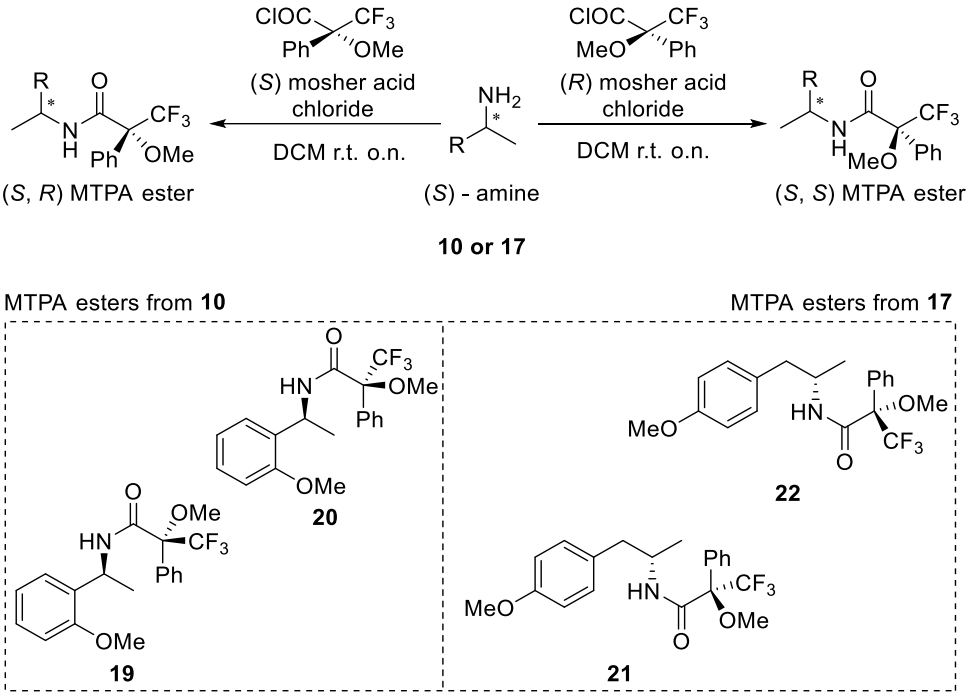

***Scheme 2.1**. Reaction of the chiral amines (**10** and **17**) with the Mosher acid chlorides in DCM at r.t. overnight.*

Reactions were monitored with thin layer chromatography (TLC) and only one new spot was detected. The new compounds were isolated and fully characterized. A single peak was observed in the ^{19}F-NMR for each individual new compound, as shown for a representative example in Figure 2.5. These results show that the spot on the TLC corresponds to a single stereoisomer, thus indicating that both starting materials, amine and Mosher acid chloride, were optically pure.

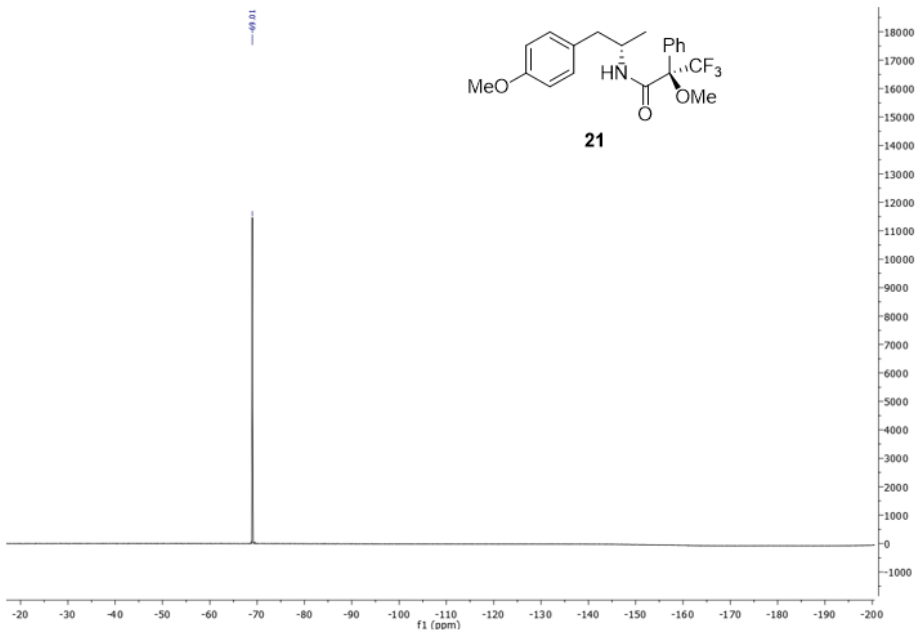

Figure 2.5. *^{19}F-NMR of compound **21**.*

In order to identify the absolute configuration of the chiral amines, ^{1}H-NMR of the corresponding (*S*)- and (*R*)-Mosher amides were compared. It is known that aryl groups, such as the phenyl ring of the Mosher moiety, impose an anisotropic, magnetic shielding effect on protons above or below the ring.[151,152] This leads to those protons appearing upfield (lower ppm) on the ^{1}H-NMR spectra.[151,152] Inspection of the ^{1}H-NMR of the Mosher amides, would reveal the protons (of one stereogenic centre) residing in close proximity to the phenyl ring (of the other stereogenic centre). These protons will be shielded and upfield in the spectra. As an example, the corresponding Mosher amides of compound **17** are discussed. Compounds (*S*,*R*)-**21** (shown in blue) and (*S*,*S*)–**22** (shown in red) were synthesized with reacting **17** with the (*S*)- and (*R*)-Mosher acid chlorides, respectively (Figure 2.6). Analysis of the two spectra showed that protons (1.0-1.25 ppm) of the methyl group adjacent to the amide group are upfield for compound (*S*,*R*)-**21**, indicating the shielding effect from the Mosher phenyl ring. The same

effect is observed for the proton (2.5-3.0 ppm) in α-position of the amide group for compound (*S,S*)-**22**, thus verifying the absolute configuration of these molecules.

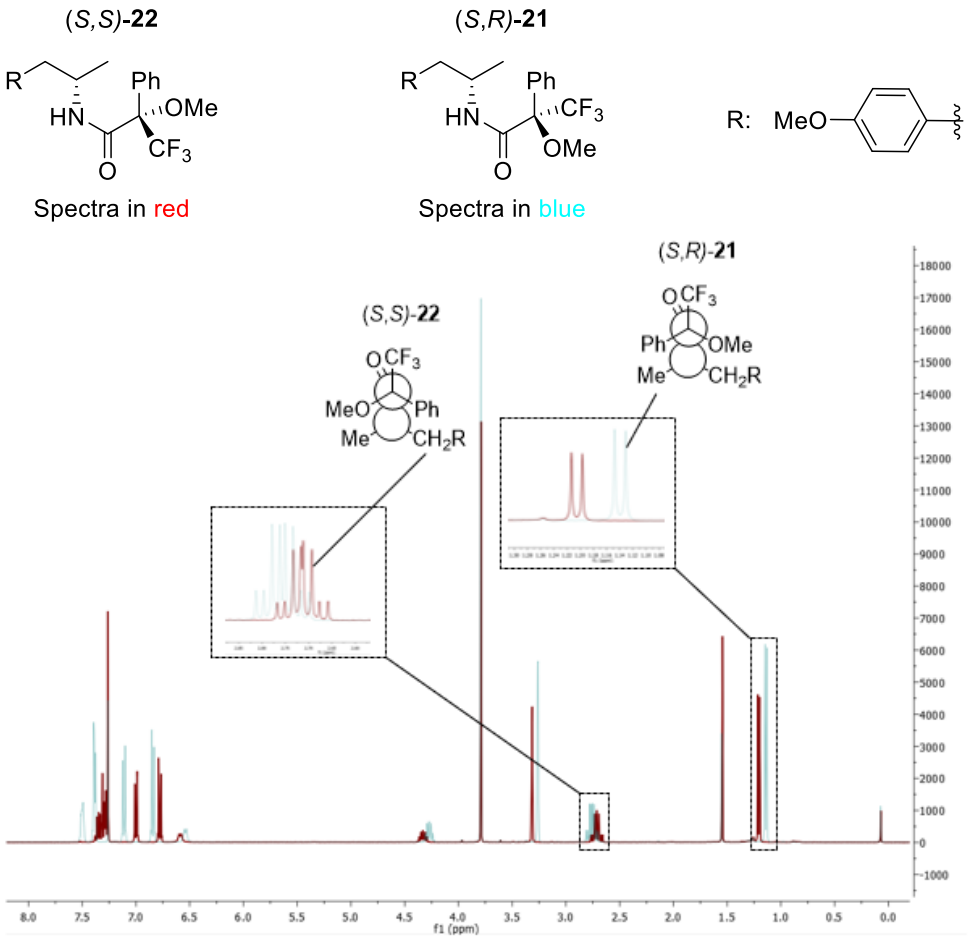

***Figure 2.6**. Aligned ^{1}H-NMR spectrum of Mosher amides (S,R)-**21** in blue and (S,S)-**22** in red.*

2.5 Conclusion

This study provides a facile route for the synthesis of chiral amines utilizing the commercially available ATA256 and 'smart' amine donors, *o*-xylylenediamine and cadaverine. The potential of *o*-xylylenediamine as a HTS donor to unveil the carbonyl substrate scope of the commercially available ATA256 was demonstarted. The colored precipitate is indicative of ATA activity, assisting in the identification of reactive amino acceptors. A general trend towards smaller carbonyl substrates is described for the

ATA256. However, the screen is not quantitative and further optimization would broaden its application.

Also, the application of cadaverine, a less expensive 'smart' amine donor, for a cost-effective production of chiral amines **10** and **17** was demonstrated. The stereoselectivity was assigned retrospectively with the Mosher esters approach and the final products (**10** and **17**) became commercially available. Commercial reagents and biocatalyst were used in this work, making this approach readily available to the general research community.

2.6 Experimental

2.6.1 General Methods and Materials

General: NMR spectra were recorded on a JEOL ECS 400 NMR spectrometer (^{1}H 400 MHz, and ^{13}C 100 MHz). The chemical shifts were recorded in ppm with the residual $CHCl_3$ signal referenced to 7.26 ppm and 77.00 ppm for ^{1}H and ^{13}C respectively. Coupling constants (*J*) are reported in Hz, are corrected and refer to the apparent peak multiplicities. Thin layer chromatography was performed on Alfa Aesar silica gel 60 F254 plates. Flash column chromatography was performed on silica gel (60 Å, 230-400 mesh). GC-MS spectra were recorded on a HP 5973, HP-5MS (30 m × 0.25 mm × 0.25 µm), Helium carrier gas, flow 1 mL/min. Infrared spectra were recorded using a Thermo Nicolet 380 FT-IR. GC-FID analysis was performed on Agilent 6850 equipped with a CP CHIRASIL-DEX CB (25 m × 0.25 mm) DF = 0.25 column. HPLC analysis was performed on an Agilent 1100 series equipped with a Lux Amylose-1 chiral column from Phenomenex. All racemic standards were prepared by mixing equimolar quantities of enantiomerically pure biotransformation products.

Materials: Commercially available reagents, purchased from Sigma Aldrich or Acros, were used throughout without further purification. Anhydrous THF, CH_2Cl_2, diethyl ether and toluene were obtained from a Pure Solvent apparatus. Commercially available transaminases, ATA113 and ATA117 were purchased from Codexis in the form of lyophilised cell extract. All biotransformations were carried out in HEPES buffer (100 mM, pH 10.9) at 30°C.

2.6.2 High-throughput screening

Commercially available Codexis® (*S*)-selective ATA 256 (2.5 mg/mL) was rehydrated in HEPES buffer (200 µL, 100 mM, pH 7) containing PLP (1 mM) and *o*-xylylenediamine (5 mM from a 500 mM stock in HEPES buffer). To this was added the ketone substrate (5 mM from a 500 mM stock in DMSO). The reaction mixture was incubated at 30°C, 200 rpm in a shaking incubator and color formation was observed after 24 and 48 hours.

2.6.3 Analytical scale biotransformations of ketones 1-9 with ATA 256 and cadaverine

Commercially available Codexis® (*S*)-selective ATA 256 (2.5 mg/mL) was rehydrated in HEPES buffer (1 mL, 100 mM, pH 10.9) containing PLP (1 mM) and cadaverine (5-300 mM from a 500 mM stock in HEPES buffer). For comparison, isopropylamine (20 mM), was tested under the same reaction conditions. To this was added the ketone substrate (5-100 mM from a 500 mM stock in DMSO) and the reaction pH was adjusted to 10.9. The reaction mixture was incubated at 30°C, 200 rpm in a shaking incubator. After 48 hours the reactions were basified (pH 12), extracted with ethylacetate (EtOAc) (750 µL), derivatised using 10 µL triethylamine (TEA) and 10 µL acetic anhydride (Ac_2O) and analysed by GC-FID.

2.6.4 GC Method

Chiral GC analysis was performed on a ThermoFisher 1310 chromatograph equipped with a flame ionising detector, an AI 1310 autosampler and a CP-Chirasil-Dex-CB chiral column (25 m x 0.25 mm x 0.36 mm) using helium as a carrier gas. The front inlet temperature was set to 230 °C and the front detector was set to 250 °C. Split flow was set to 170 mL/ min and the helium gas was set to a constant flow of 1.7 mL/min GC-FID temperature program for all compounds was the following; 40 °C hold for 2 minutes followed by 20 °C/min temperature rise to 150 °C and then a hold for 5 minutes followed by a 30°C/min temperature rise to 225 °C and a further hold for 8 minutes.

2.6.5 Measurement of conversion

Conversions were measured by comparing the relative areas between the peak of the starting material and a newly formed peak, which is present in the reaction mixture but not in the negative control. The negative control is the same reaction but without the addition of the enzyme. The total of peak areas is assumed to represent all molecules in the system and the conversion is calculated as follows:

$$conversion\,\% = \frac{A}{A+B} * 100$$

A: peak area of the product (equals to moles of product produced)
B: peak area of the starting material (equals to remaining moles of the starting material)

Additional peaks of solvent, triethylamine and acetic anhydrate are also present, but are not incorporated in the calculation, as they are added in excess.

2.6.6 Analytical scale biotransformations of ketone 1 and 8 with ATA256 and cadaverine using various co-solvents

Commercially available (*S*)-selective ATA 256 (2.5 mg/mL) was rehydrated in HEPES buffer (1 mL, 100 mM, pH 10.9) containing PLP (1 mM) and cadaverine (60 mM from a 500 mM stock in HEPES buffer). To this was added the ketone substrate (20 mM from a 200 mM stock in co-solvent tested) and the reaction pH was adjusted to 10.9. The reaction mixture was incubated at 30°C, 200 rpm in a shaking incubator. After 48 hours the reactions were basified (pH 12), extracted with EtOAc (750 µL), derivatised with 10 µL triethylamine and 10 µL acetic anhydride and analysed by GC-FID.

2.6.7 Preparative scale biotransformations of compounds 10, 17

10. (*S*)-1-(2-methoxyphenyl)ethan-1-amine[133]

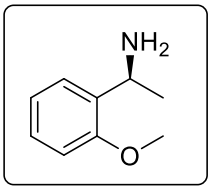

Commercially available (*S*)-selective ATA 256 (2.5 mg/mL) was rehydrated in HEPES buffer (3x10 mL, 100 mM, pH 10.9) containing PLP (1 mM) and cadaverine (60 mM). To this was added 4-methoxyphenylacetone **1** (20 mM dissolved in 5% methanol) and the mixture was incubated at 30° C for 48 hours in a shaking incubator (200 rpm). The pH of the mixture was then adjusted to 2 and extracted with ethyl acetate (10 mL). The pH of the aqueous phase was then adjusted to 14 and extracted with ethyl acetate (6 x 10 mL). The combined organic fractions were dried over magnesium sulphate and the solvent was removed *in vacuo*; the crude product was purified by column chromatography using flash silica gel (eluent: 100% DCM) to afford the product (63 mg, 70%) as a white solid. ^{1}H NMR (400 MHz, $CDCl_3$) δ 7.33 (dd, *J* = 7.5, 1.7 Hz, 1H), 7.21 (ddd, *J* = 8.2, 7.5, 1.7 Hz, 1H), 6.94 (td, *J* = 7.5, 1.1 Hz, 1H), 6.87 (dd, *J* = 8.2, 1.1 Hz, 1H), 4.36 (q, *J* = 6.7 Hz, 1H), 3.85 (s, 3H), 1.40 (d, *J* = 6.7 Hz, 3H). ^{13}C NMR (101 MHz, $CDCl_3$) δ 156.9, 127.8, 125.9, 120.8, 110.6, 110.1, 55.4, 46.2, 23.3. MS (EI) m/z: Calculated $C_9H_{14}NO^+$ $[M+H]^+$ 152.0997; found 152.1076. Spectra in accordance with literature values.[133]

17. (*S*)-1-(4-methoxyphenyl)propan-2-amine hydrochloride[153]

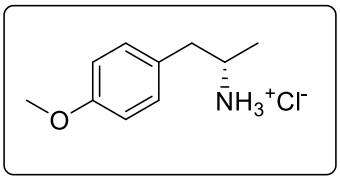

Commercially available (*S*)-selective ATA256 (2.5 mg/mL) was rehydrated in HEPES buffer (5 x 10 mL, 100 mM, pH 10.9) containing PLP (1 mM) and cadaverine (150 mM). To this was added 4-methoxyphenylacetone **8** (100 mM dissolved in 5% DMSO) and the mixture was incubated at 30° C for 48 hours in a shaking incubator (200 rpm). The pH of the mixture was then adjusted to 2 and extracted with ethyl acetate (30 mL). The pH of the aqueous phase was then adjusted to 14 and

extracted with ethyl acetate (6 x 30 mL). The combined organic fractions were dried over magnesium sulphate, filtered and the solvent was removed in *vacuo*; the crude product was purified by column chromatography using flash silica gel (eluent: DCM:MeOH 9:1) to afford the product (200 mg, 49%) as a white solid. This was re-dissolved in 15 mL of anhydrous tetrahydrofuran (THF) and HCl (4N in diethyl ether) was added dropwise until no more precipitate was formed. The residual solvent was removed *ex vacuo* to afford the final product (2*S*)-1-(4- methoxyphenyl)propan-2-amine as the hydrochloride salt (162 mg, 39%) as a white solid. ^{1}H NMR (400 MHz, D_2O) δ 7.35 – 7.19 (m, 2H), 7.09 – 6.92 (m, 2H), 3.84 (s, 3H), 3.60 (m, 1H), 2.90 (m, 2H), 1.31 (d, *J* = 6.6 Hz, 3H). ^{13}C NMR (101 MHz, D_2O) δ 158.0, 130.6, 128.6, 114.4, 55.4, 49.2, 39.2, 17.4. MS (EI) m/z: Calculated $C_{10}H_{16}NO^+$ $[M+H]^+$ 166.0764; found 166.0732. Spectra in accordance with literature values.[153]

2.6.8 Standard procedure for derivatizing free amines with Mosher's Acid Chloride

The amine (1 eq) was dissolved in DCM. To this were added triethylamine (3 eq) and (*S*)- or (*R*)-(+)-α-methoxy-α-trifluoromethylphenylacetyl chloride (2 eq) and the reaction was stirred at room temperature overnight. Upon completion, the reaction was quenched with H_2O and extracted three times with DCM. The organic phases were combined, dried over $MgSO_4$ and the solvent was removed *in vacuo*. The crude was then purified via column chromatography to afford pure final product, which was analyzed *via* NMR and MS.

19. (*S*)-3,3,3-trifluoro-2-methoxy-*N*-((*S*)-1-(2-methoxyphenyl)ethyl)-2-phenylpropanamide

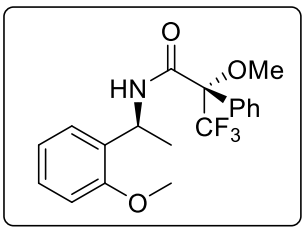

White solid (24mg, 25%) ^{1}H NMR (400 MHz, $CDCl_3$) δ 7.64 – 7.58 (m, 2H), 7.53 (d, *J* = 8.9 Hz, 1H), 7.47 – 7.38 (m, 3H), 7.33 – 7.20 (m, 2H), 7.00 – 6.87 (m, 2H), 5.34 (m, 1H), 3.86 (s, 3H), 3.42 (m, 3H), 1.47 (d, *J* = 6.9 Hz, 3H). ^{13}C NMR (101 MHz, $CDCl_3$) δ 165.0, 157.2, 133.3, 130.2, 129.5, 128.8, 128.6, 128.1, 127.8, 123.9 (q, *J* = 289.8 Hz), 121.0, 111.1, 84.1 (q, *J* = 26.2 Hz), 55.3, 55.0, 47.3, 21.1. ^{19}F NMR (376 MHz, $CDCl_3$) δ -68.89. IR (ART cm^{-1}) 3459, 2948, 2842, 1687. MS (EI) m/z: calculated $C_{19}H_{21}F_3NO_3^+$ $[M+H]^+$ 368.1395; found: 368.1375.

20. (*R*)-3,3,3-trifluoro-2-methoxy-*N*-((*S*)-1-(2-methoxyphenyl)ethyl)-2-phenylpropanamide

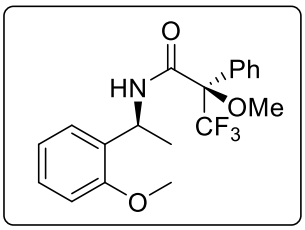

White solid (17 mg, 18%) ^{1}H NMR (400 MHz, $CDCl_3$) δ 7.54 (d, *J* = 8.9 Hz, 1H), 7.48 – 7.42 (m, 2H), 7.38 – 7.24 (m, 4H), 7.19 (dd, *J* = 7.5, 1.8 Hz, 1H), 6.93 (td, *J* = 7.5, 1.1 Hz, 1H), 6.87 (dd, *J* = 8.2, 1.0 Hz, 1H), 5.32 (m, 1H), 3.76 (s, 3H), 3.47 (m, 3H), 1.53 (d, *J* = 7.0 Hz, 3H). ^{13}C NMR (101 MHz, $CDCl_3$) δ 165.1, 157.1, 132.9, 130.1, 129.4, 128.7, 128.4, 128.2, 127.9, 125.4(q, *J* = 289.5 Hz), 111.1, 84.2 (q, *J* = 26.2 Hz), 55.2, 55.0, 47.5, 21.1. ^{19}F NMR (376 MHz, $CDCl_3$) δ -69.20. IR (ART cm^{-1}) 3419, 2948, 2842, 1687. MS (EI) m/z: calculated $C_{19}H_{21}F_3NO_3^+$ $[M+H]^+$ 368.1395; found 368.1380.

21. (*R*)-3,3,3-trifluoro-2-methoxy-*N*-((*S*)-1-(4-methoxyphenyl)propan-2-yl)-2- phenylpropanamide

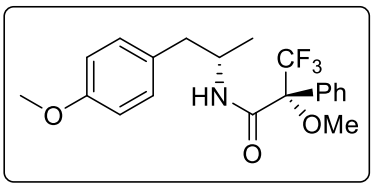

White solid (28 mg, 49%). ^{1}H NMR (400 MHz, $CDCl_3$) δ 7.39 – 7.25 (m, 5H), 7.03 – 6.96 (m, 2H), 6.80 – 6.76 (m, 2H), 6.60 (d, *J* = 8.8 Hz, 1H), 4.33 (m, 1H), 3.79 (s, 3H), 3.31 (m, 3H), 2.79 – 2.64 (m, 2H), 1.21 (d, *J* = 6.7 Hz, 3H) ppm. ^{13}C NMR (101 MHz, $CDCl_3$) δ 165.4, 158.3, 132.4, 130.3, 129.7, 129.3, 128.5, 127.7, 123.9 (q, *J* = 289.8 Hz), 113.8, 83.9 (q, *J* = 26.2 Hz), 55.2, 54.8, 46.3, 41.6, 20.4. ^{19}F NMR (376 MHz, $CDCl_3$) δ -69.00. IR (ART cm^{-1}) 3305, 3013, 2839, 1660. MS (EI) m/z: calculated $C_{20}H_{23}F_3NO_3^+$ $[M+H]^+$ 382.1652, found: 382.1639.

22. (*S*)-3,3,3-trifluoro-2-methoxy-*N*-((*S*)-1-(4-methoxyphenyl)propan-2-yl)-2- phenylpropanamide

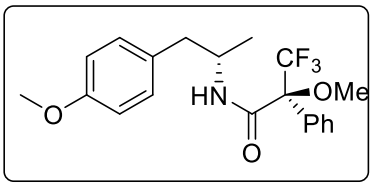

White solid (27.4 mg, 49%). ^{1}H NMR (400 MHz, $CDCl_3$) δ 7.53 – 7.48 (m, 2H), 7.42 – 7.35 (m, 3H), 7.14 – 7.09 (m, 2H), 6.87 – 6.81 (m, 2H), 6.55 (d, *J* = 8.3 Hz, 1H), 4.27 (m, 1H), 3.79 (s, 3H), 3.26 (m, 3H), 2.82 – 2.68 (m, 2H), 1.14 (d, *J* = 6.6 Hz, 3H). ^{13}C NMR (101 MHz, $CDCl_3$) δ 165.6, 158.5, 133.1, 130.4, 129.7, 129.5, 128.6, 127.7, 123.9 (q, *J* = 290.1 Hz), 114.0, 84.1 (q, *J* = 26.1 Hz), 55.4, 55.0, 46.7, 41.5, 19.9. ^{19}F NMR (376 MHz, $CDCl_3$) δ -68.71. IR (ART cm^{-1}) 3339, 3013, 2839, 1660. MS (EI) m/z: calculated $C_{20}H_{23}F_3NO_3^+$ $[M+H]^+$ 382.1552, found: 382.1536.

3. Development of a self-sufficient whole-cell biocatalyst for chiral amine synthesis

3.1 Introduction

The development of bacterial strains producing 'smart' amine donors has been reported.[154–159] *Corynebacterium glutamicum* is an organism currently used for the industrial production of L-lysine and other amino acids on multi-tonne scale.[160] In 2007, Yamada and co-workers developed a *C. glutamicum* strain (named: GRLys1) capable of producing 2.6 g L^{-1} cadaverine from L-lysine, by overexpressing lysine decarboxylase (*ldcC*) from *E. coli* (Figure 3.1a).[156] In 2012, Volker and co-workers engineered *C. glutamicum* ATCC13032 for the production of putrescine,[155] and in 2015, they improved their system through metabolic engineering.[1] The new strain (named NA6) harbors many mutations in the genome, such as deletion of *snaA* gene encoding a spermi(di)ne N-acetyltransferase, allowing the accumulation of the precursor L-ornithine, which is converted to putrescine (up to 58 mM) from a recombinant ornithine decarboxylase (*speC*) with a volumetric productivity of 0.21 g L^{-1} h^{-1} (Figure 3.1b).[154]

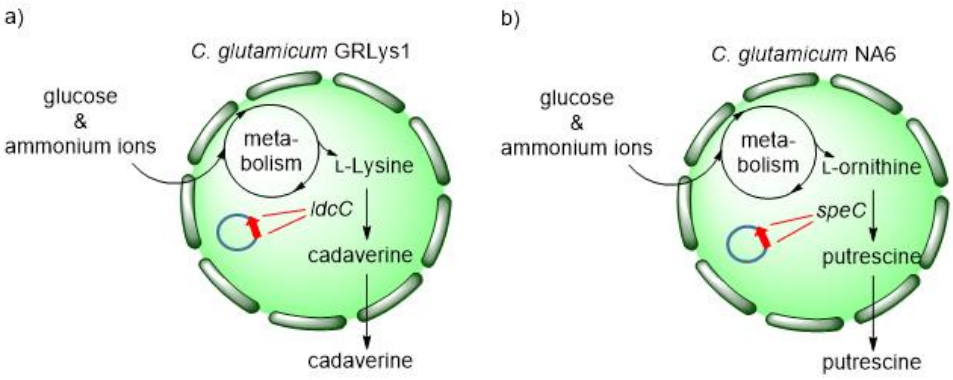

***Figure 3.1**. Production of a) cadaverine[156] and b) putrescine[154] from engineered C. glutamicum strains.*

Kim *et al*. 2013, utilized *C. glutamicum* strains for the heterologous expression of the branched chain aminotransferase (BCAT) IlvE from *E.*

coli.[161] This is an α-TA that has been previously described in the production of non-proteinogenic amino acids, 2-(3-hydroxy-1-adamantyl)-(2*S*)-amino-oxoethanoic acid (HAAE) and L-Tle, utilizing *E. coli* K12 as host cells (Scheme 3.1). This previous work required the external addition of L-glutamate (L-glu) donor and a coupled enzymatic system to tackle inhibition from the co-product leading to 90 mM and 37 mM of HAAE and L-Tle, respectively, when aspartate TA (AspTA) was co-expressed. [162]

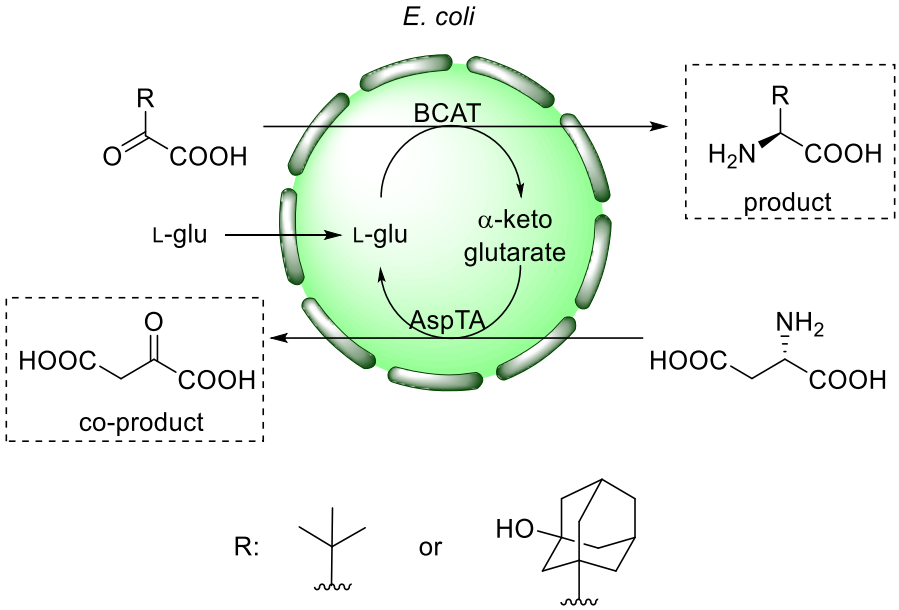

***Scheme 18**. Production of HAAE and L-Tle utilizing E. coli cells biocatalysts.*[162]

Kim *et al.* 2017, demonstrated an optimized whole cell system, by swapping to *C. glutamicum* ATCC13032 host cells, which naturally overproduces L-glutamate[163] and has high tolerance to organic molecules.[164–166] The new system, which only requires the heterologous expression of BCAT without a coupled enzymatic system or external additives (Scheme 19), afforded up to 40 mM and 35 mM of HAAE and L-Tle, respectively.[161]

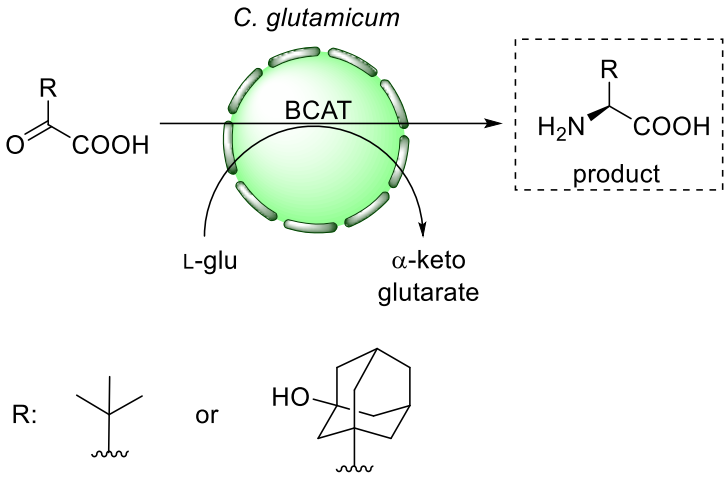

***Scheme 19**. Production of HAAE and L-Tle utilizing C. glutamicum cell biocatalysts.*[161]

This work showcased *C. glutamicum* as a superior host for whole cell biocatalysis and is the only example in the literature describing the overexpression of recombinant TA in such bacteria. However, α-TAs only accept α-amino and keto acid substrates, thus limiting the application of the system. Heterologous expression of ATAs in *C. glutamicum* would provide access to a broader range of high-value chemicals and enhance its application.

3.2 Aims and objectives

The aim of this chapter is to develop a whole cell biocatalyst capable of the *in situ* production of the target transaminase and of a suitable 'smart' amine donor, allowing the synthesis of high-value chiral products, starting from inexpensive starting materials. More specifically, this work aims to:

- Identify ATAs capable of accepting 'smart' amine donors
- Explore engineered strains producing 'smart' amine donors
- Investigate ATA expression in engineered strains
- Evaluate the efficiency of the whole cell system in converting ketone substrates

3.3 Identification of ATAs accepting the smart amine donors

A selection of ATAs, consisting of the (*R*)-selective ATAs from *Aspergillus oryzae* (AspOry),[114] *Aspergillus fumigatus* (AspFum),[167,168] *Mycobacterium vanbaalenii* (MycVan),[168] *Neosartoria fischeri* (NeoFis)[167,168] and the (*S*)-selective from *Chromobacterium violaceum* (ChrVio),[169–172] *Vibrio fluvialis* (VibFlu),[172–175] *Silicibacter pomeroyi* (referred by its Protein Data Bank code: 3HMU)[167,176] and *Rhodobacter sphaeroides KD131* (referred by its Protein Data Bank code: 3I5T),[167,176] was successfully expressed in *E. coli* BL21 (DE3) using isopropyl β-D-1-thiogalactopyranoside (IPTG) or rhamnose induced system, depending on the plasmid (see section 3.8.8.1). Individual cultures expressing one of the above ATAs were pelleted with centrifugation and the cells were sonicated to afford a clarified extract, which was analyzed *via* sodium dodecyl sulfate-polyacrylamide gel electrophoresis (SDS-PAGE) as described in section 3.8.10 (Figure 3.2a). Intense bands were observed at 50 kDa and 37 kDa, for the (*S*)- and (*R*)-selective, respectively, except for the AspOry ATA, where no intense band was detected. The activity of the clarified crude extracts was estimated utilizing the acetophenone assay (see section 3.8.11), where methylbenzylamine is used as amine donor and the formation of acetophenone is followed by the increase in absorbance at 245 nm (Figure 3.2b). [177] A more detailed explanation on how the activity is measured through the acetophenone assay is described in the Appendix A.2.1.

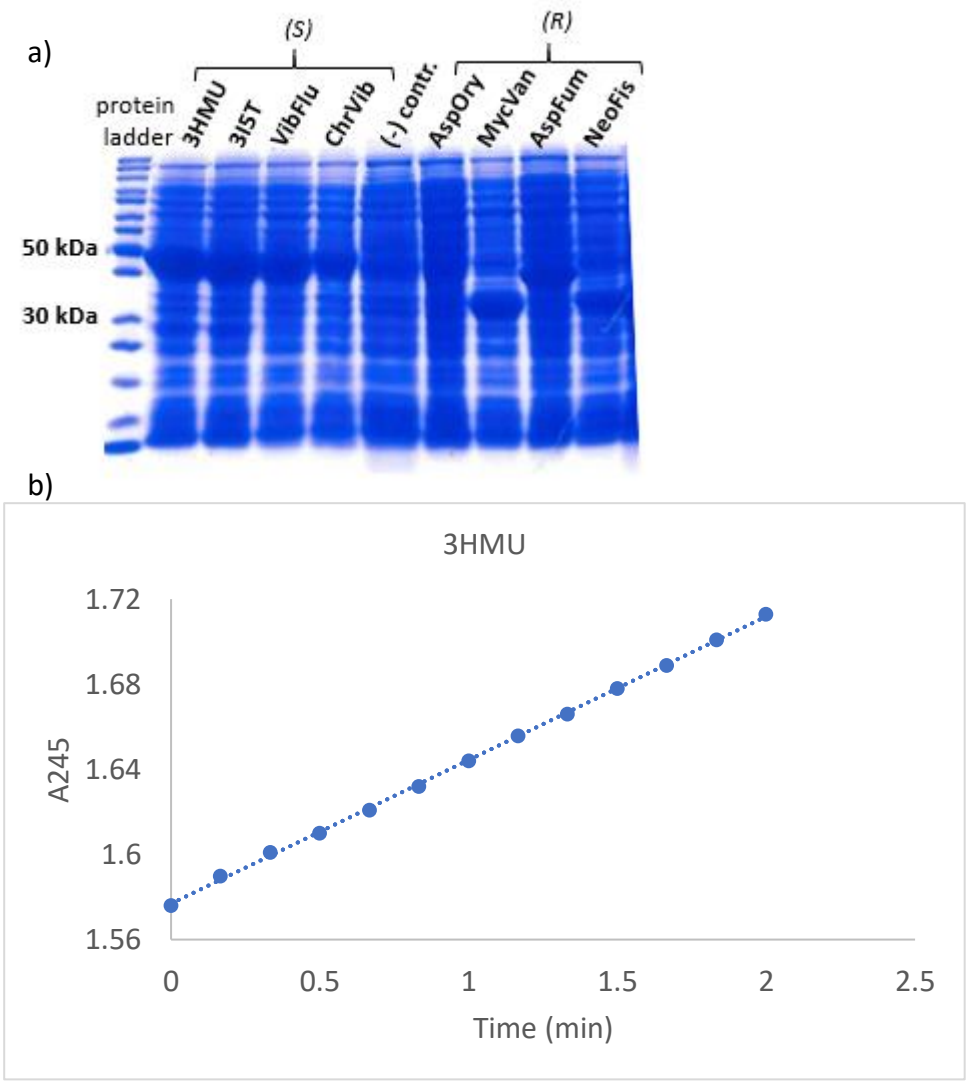

***Figure 3.2**. A sample a) SDS-PAGE of clarified crude extracts of ATAs from E. coli and b) graph of the acetophenone assay for 3HMU.*

ATAs (as clarified extracts) were screened against a panel of 'smart' amine donors (see section 3.8.13.1) utilizing 4-phenyl-2-butanone (**23**) as a model ketone substrate, in a ratio 1:1 (Figure 3.3), and the conversions were measured on GC-FID as previously described (see section 2.6.5). This ketone comprises a methyl substituent on one side of the carbonyl and an aliphatic chain with a bulky phenyl ring on the other side, and was expected to represent a suitable substrate for the active site of the ATA.[178] As shown in Figure 3.3, there was no detected ATA activity for any of the (*R*)-selective ATAs. AspOry was not tested, as it was found inactive. The majority of the

(*S*)-selective ATAs gave poor conversions. A moderate conversion of 20% was observed for 3HMU.

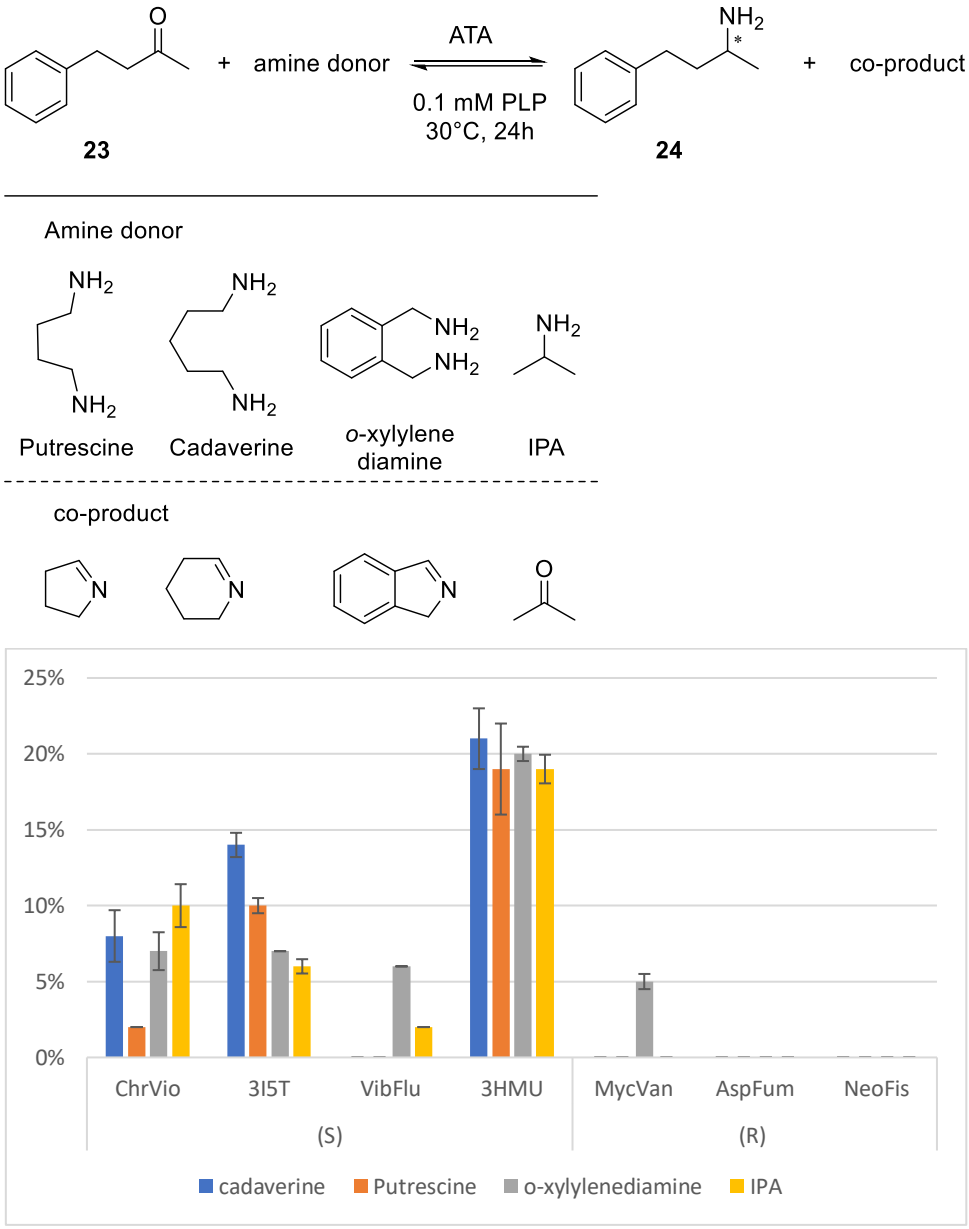

***Figure 3.3**. Reaction scheme and conversions (n=3, error bars show std) of **23** to its corresponding chiral amine utilizing clarified extract of (R)- or (S)-selective ATAs. Conversions are measured as previously described in section 2.6.5.*

3.3.1 Investigation of the carbonyl substrate of 3HMU

Following these findings, 3HMU was expressed in *E. coli* in 100-200 mL cultures (see section 3.8.8.1) and its clarified extract was collected for subsequent experiments. 3HMU was screened against different smart amine donors utilizing two more ketone substrates (see section 3.8.13.1). Acetophenone (**25**) is an interesting and challenging substrate, because the ATA reaction equilibria is displaced towards the ketone. Compound **25** is more thermodynamically stable than its corresponding amine, due to the conjugation of the carbonyl group with the aromatic ring. The less challenging substrate 1-phenyl-1,4-pentanedione (**27**) was also tested. This substrate is particularly interesting, because the amine formed upon transamination spontaneous cyclizes to afford an imine, thus driving the equilibrium forward. [179] As shown in Table 3.1, 3HMU performed well with **27**, achieving conversions of up to 75%, when cadaverine or o-xylylenediamine were used as co-substrates. On the other hand, there was no detectable conversion of **25**, regardless of the amine donor used. For comparison the widely used amine donors L-alanine and IPA were tested under the same conditions, without a coupled system for co-product removal. L-lysine was also tested as a potential 'smart' amine donor, which has not been previously explored, to the best of our knowledge. As shown in Table 3.1, L-lysine outperformed L-alanine, affording 18% conversion of **27**, which can be attributed to the cyclization of the co-product formed.[180,181] To the best of our knowledge, these results are the first evidences ever reported, showing L-lysine as a sacrificial amine donor for an ATA reaction. On the other hand, the industrial amine donor, IPA, outperformed both amino acids, achieving 70% conversion of **27** under the same reaction conditions. IPA gave comparable results to the 'smart' amine donors for all ketone substrates tested. These findings indicate that 3HMU can afford good conversions with low concentrations of IPA, showcasing the industrial relevance of this ATA.

***Table 3.1**. Reaction scheme and conversions (from triplicated, n=3, std <1%) of **23, 25** and **27** to their corresponding chiral amines utilizing clarified crude extract of 3HMU (2 mg mL^{-1}) and 1 equiv amine donor. Co-products are also shown. Conversions were measured as previously described in section 2.6.5.*

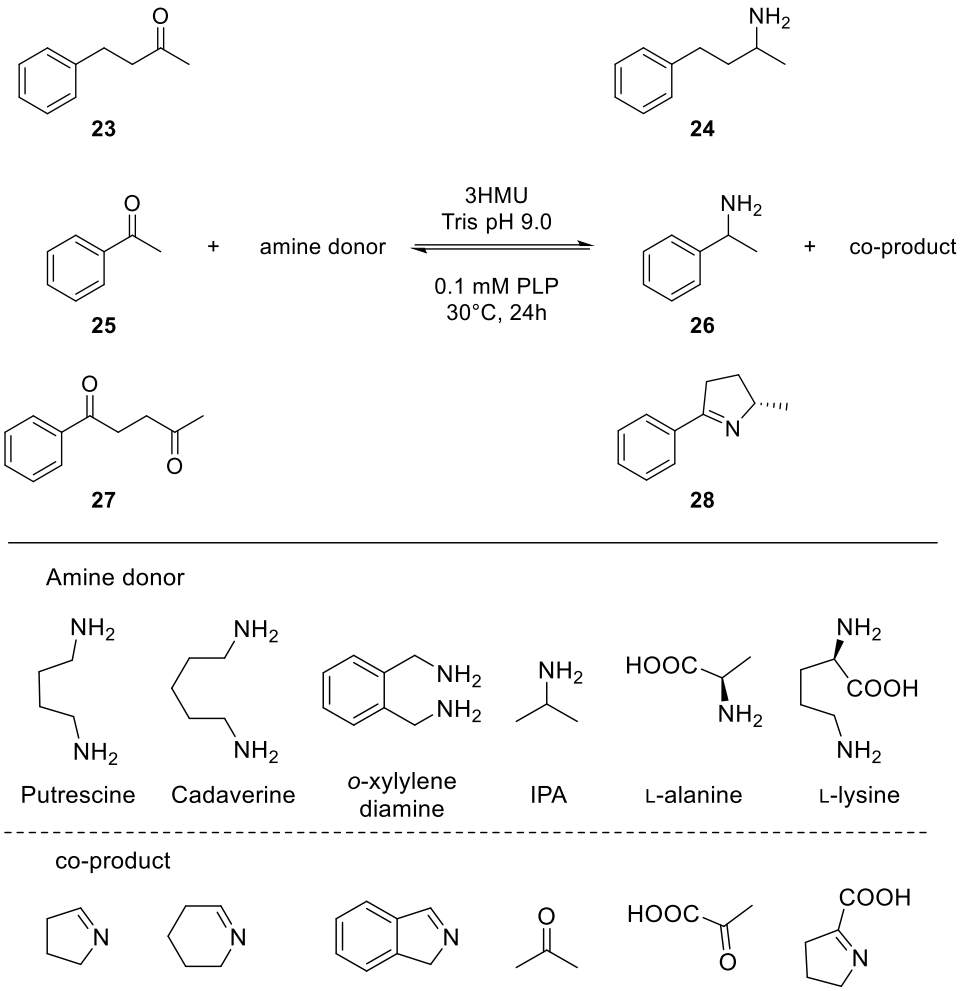

Ketone	Conversion					
	Putr.	Cadav.	*o*-xylylene-diamine	IPA	L-alanine	L-lysine
23	19%	21%	20%	19%	n.d.	n.d.
25	n.d.	n.d.	n.d.	n.d.	n.d.	n.d.
27	72%	75%	74%	71%	12%	18%

n.d.: not detected

3.3.2 Transamination with bacterial supply of 'smart' amine donor

Further investigation of the transamination of **27** with 3HMU was underway, utilizing conditioned medium from *C. glutamicum* strains engineered to over-produce putrescine[155] and cadaverine.[156] For this experiment, His-tagged 3HMU ATA was expressed in *E. coli* BL21 (see section 3.8.8.1) and purified *via* nickel affinity chromatography on Akta (see section 3.8.9). Fragments were collected and concentrated *via* centrifugation, and the purity was examined on SDS-PAGE as shown in figure 3.4 (and described in section 3.8.10).

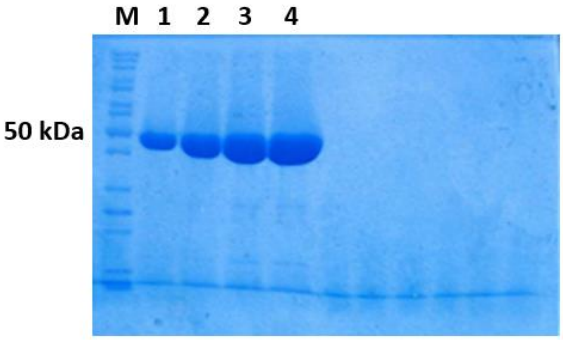

M: PageRuler protein ladder
1: 2 µL purified extract of 3HMU
2: 4 µL purified extract of 3HMU
3: 6 µL purified extract of 3HMU
4: 8 µL purified extract of 3HMU

Figure 3.4*. SDS-PAGE analysis of different dilution of purified extract of 3HMU.* ***M****: molecular marker,* ***1-4****: 2, 4, 6 or 8 µL of purified extract of 3HMU, respectively.*

A fraction of the purified extract was then used for the biotransformation of ketone **27** in conditioned medium from *the C. glutamicum* cultures (see section 3.8.13.2). As shown in Table 3.2, complete conversion was observed, when two-day (2d) mature culture of the cadaverine-producing strain GRLys1 was used, which is double compared to a one-day (1d) mature culture of the same strain. On the other hand, the conversions remained at 80% for both one-day and two-day mature culture of the putrescine producing strain NA6. Significant conversion (14%) was observed with the wild type (WT) *C. glutamicum* ATCC 13032, which can be attributed to the accumulation of L-lysine that naturally occurs in this

organism.[160] Previous results have already shown that 3HMU accepts L-lysine to a certain extent, thus providing a likely explanation for these results. These findings indicate that sufficient 'smart' amine donor is produced from the engineered strains and demonstrate that *C. glutamicum* NA6 and GRLys1 strains can be exploited as hosts for the development of a self-sufficient whole cell system mediating ATA reaction.

***Table 3.2**. Conversion (n=3, std <1%) of **27** to its corresponding chiral amine, utilizing purified extract of 3HMU (1 mg/mL) in conditioned culture medium (WT, NA6 or GRLys1). Conversions were measured as previously described in section 2.6.5.*

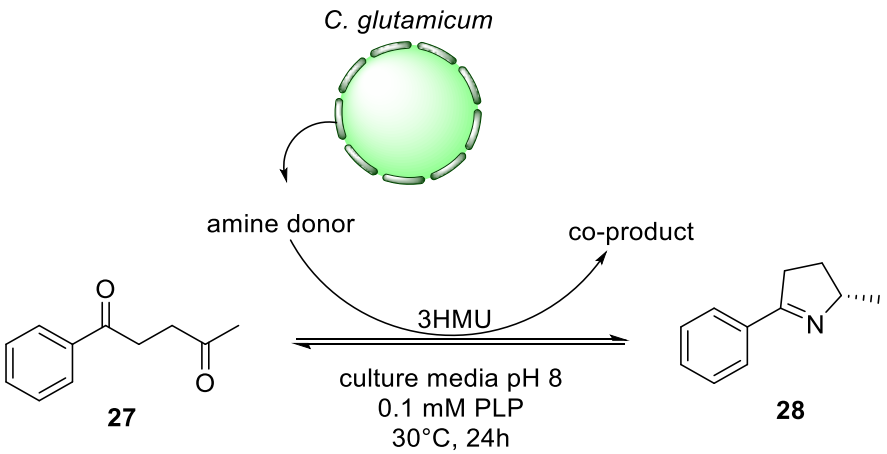

C. glutamicum culture	Conversion using medium from culture after incubating for	
	1d	2d
Wild type	15%	15%
NA6	81%	83%
GRLys	55%	98%

3.4 Expression of 3HMU in *C. glutamicum* strains

The *C. glutamicum* strains already harbour a vector and thus the compatible shuttle vector, pEKEx3,[182,183] was chosen for ATA expression. The 3HMU insert was amplified from its plasmid utilizing the SG1_F and SG2_R primer pair *via* PCR and successfully cloned into the shuttle vector, pEKEx3,[182,183]

which was transformed in *E. coli* DH5a (see section 3.8.4.1). Restriction analysis with SalI and EcoRI of the newly formed plasmid (pEKEx3-3HMU) confirmed the presence of the 3HMU insert (Figure 3.5).

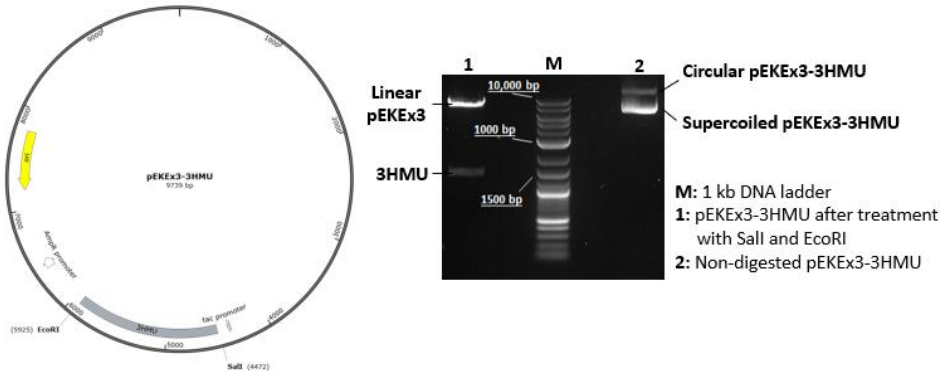

Figure 3.5*. Map of the plasmid pEKEx3-3HMU (on the left) and restriction analysis on agarose gel (1%) (on the right).* ***1)*** *pEKEx3-3HMU (isolated from E. coli DH5a), after digestion with SalI and EcorI and* ***2)*** *before digestion,* ***M****: 1 kb DNA ladder.*

The plasmid was isolated from *E. coli* DH5a (30 uL of 500-700 ng/uL) and transformed in *C. glutamicum* strains (see section 3.8.4.2). Four colonies were picked after the transformation and their plasmids were isolated and treated with SalI and EcoRI (see section 3.8.6). As shown in Figure 3.6, a band at 1.5 kb is present in all lanes, corresponding to the 3HMU gene. Lanes **1** and **2**, gave more bands, which could be attributed to potential star activity of EcoRI with prolonged incubation times. The colony from lane **4** was selected for future experiments, as it clearly contains the plasmid with 3HMU with no extra bands shown on the agarose gel.

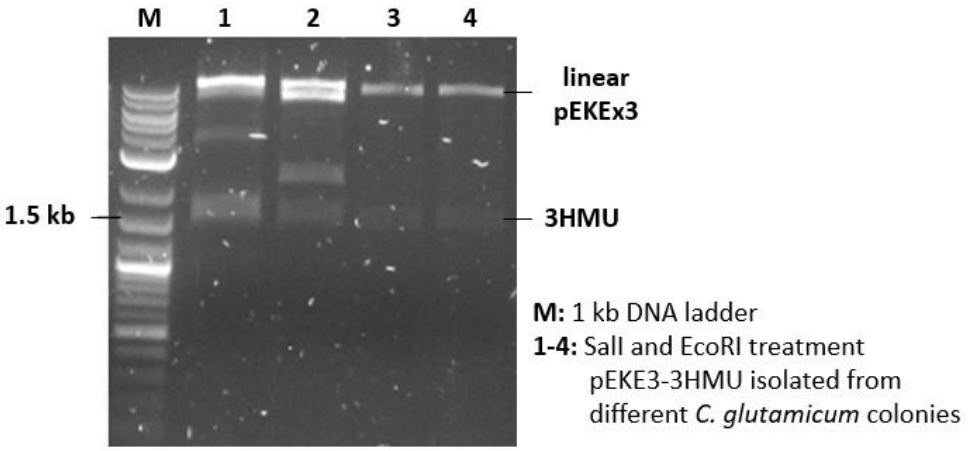

***Figure 3.6**. Agarose gel (1%) of **1-4:** the isolated plasmid pEKEx3-3HMU from different C. glutamicum NA6 colonies after restriction digestion with SalI and EcoRI. **M**: 1 kb DNA ladder.*

Preliminary tests on the cell-free crude extract of the newly transformed *C. glutamicum* strains did not exhibit ATA activity. In those experiments, concentration of 1 mM IPTG was selected, which is widely used in whole cell biocatalysis with *C. glutamicum* strains. For comparison, a higher concentration (2 mM) and dilutions (0.5 and 0.1 mM) were tested. Unfortunately, expression of 3HMU in the engineered strains was not detectable with neither SDS-PAGE (Figure 3.7a) nor the acetophenone assay (Figure 3.7b) in any of the experiments. The same results were observed for a range of different conditions, including temperatures, media and induction time-lengths.

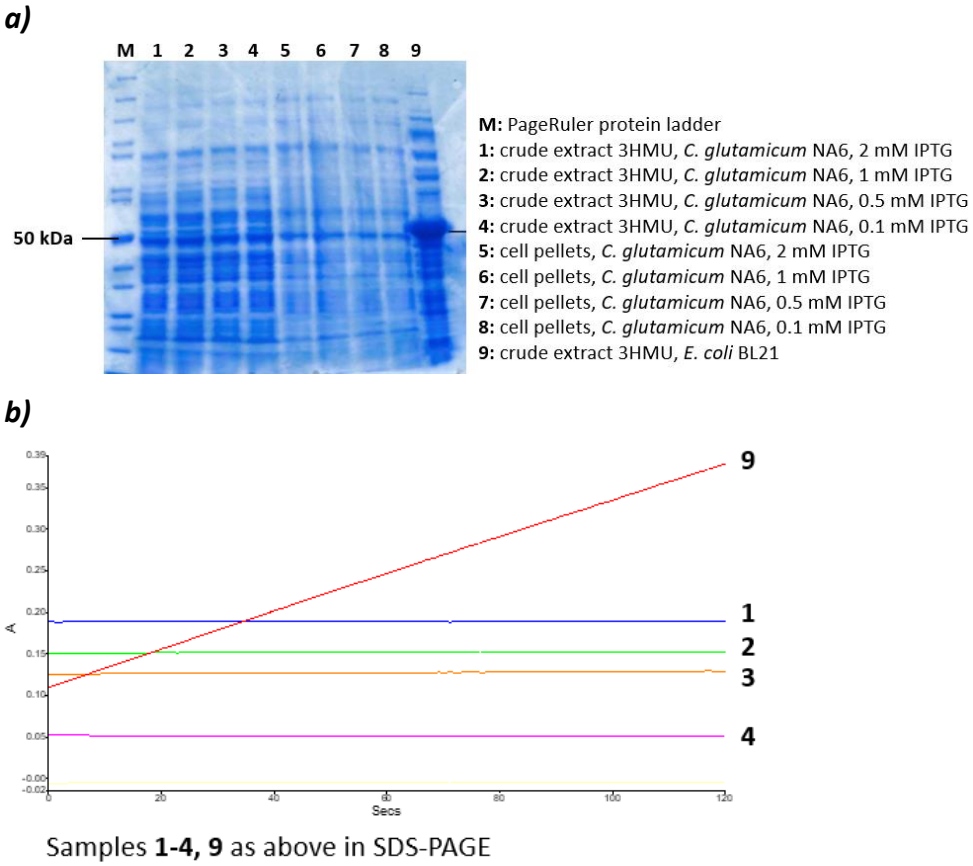

***Figure 3.7**. An **a**) SDS-PAGE of **M:** protein ladder, **1-4:** crude extract of 3HMU expressed in C. glutamicum NA6 utilising 2, 1, 0.5 or 0.1 mM IPTG, respectively, **5-8:** the equivalent cell pellets and **9:** crude extract of 3HMU expressed in E. coli BL21. **b)** a graph of the acetophenone assay of the extracts **1-4, 9** described above. Note that **9** is included as a positive control.*

3.4.1 Investigation of expression system

In the above system, the ribosomal binding site (RBS) in the pEKEx3 vector was introduced for the expression of 3HMU in *C. glutamicum* strains. Due to the lack of observed expression, the expression system itself was tested using a reporter gene; the wild type green fluorescence protein (GFP) from the jellyfish *Aequorea victoria*.[184–186] A vector containing the GFP insert was provided from Dr. Phil Hill. The GFP insert was successfully amplified *via* PCR using the SG3_F and SG4_R primers, cloned into the shuttle vector pEKEx3 and transformed in *E. coli* DH5a. The newly formed plasmid (pEKEx3-GFP) was isolated and the sequence of GFP was verified from

Eurofins sequencing services. The plasmid was isolated from *E. coli* DH5a (30 uL of 500-700 ng/uL) and transformed in *C. glutamicum* NA6 for testing (see section 3.8.4.2). The fluorescence intensity of the clarified extract of the new strain was measured using a TECAN Infinite M1000 Pro. As shown in Figure 3.8, the clarified extract of GFP expressed overnight from *C. glutamicum* (grey line) behaved similar to the positive control (yellow line), with an excitation (Figure 3.8a) and emission (Figure 3.8b) maximum of 510 and 395 nm, respectively, which match those reported in the literature.[184–186]

a)

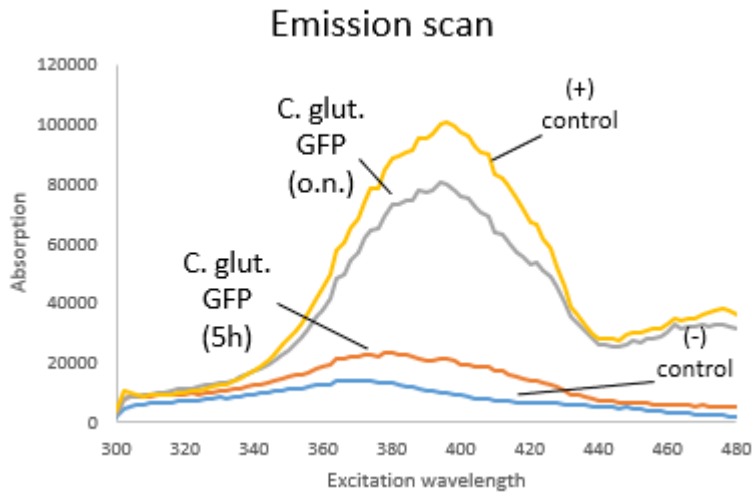

b)

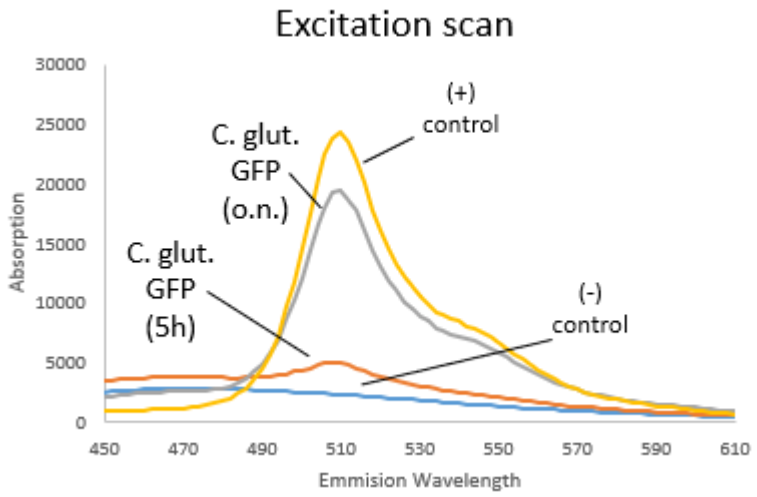

***Figure 3.8**. The **a**) emission and **b**) excitation scan of GFP in the clarified crude extracts of recombinant C. glutamicum strains (**grey line** for overnight*

expression, ***red line*** *for 5-hours expression), E. coli DH5a (****yellow line****) and wild type (non-recombinant) C. glutamicum (****blue line****), are compared.*

These results indicate that the RBS used is not at fault and thus further investigation is required.

3.4.2 Investigation of toxicity and rare codons

Potential toxicity associated with 3HMU activity could hamper expression or lead to inactive mutants. In order to further investigate this theory, an inactive mutant of the 3HMU was developed by changing the catalytic lysine residue (K292) to alanine using the internal primers SG5_F and SG6_R and the external SG1_F and SG2_R. The newly formed plasmid containing the 3HMU mutant (pEKEx3-3HMU_K292A) was isolated from *E. coli* DH5a and the mutation was verified *via* sequencing service from Eurofins. The plasmid was then transformed in *E. coli* BL21 and the mutated 3HMU was successfully expressed and was found inactive. The 3HMU_K292A was subsequently transformed and expressed in *C. glutamicum* strains. Different concentration of IPTG were tested on *C. glutamicum* NA6 with pEKEx3-3HMU_K292A. As shown in Figure 3.9, SDS-PAGE and mass spectrometry MALDI-TOF analysis showed that the inactive mutant was not expressed, thus indicating potential complications with the transcription of the gene.

a)

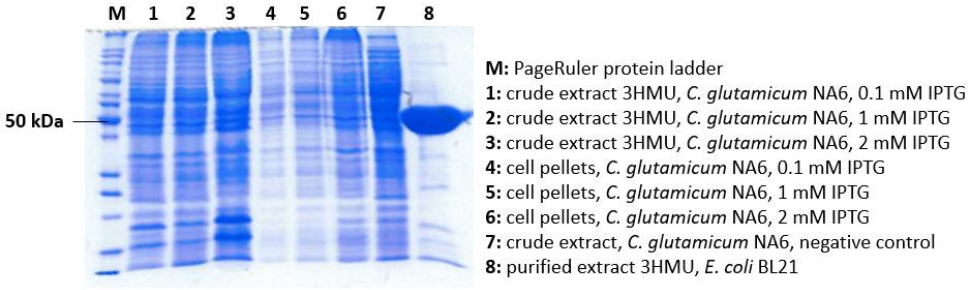

b)

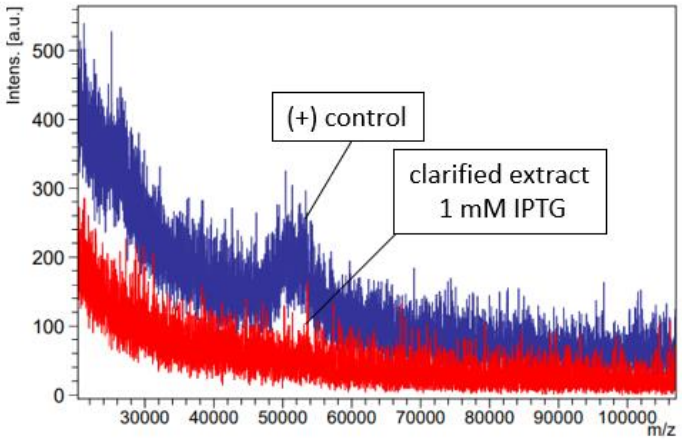

***Figure 3.9**. An **a**) SDS-PAGE of **M:** protein ladder, **1-3:** crude extract of 3HMU expressed in C. glutamicum NA6 utilising 0.1, 1, or 2 mM IPTG, respectively, **4-6:** the equivalent cell pellets, **7:** crude extract from C. glutamicum NA6 (negative control) and **8:** purified extract of 3HMU expressed in E. coli BL21, and **b**) mass spectrometry MALDI-TOF analysis of the crude extract of 3HMU expressed in C. glutamicum NA6 with 1 mM IPTG, shown in red*. A positive control is included in blue.

To investigate potential complications at the transcription level, codon optimisation of the 3HMU sequence was carried out for expression in *C. glutamicum*. The investigation of rare codons in the sequence was performed utilizing an open access platform[187] and importing the codon usage table of *C. glutamicum* ATCC 13032.[188] There was no rare codon in the sequence of 3HMU, indicating that some other factors were interfering with the expression. At this point, the investigation for expression failure of 3HMU was stopped, and alternative ATA candidates were explored.

3.5 Identification of a putrescine ATA from *Halomonas elongata*

Paradisi and co-workers reported a wild type putrescine ATA from *Halomonas elongata* (HEWT)[189] capable of converting benzaldehyde to benzylamine in the presence of *o*-xylylenediamine (Scheme 20).[189] These promising results prompted a further investigation of HEWT.

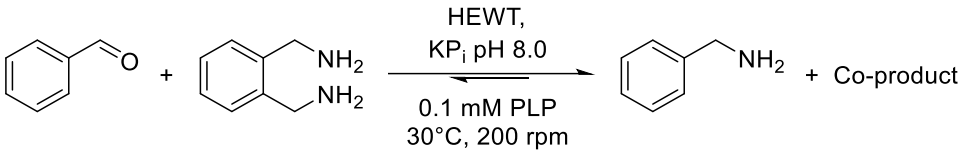

***Scheme 20**. Transamination of benzaldehyde from HEWT.*[189]

3.5.1 Substrate scope of HEWT

The plasmid containing the HEWT insert was kindly offered from prof. Fransesca Paradisi. It was transformed in *E. coli* DH5a, and a stock was made to reserve the plasmid, as well as in *E. coli* BL21, for subsequent *in vitro* biotransformations. HEWT was expressed in *E. coli* BL21 (see section 3.8.8.1) and the clarified extract was used to screen a panel of carbonyl-containing substrates and the 'smart' amine donors, putrescine and cadaverine (see section 3.8.13.1). Biotransformations were analysed *via* GC-FID and the conversion are reported in Table 3.3. Cerioli *et al*. 2015, had previously screened against hydrophilic ketones[189] and thus cyclic and aromatic hydrophobic ketones, as well as benzaldehyde were tested in this study. As shown in Table 3.3, HEWT performed poorly with the majority of the ketone substrates. A moderate conversion of 40% was observed with tetrahydro-4*H*-thiopyran-4-one (**37)** when cadaverine was used as the donor, but two new peaks appeared, potentially corresponding to the different enantiomers at 1:4 ration. On the other hand, benzaldehyde (**34)** was an excellent substrate with conversions between 77% and 90% achieved.

***Table 3.3**. Conversion (n=3, std <1%) of various carbonyl substrates utilizing putrescine or cadaverine and clarified extract of HEWT (2 mg mL^{-1}). Conversions were measured as previously described in section 2.6.5.*

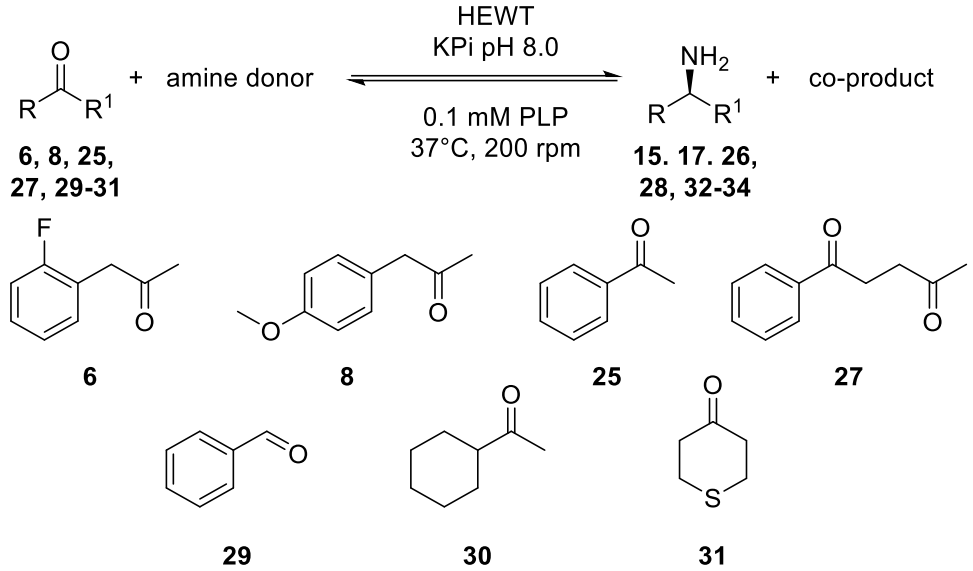

Carbonyl substrate	conversion	
	Cadaverine	Putrescine
6	8%	0%
8	8%	4%
25	6%	3%
27	4%	2%
29	92%	76%
30	n.d.	n.d.
31	n.d.	n.d.

3.5.2 Expression of HEWT in *C. glutamicum* strains

HEWT insert was amplified from its plasmid utilizing the SG7_F and SG8_R primer pair *via* PCR and successfully cloned into the shuttle vector, pEKEx3, which was transformed in *E. coli* DH5a. Restriction analysis with BamHI of the newly formed plasmid (pEKEx3HEWT) confirmed the presence of the HEWT insert (Figure 3.10).

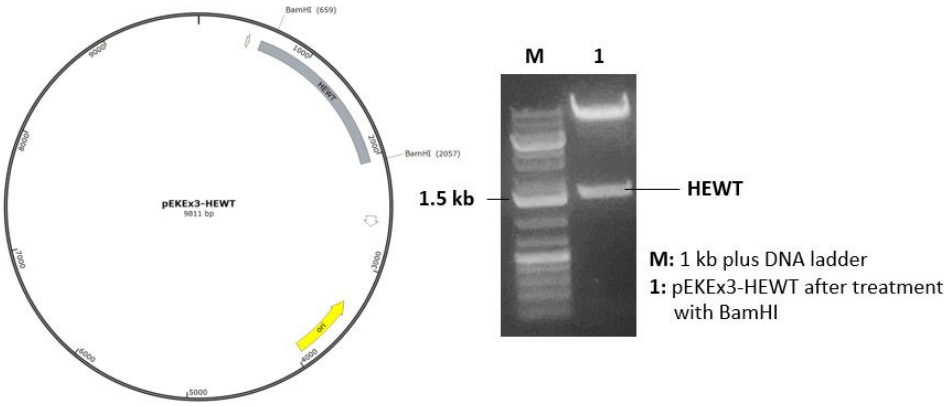

Figure 3.10. *Agarose gel (1%) of* ***1****: the isolated plasmid pEKEx3-HEWT from E. coli DH5a after restriction digest with BamHI.* ***M****: 1kb plus DNA ladder.*

The plasmid was isolated from *E. coli* DH5a (30 uL of 500-700 ng/uL) and transformed in *C. glutamicum* strains (see section 3.8.4.2). As shown in Figure 3.11, digestion of the plasmid with BamHI afforded a band at 1.5 kb, corresponding to the HEWT gene.

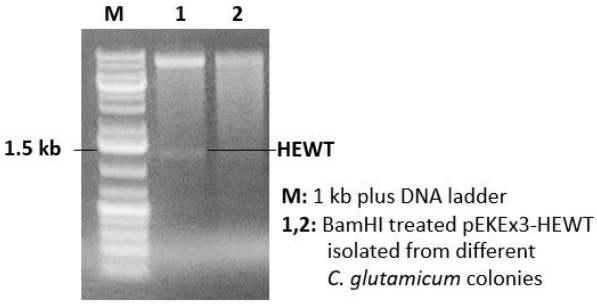

Figure 3.11. *Agarose gel (1%) of* ***1-2****: the isolated plasmid pEKEx3-HEWT from different C. glutamicum colonies after restriction digest with BamHI.* ***M****: 1 kb plus DNA ladder.*

The transamination of benzaldehyde was tested using whole cells of the newly developed strains (see section 3.8.13.3) and conversions were measured with GC-FID (method described in section 2.6.4). As shown in Table 3.4, side reaction(s) lead to complete consumption of benzaldehyde and production of benzylalcohol. The production of benzylalcohol can be attributed to endogenous alcohol dehydrogenases (ADHs).[190–194] Also,

endogenous aldehyde dehydrogenases (AldDHs)[195,196] can oxidise benzaldehyde to benzoic acid, which cannot easily be extracted and detected on GC-FID, thus not reported. Also, the ATA reaction rate is significantly lower inside the cell (neutral conditions), since HEWT maintain only 20% of its relative activity at pH 7.0.[189] The alcohol and/or aldehyde dehydrogenases are possibly more reactive at those conditions, thus explaining the depletion of benzaldehyde and the production of benzylalcohol.

***Table 3.4**. Conversion (n=3, std <1%) of **29** after 24h and 48h, using C. glutamicum whole cell overexpressing HEWT. Note that possible formation of co-product **36** cannot be measured by analysis methods used herein. Conversions were measured as previously described in section 2.6.5.*

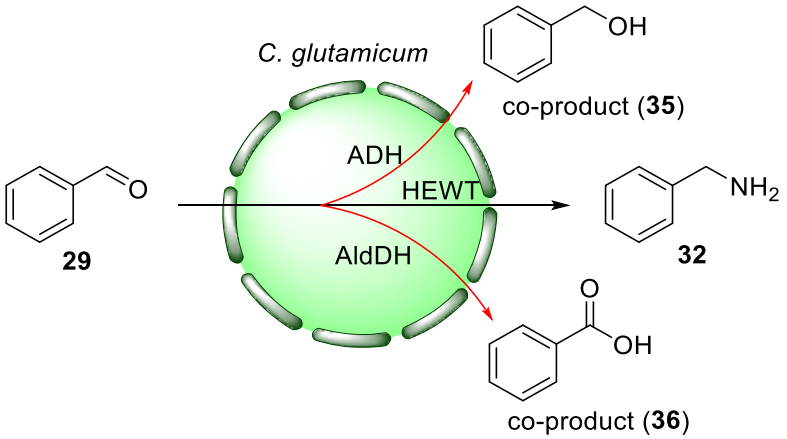

C. glutamicum strain	Conversion (24h)		Conversion (48h)	
	32	**35**	**32**	**35**
Wild Type	n.d.	99%	n.d.	99%
NA6	n.d.	99%	n.d.	99%
GRLys1	n.d.	99%	n.d.	99%

n.d.: not detected

Flitsch and co-workers 2017, encountered similar problems with the ATA step of a whole cell bio-cascade.[197] The group followed an approach that mimics nature[198,199] and managed to overcome this difficulty by incorporating a second copy of the ATA gene in the plasmid.[197] Inspired by

their work, a solution was sought by increasing the amount of HEWT produced in a similar way. Two different approaches were tested; i) the expression of a double insert under the same promoter (HEWTx2) and ii) the use of separate promoters for the expression of the two inserts (pHEWTtx2). The primer pairs SG9-SG12 (for (i)) and SG13-SG16 (for (ii)) were used, and the constructs were synthesized with HiFi DNA assembly, following NEB's protocol. The two constructs were successfully cloned in pEKEx3 vector and verified *via* restriction analysis. As shown in Figure 3.12, the vectors were digested with BamHI, which cuts at the beginning of HEWT sequence. The band observed at 1.5 kb corresponds to the HEWT gene. An additional BamHI restriction site was introduced right after the HEWT gene, during the cloning of pHEWTtx2. The band around 600 bp observed for the pHEWTtx2 (Figure 3.12b), corresponds to the terminator of insert 1 and promoter of insert 2, indicating the introduction of a second promoter.

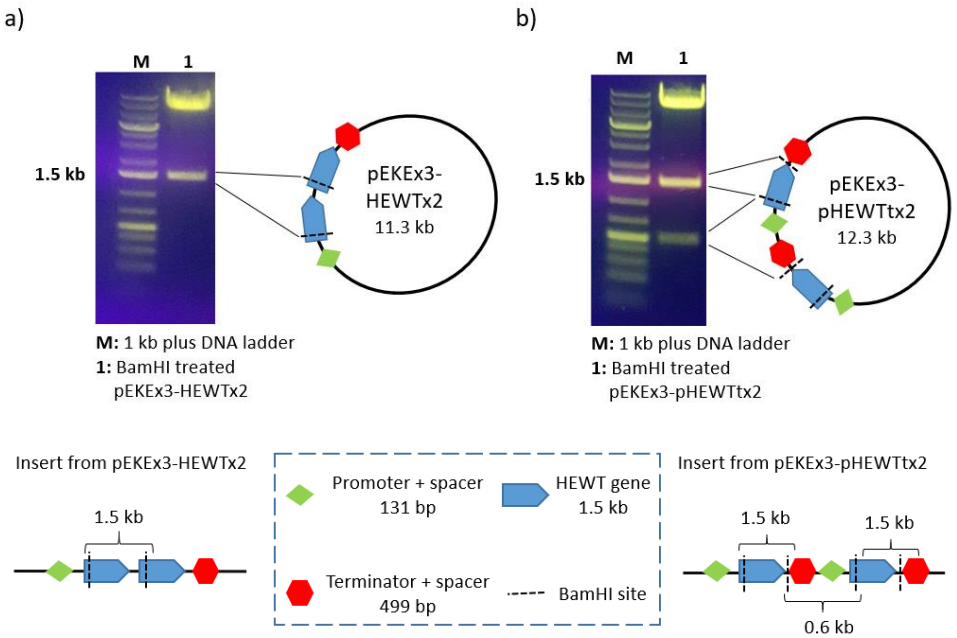

***Figure 3.12**. Agarose gel (1%) of **a**) pEKEx3-HEWTx2 (**1**) and **b**) pEKEx3-pHEWTtx2 (**1**), isolated from E. coli DH5a, after restriction digest with BamHI. **M**: 1kb plus DNA ladder.*

Different induction time-lengths were tested utilising the new strains. An SDS-PAGE analysis (shown in Figure 3.13a), verified the production of HEWT (see squared section), when comparing the samples (lanes **1**,**3**,**6**,**8**) to a negative (lane **5**, **10**) and a positive (lane **11**) control. Also, there is nothing present in the pellets (lanes **2**, **4**, **7**, **9**), indicating that all protein is in the soluble fraction. The activity of the clarified crude extracts can be accurately measured *via* the acetophenone assay (see section 3.8.11 and Appendix A.2.1),[177] and therefore was used as means to estimate the amount of enzyme produced. A detailed explanation on how to estimate the amount of HEWT is described in Appendix A.2.2. The results (Figure 3.13) show up to four-fold increase for the wild type and NA6 strains, which is significantly higher than the 50% increase observed for the GRLys1. This was verified with statistical analysis presented in Appendix A.2.3 (null hypothesis 3). In all strains, the use of separate promoters for the expression of the two inserts (approach ii) lead to maximum HEWT production.

a) SDS-PAGE

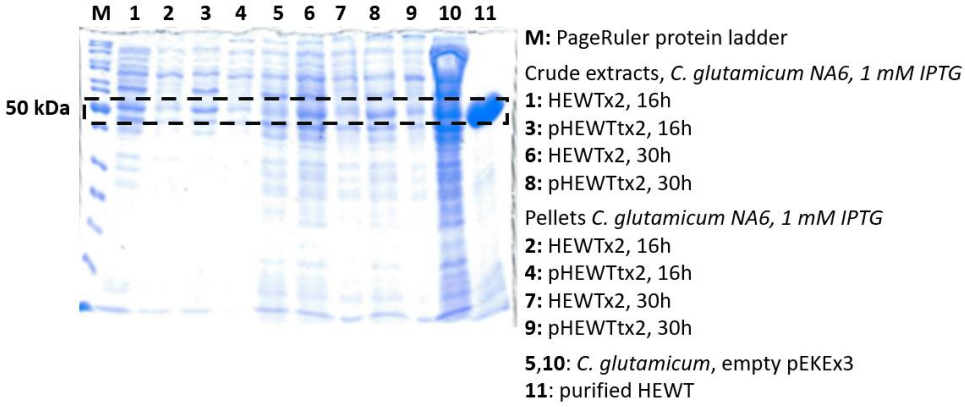

b)

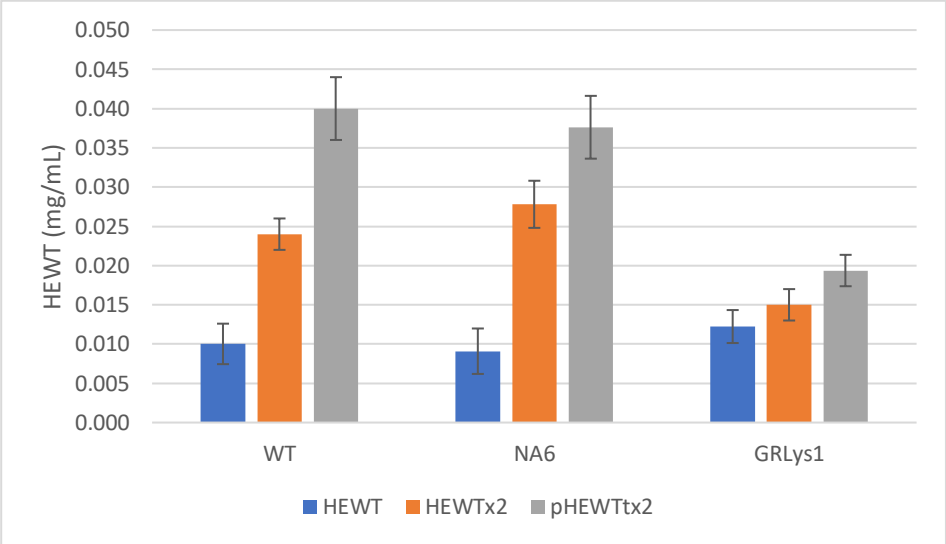

***Figure 3.13**. **a**) Comparison of the expression levels in different IPTG concentration on SDS-PAGE. **M**: PageRuler protein ladder, crude extracts of C. glutamicum NA6 expressing HEWTx2; **1**: 0.1 mM IPTG, 16h, **3**: 5 mM IPTG, 16h, **6**: 0.1 mM IPTG, 30h, **8**: 5 mM IPTG, 30h. The equivalent pellets; **2**: 0.1 mM IPTG, 16h, **4**: 5 mM IPTG, 16h, **7**: 0.1 mM IPTG, 30h, **9**: 5 mM IPTG, 30h; crude extract of C. glutamicum carrying the empty vector pEKEx3 **5**: 1 mM, 16h, **10**: 1 mM, 30h; and the positive control **11**: purified extract HEWT. **b**) Comparison of the estimated amount of HEWT (mg) in 1 mL clarified extract produced from the different strains (n=3, error bars show std). Only the results of the best conditions (1 mM IPTG, 16h) are shown in the latter (for results from all conditions see table A.2.4.2).*

The strains containing separate promoters for the expression of two HEWT genes, were employed for the biotransformation of benzylaldehyde.

Despite the increased production of HEWT, benzylalcohol remained the main product of this biotransformation. Only the NA6 strain showed a minor improvement, reaching 5% conversion to benzylamine **32** (Table 3.5).

***Table 3.5**. Conversion (n=3, std <1%) of **29** utilizing whole cell of C. glutamicum overexpressing HEWT with pHEWTtx2. Conversions were measured as previously described in section 2.6.5.*

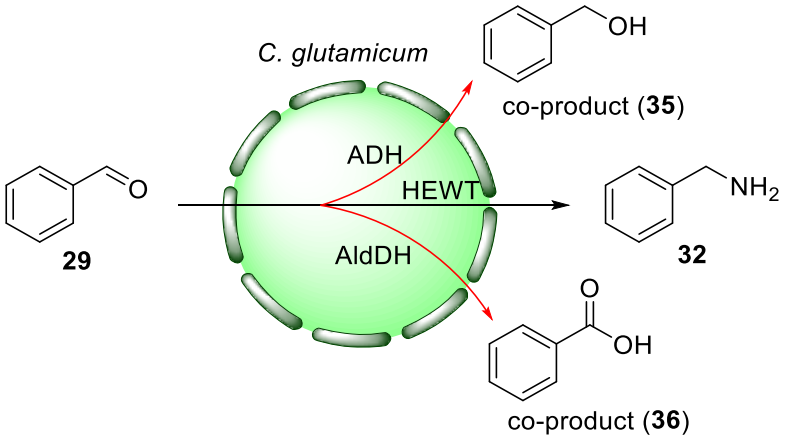

C. glutamicum strain	Conversion (24h)		Conversion (48h)	
	32	**35**	**32**	**35**
Wild type pHEWTtx2	n.d.	99%	n.d.	99%
NA6 pHEWTtx2	5%	95%	5%	95%
GRLys1 pHEWTtx2	n.d.	99%	n.d.	99%

n.d.: not detected

These results indicate that the side reactions still occur more readily than transamination. Metabolic engineering offers an attractive solution, where the endogenous production of ADHs and AldDHs can be regulated. Knocking-out the ADH and AldDH genes or switching to weaker promoters for reduced expression, could lead to increased production of benzylamine. However, tampering with the metabolic pathway could lead to complications and thus was avoided. In the interest of progress some positive preliminary results from other putrescine ATAs were followed instead.

3.6 Investigation of three additional putrescine ATAs

Galman *et al*. 2017, identified three novel ATAs from *Pseudomonas* species *P. chlororaphis subsp. Aureofaceins* (PcATA), *P. fluorescens* (PfATA) and *P. putida* (PpATA) through a Basic Local Alignment Search Tool (BLAST) analysis of the characterised *spuC* gene from *P. aeruginosa*. [200,201] Characterization of these amines revealed high specific activity towards diamines, with up to 27.3 U mg^{-1} for cadaverine with the PpATA,[201] where one unit of activity was defined as the amount of enzyme that produced 1 µmol of product per min at 30˚C. Turner and co-workers kindly offered these ATAs to test.

3.6.1 Elucidation of substrate scope

Galman *et al*. 2017, have previously reported the successful transamination of a range of ketone substrates, utilizing 2 mg mL^{-1} purified putrescine ATAs.[201] Based on previous observations (section 3.5.2), *C. glutamicum* strains (from this study) will not be able to produce such high concentrations of enzyme. Thus, the putrescine ATAs were screened with a panel of ketone substrates, utilizing 1.5 mg mL^{-1} of clarified crude extract (see section 3.8.13.1). The panel included substrates **23, 25** and **27** were selected for reasons mentioned in section 3.3.1. Galman *et al*. 2017 reported good to excellent conversions of substrates **37**-**40** with pc, pf or ppATA in the presence of 'smart' amine donors, thus were included in the panel. Diketones **41** and **42** were kindly offered from my colleague Freya Taday, who wished to investigate their potential for a transaminase reaction. Conversions of the above ketones were measured *via* GC-FID (described in previous section 2.6.5). As shown in Figure 3.14, there was no detected conversion for substrates **25**, **37** and **42**. A conversion of up to 25% was observed for substrate **23** with PfATA and cadaverine, which was the highest among the mono-carbonyl substrates. Compound **41** was similar trend to **23**, seeing a maximum conversion of 29% under the same reaction conditions, however more peaks were formed possibly due to side-

reactions. Substrate **27** outperformed all compounds in all reaction conditions, reaching above 50% conversion (results in square). The rest of the substrates (**38**-**40**) afforded poor conversions (<40%).

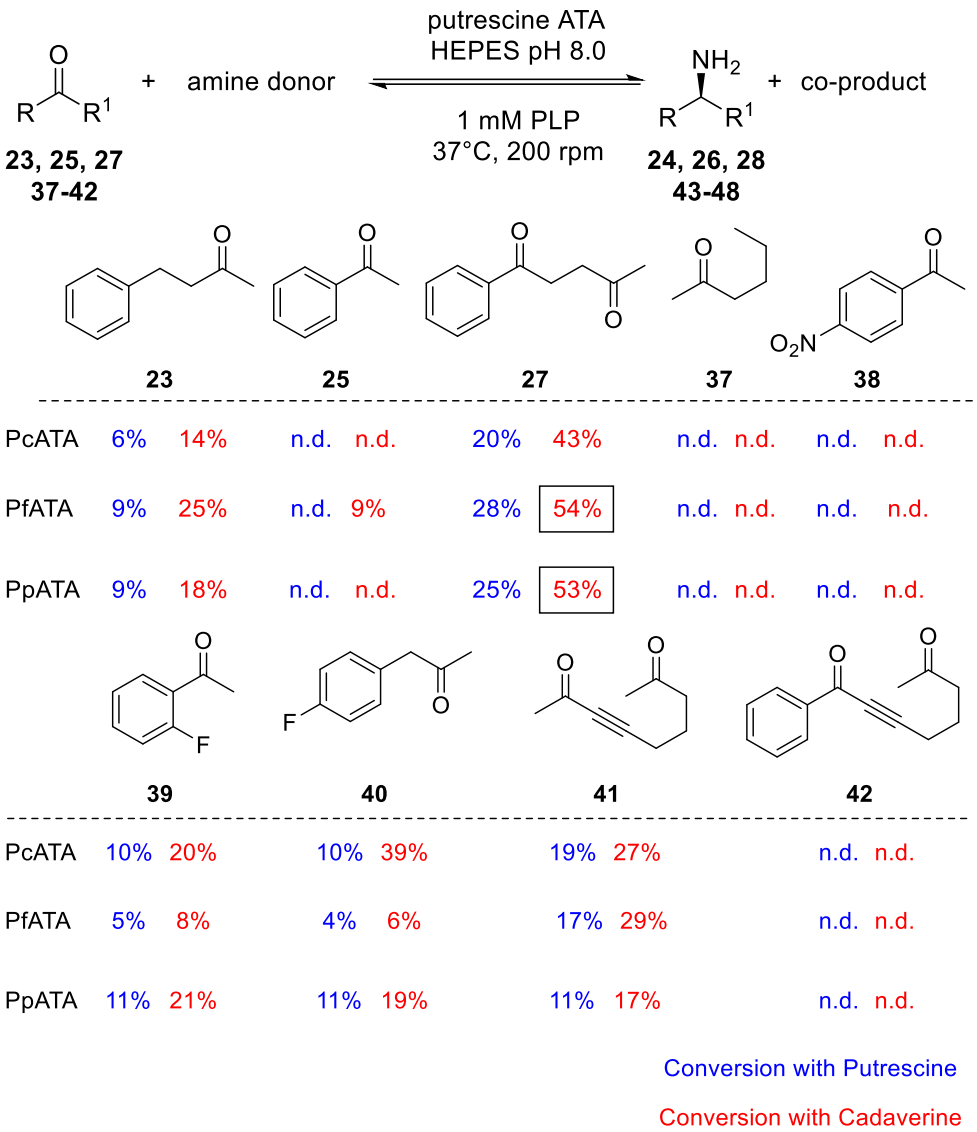

***Figure 3.14**. Conversion (n=3, std <5%) of the transamination of a range of ketones utilizing 1.5 mg mL^{-1} clarified crude extract of putrescine ATAs and 'smart' amine donor (1 equiv.). Some of the highest conversions are indicated in black boxes. Conversions were measured as previously described in section 2.6.5.*

The best substrate (**27**) was selected for further experiments using three equivalents of putrescine or cadaverine (Figure 3.15). Conversion values

doubled for PcATA, when 3 eq. of 'smart' amine donors were used, reaching as high as 75%. A similar trend was observed for PpATA with putrescine, affording up to 50% conversion, but not with cadaverine, where values slightly increased to 65%. Negligible differences in conversion observed for PfATA, stagnating at 30% and 60% with 3 eq. of putrescine or cadaverine, respectively.

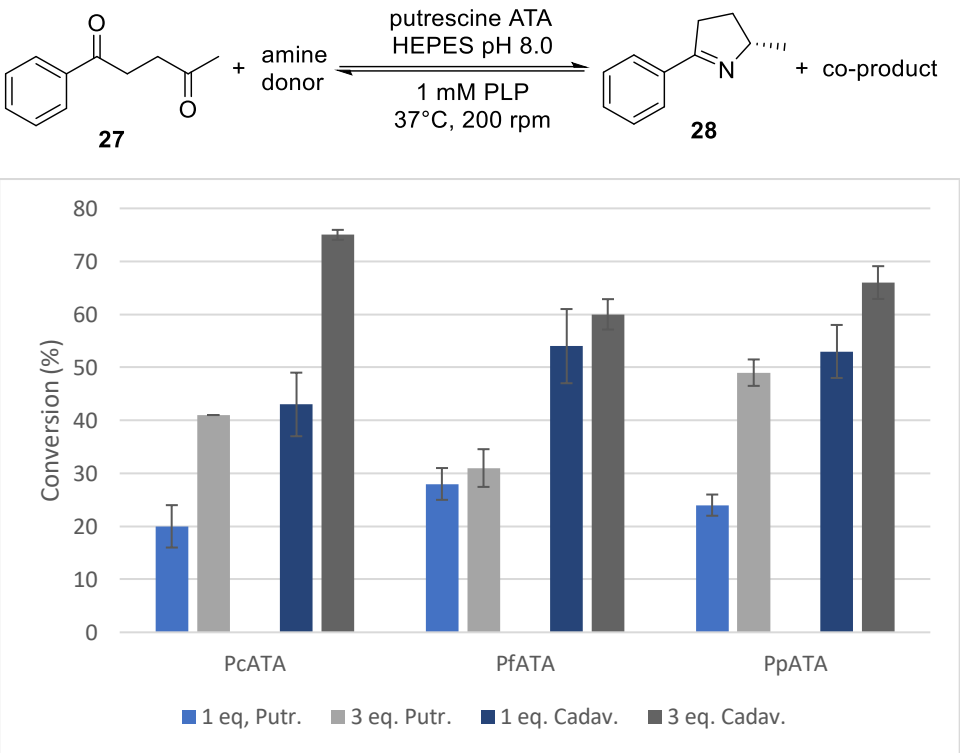

***Figure 3.15**. Comparison of conversion (n=3, error bars show std) of **27** utilizing 1.5 mg mL^{-1} clarified extract of putrescine ATA in the presence of 1 or 3 equivalent putresine or cadaverine, as indicated. Conversions were measured as previously described in section 2.6.5.*

All putrescine ATAs were His-tagged and were expressed from *E. coli* BL21 (see section 3.8.8.1) and purified with nickel affinity chromatography (see section 3.8.9) for subsequent experiments. The purity of the isolated fractions was estimated with SDS-PAGE analysis (see section 3.8.10), as shown in Figure 3.16 for the pfATA.

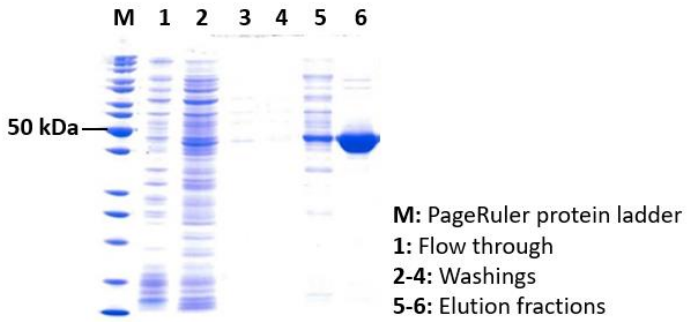

***Figure 3.16**. SDS-PAGE analysis of the different fractions from Ni-affinity chromatography purification of PfATA. **M**: protein ladder, **1**: flow through, **2-4**: washings, **5-6**: elution fractions.*

The production of putrescine or cadaverine from *C. glutamicum* NA6 and GRLys1 strains, respectively, was tested on the transamination of ketone **27**, utilizing 1 mg mL^{-1} purified extract of the putrescine ATAs (see section 3.8.13.2). Purified extract was used for consistency with previous experiments (see section 3.3.2). For this experiment individual cultures of *C. glutamicum* NA6 and GRLys1 were grown, as reported in the literature. A sample was taken every 24h and the cells were removed with centrifugation. The supernatant was then supplemented with ketone **27** and purified extract of pc, pf or pp ATA, allowed to react for 24h and the conversion were measured with GC-FID. As shown in Table 3.6, GRLys1 reached similar conversions (60-78%) to NA6 strain, when 48h mature culture of GRLys1 was used. This indicates that longer incubation time of the culture (48h mature culture) is required for the GRLys1 strain to reach maximum OD and produce enough cadaverine for the biotransformations. This is not the case for the NA6 strain, as there was not significant difference between 24h and 48h mature culture media. OD measurements (not shown) support this theory, as GRLys1 was still growing when a sample was taken after 24h.

***Table 3.6**. Conversion (n=3, std <5%) of **27** utilizing purified extract of putrescine ATAs (1 mg/mL) in 24h or 48h mature conditioned culture medium (WT, NA6 or GRLys1). Conversions were measured as previously described in section 2.6.5.*

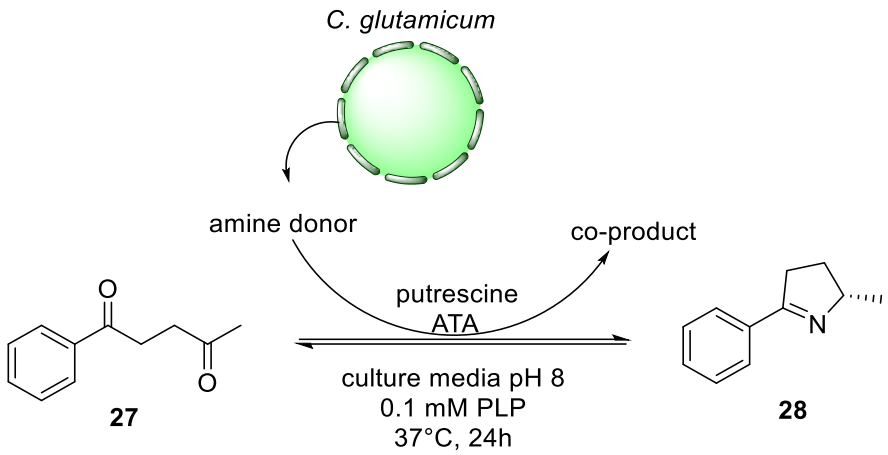

Culture	ATA	Conversion (%)	
		24h matured medium	48h matured medium
Wild type	Pc	n.d.	n.d.
	Pf	n.d.	n.d.
	Pp	n.d.	n.d.
NA6	Pc	75%	76%
	Pf	68%	70%
	Pp	71%	73%
GRLys1	Pc	26%	78%
	Pf	26%	70%
	Pp	27%	60%

n.d.: not detected

3.6.2 expression of putrescine ATAs in *C. glutamicum* strains

All putrescine ATAs were successfully cloned in pEKEx3 vector utilizing the primer pairs SG17_F and SG18_R for PcATA, SG19_F and SG20_R for PfATA and SG19_F and SG21_R for PpATA. The constructs were transformed in *E. coli* DH5a (see section 3.8.4.1) and they were verified by restriction analysis (Figure 3.17) and sequencing.

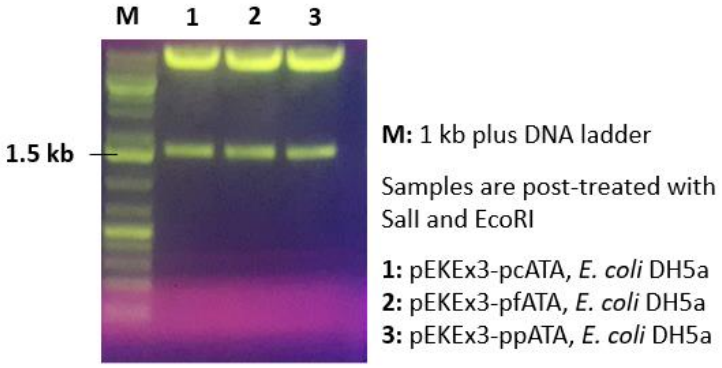

***Figure 3.17**. Agarose gel (1%) of the restriction analysis of plasmids **1**: pEKEx3-pcATA, **2**: pEKEx3-pfATA, **3**: pEKEx3-ppATA isolated from E. coli DH5a utilizing EcoRI and SalI. **M**: 1kb plus DNA ladder*

The plasmid was isolated from *E. coli* DH5a (30 uL of 500-700 ng/uL) and transformed in *C. glutamicum* strains (see section 3.8.4.2). The ATA activity of the new strains was evaluated from a colony based solid-phase screen utilizing *o*-xylylenediamine (see section 3.8.12).[130] The screen utilizes o-xylylenediamine and pyruvate, which diffuse through the cells and undergo transamination to afford a coloured precipitate that darkens colonies of bacteria overproducing an ATA.[130] A representative example is shown in Figure 3.18, where all strains overexpressing a putrescine ATA turned black, while the control (empty vector) remained plain.

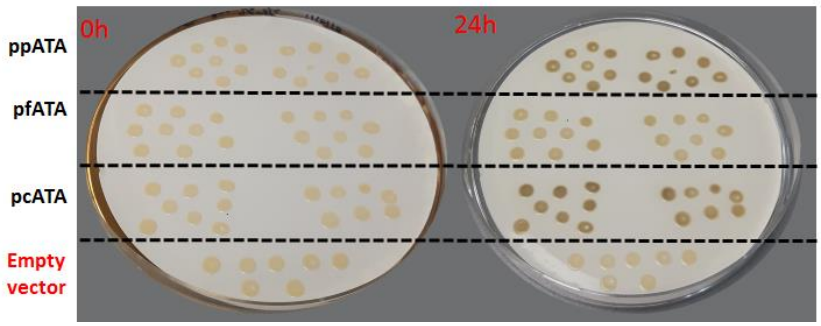

***Figure 3.18**. Results from a colony-based screen with o-xylylenediamine and C. glutamicum GRLys1 strains overexpressing putrescine ATAs.*

The ability of the new strains, as well as the ones to follow, to mediate an ATA reaction in a self-sufficient manner, was evaluated utilizing compound **27** as a model ketone substrate (Scheme 21).

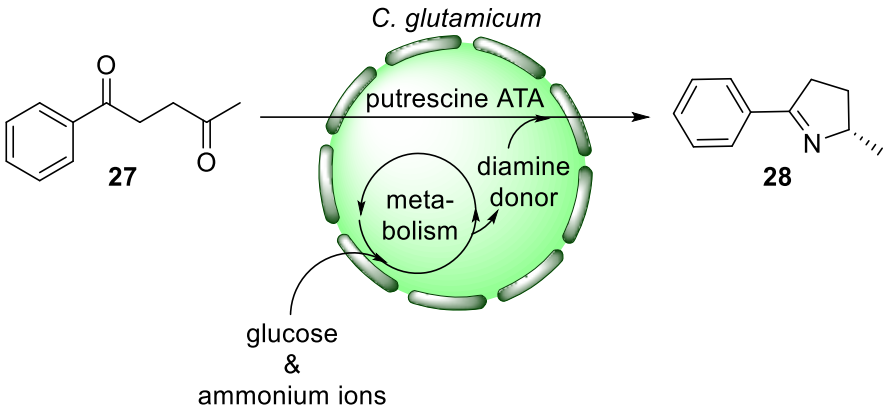

***Scheme 21**. General reaction scheme for the whole cell transamination of compound **27**.*

Galman *et al*. 2017, reportedly used 40°C for biotransformations with these putrescine ATAs,[201] which is 10°C higher than the temperature used to grow *C. glutamicum*.[202] Thus, higher temperatures were tested as they could lead to higher conversions of **27** utilizing whole cells *C. glutamicum* overexpressing the ATA (see section 3.8.13.3). The results shown in Table 3.7 are indicative of lower conversion at higher temperatures. The bacteria are potentially under additional metabolic stress, which would lead to poor performance. The highest conversion observed was just above 10% for the GRLys1 with PcATA, which is slightly higher than the rest of the GRLys1 strains. The NA6 strains performed as poorly as wild type, achieving conversions below 5%. The NA6 with PcATA was the sole exception, affording 9% conversion.

***Table 3.7**. Conversions (n=3, std <1%) of **27** utilizing C. glutamicum whole cells overproducing PcATA, PfATA or PpATA and putrescine or cadaverine, at 30°C and 37°C. Conversions were measured as previously described in section 2.6.5.*

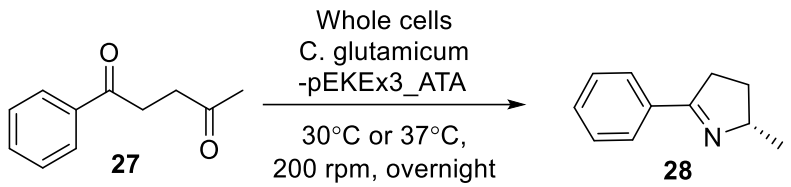

Strain	ATA	Conversion	
		30°C	37°C
WT	Pc	5%	4%
NA6	Pc	9%	5%
	Pf	3%	3%
	Pp	2%	n.d.
GRLys1	Pc	12%	7%
	Pf	8%	6%
	Pp	9%	5%

n.d.: not detected

Galman *et al.* 2017, reportedly used pH 9.0 for biotransformations, thus indicating higher activity at higher pH.[201] In order to investigate the effect of the pH in the activity of the putrescine ATAs, their specific activity at different pH was measured utilizing the acetophenone assay (Figure 3.19).[177] The activity of PpATA (grey square) fell from 50 U mg^{-1} (pH 9.0) to 8 U mg^{-1}, when pH 8.0 was used, with a further decrease to 1 U mg^{-1} at pH 7.0. A similar but less significant drop is observed with PfATA (orange diamond) at lower pHs. There is also a clear indication of higher activity at pH 9.0 for PcATA (blue circle), despite its poor overall performance. Altogether, the poor performance of the whole-cells can be attributed to lower activities observed for the putrescine ATAs at neutral pH.

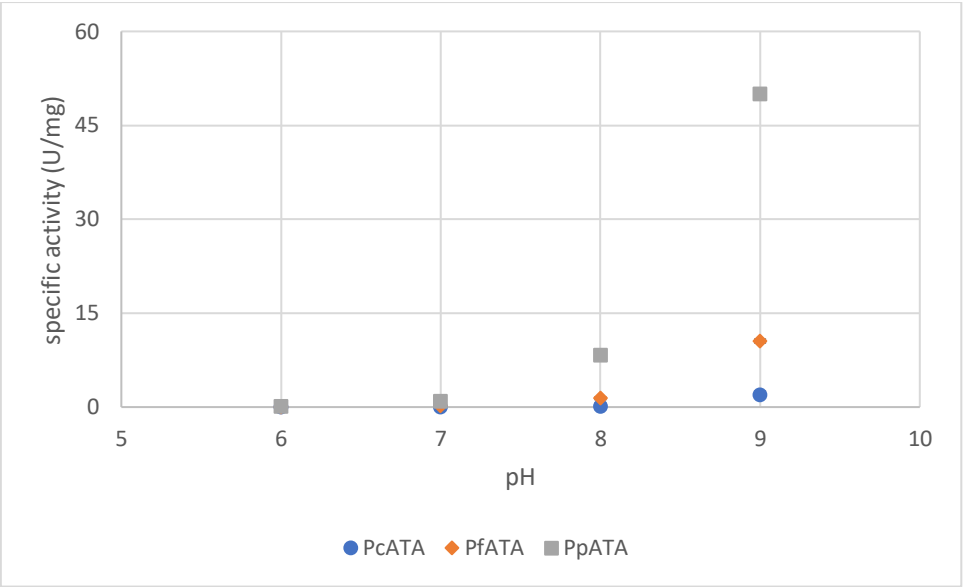

***Figure 3.19**. Measurement of the specific activity of purified extract of putrescine ATAs at different pH (see Appendix A.2.1), utilizing the acetophenone assay. One unit of enzyme activity is defined as the amount of enzyme that produced 1 µmol of acetophenone per min at 30˚C.*

Intracellular pH cannot be altered, but the amount of ATA produced inside the cells could be increased for improved performance. Following previous observations (see section 3.5.2), a construct for the expression of a double PcATA gene under the same promoter was prepared using the primers SG22_F with SG23_R and SG24_F with SG25_R. The plasmid pEKEx3-PcATAx2 was isolated from three different colonies and digested using SmaI (Figure 3.20). Agarose gel electrophoresis analysis showed that one of the three plasmids was successfully cut (lane 3), which was used for subsequent experiments.

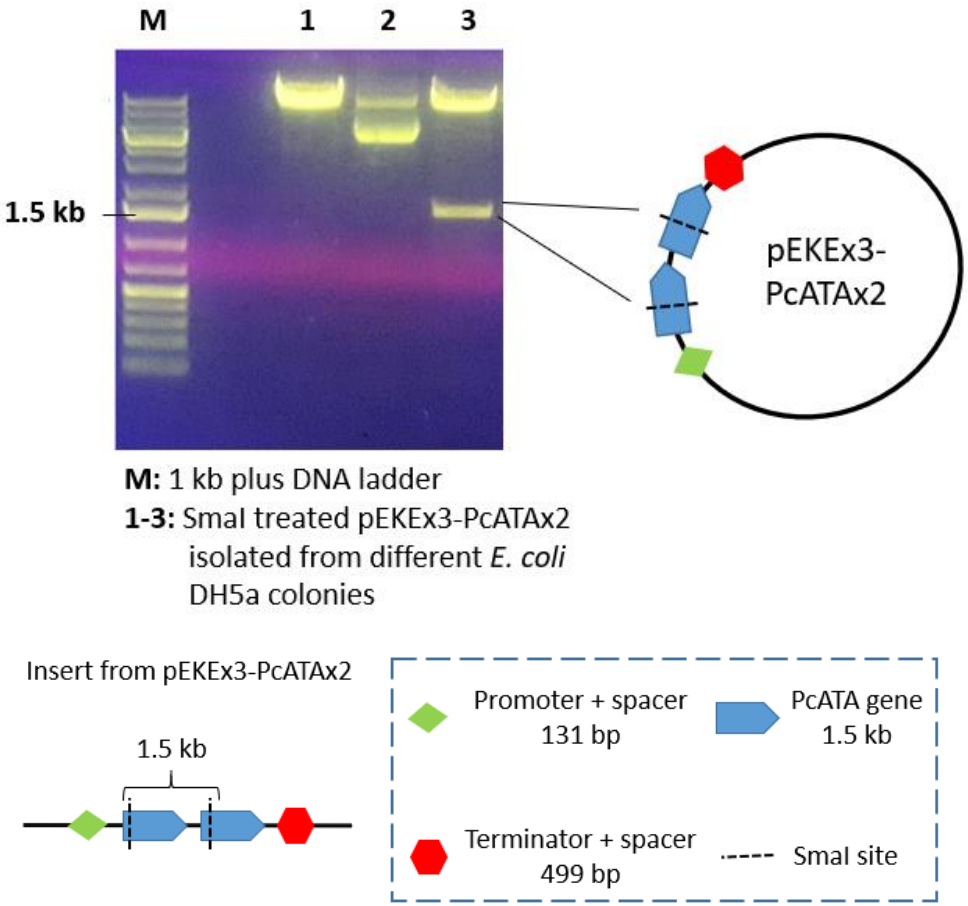

***Figure 3.20**. Agarose gel (1%) of **1-3:** the isolated plasmid pEKEx3-PcATAx2 from different E. coli DH5a colonies after restriction digestion with SmaI. **M**: 1 kb plus DNA ladder*

The verified plasmid was transformed in *C. glutamicum* strains (see section 3.8.4.2). Biotransformations of both the old and the new strains were tested under the same reaction conditions (see section 3.8.13.3) and the conversions were measured after one and two days incubation at 30°C (Figure 3.21). The conversions almost tripled from 12% to 32% for the NA6 strains expressing the double insert (PcATAx2), after two days incubation. Expression of the double insert had little effect on the GRLys1 strains, where conversions remained below 20%. This can be explained from previous observations, where the expression of the double-insert had little impact in the production of ATA in GRLys1 strains (see section 3.5.2).

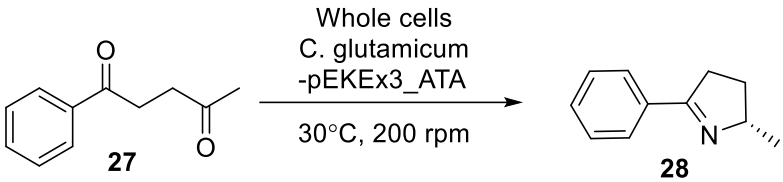

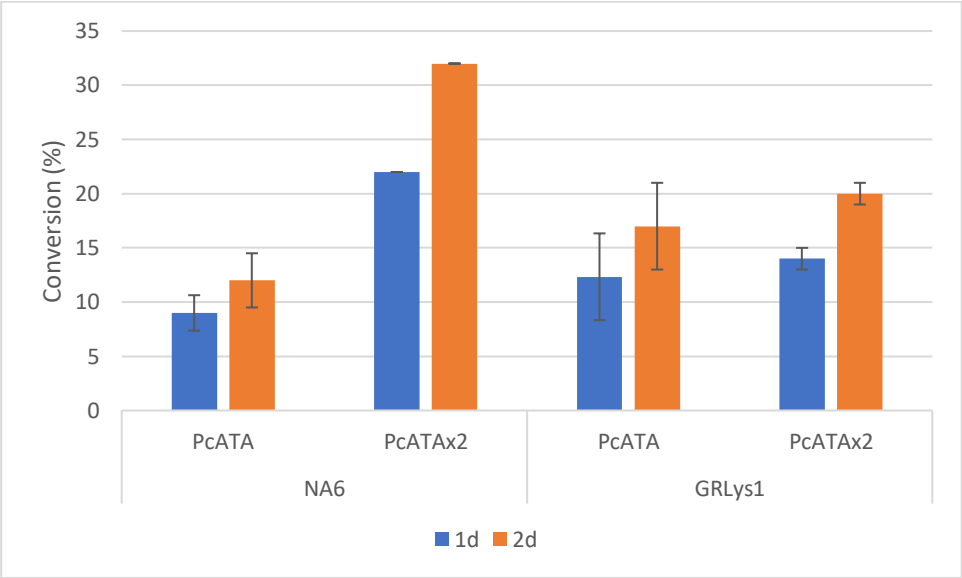

***Figure 3.21**. Conversion (n=3, error bars show std) of **27** between NA6 and GRLys1 strains with single (PcATA) and double (PcATAx2) insert. Conversions were measured as previously described in section 2.6.5.*

Increased conversion was observed when using *C. glutamicum* strains expressing the double insert PcATA. These results are indicative of improved overall performance with increased production of ATA and are further supported by statistical analysis (see Appendix A.2.3, null hypothesis 4). It was envisaged that utilizing the high copy number plasmid, pVWEx1,[163,203] for the expression of ATA would lead to increased conversion. As mentioned in section 3.1, the engineered strains NA6 and GRLys1 already contain this vector expressing genes essential for the production of putrescine and cadaverine, respectively. In order to create new strains with increased ATA production, the genes of the putrescine ATAs were cloned along with the *ldcC* and *speC* genes (GRLys1 and NA6 respectively) in pVWEx1. The *ldcC* and *speC* genes were amplified from genomic DNA of *E. coli* using the pairs SG26_F with SG27_R and SG28_F with SG29_R, respectively. New primers were designed for the

amplification of putrescine ATAs; the pairs SG30_F with SG31_R, SG32_F with SG33_R and SG34_F with SG35_R were used for the amplification of PcATA, PfATA and PpATA respectively. The newly formed plasmids were transformed in *E. coli* DH5a and verified with restriction analysis, as shown for the pVWEx1-*ldcC*_pcATA in Figure 3.22.

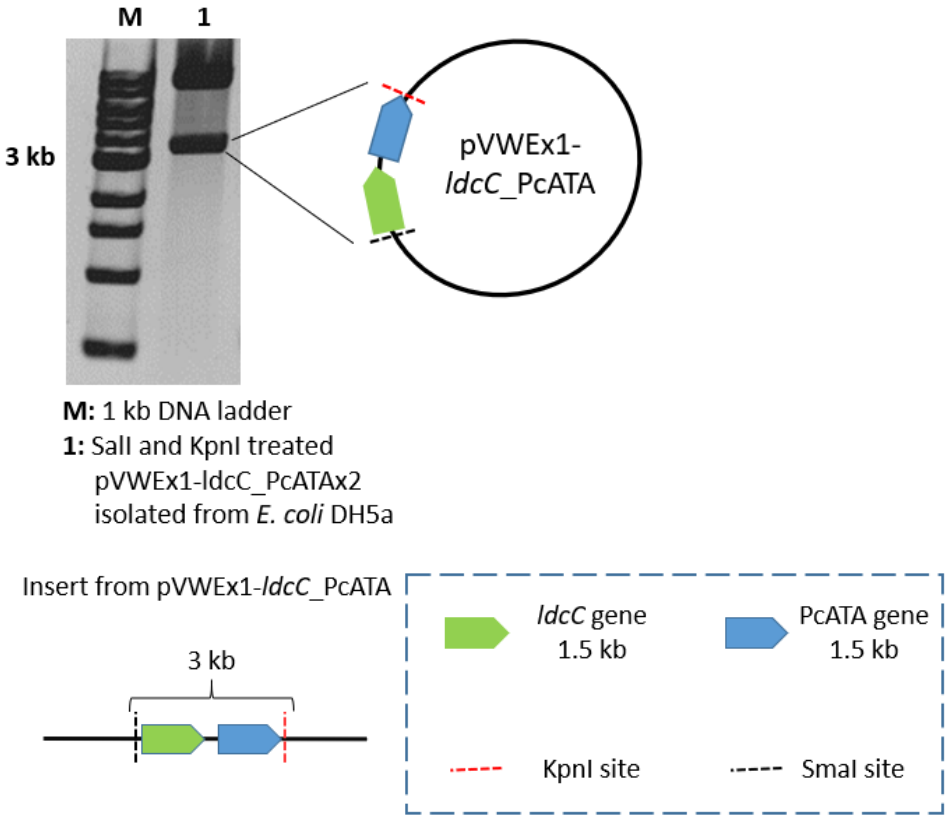

***Figure 3.22**. Agarose gel (1%) of **1**: pVWEx1 with ldcC and PcATA isolated from E. coli DH5a, after restriction digestion with SalI and KpnI. **M**: 1kb DNA ladder.*

The vector pVWEx1 with the ornithine decarboxylase (*speC*) and putrescine ATA gene has a size of 12 kb, which is already large enough to make the transformation challenging. In order to avoid such complications, the NA6 strain was replaced with the NA2b. The latter does not contain the genes for pyruvate carboxylase (*pyc*), glyceraldehyde 3-phosphate dehydrogenase (*gapA*), N-acetylglutamate kinase (*argB*) and ornithine transcarbamoylase ($argF_{21}$), which are co-expressed with *speC* in NA6. [155]

The new constructs were verified *via* sequencing and the new strains were tested in the transamination of 5 mM of compound **27** (Table 3.9). A significant drop in conversion was observed for the NA2 strains (entries 1-3), which can be attributed to the decreased production of putrescine. A significant improvement was observed for all GRLys1 strains (entries 4-6), affording conversions above 25%. GRLys1 with PcATA achieved the highest conversion (36%) after 24h, followed by a slight increase after 48h (entry 4). These are the best conversions observed utilizing whole cells, and thus the GRLys1 strain co-expressing *ldcC* and PcATA was further investigated and the reaction conditions were optimized.

Table 3.9*. Conversion (n=3, std <1%) of* ***27*** *utilizing whole cells C. glutamicum GRLys1 or NA2 overexpressing putrescine ATA (Pc, Pf or Pp) from pVWEx1 vector, at 30°C, after 24h, 48h and 72h. Conversions were measured as previously described in section 2.6.5.*

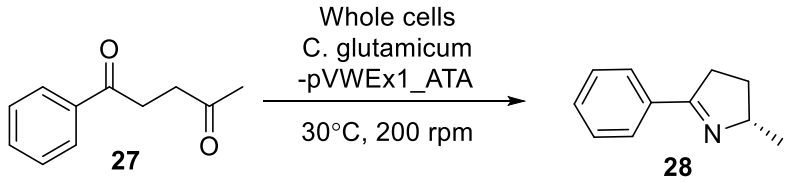

Entry	Strain	ATA	Conversion		
			24h	48h	72h
1	NA2	Pc	n.d.	7%	8%
2		Pf	n.d.	5%	5%
3		Pp	n.d.	5%	5%
4	GRLys1	Pc	36%	41%	41%
5		Pf	32%	35%	35%
6		Pp	26%	33%	35%

3.6.3 Optimization of *in vivo* Whole cell biotransformations

Different reaction conditions were tested with the *C. glutamicum* GRLys1 co-expressing *ldcC* and PcATA. Initially, different concentrations of cells were tested (Figure 3.15). Higher cell density would result in higher probability of compound **27** encountering the cells and undergo transamination. Previous reaction conditions with whole cells employed 50

mL expression culture (see section 3.8.8.2 for expression and section 3.8.13.3 for biotransformation), which corresponded to 20 mg mL^{-1} wet cell pellets (WCP). Conversions significantly increased with higher cell densities, reaching a plateau of 72% with 100 mg mL^{-1} WCP. This is a tremendous improvement, as values are comparable with the *in vitro* experiments described in section 3.6.1. Also, statistical analysis (see Appendix A.2.3, null hypothesis 5) reinforce the above statement, confirming that higher cell density brought a statistically significant increase in the yield. Biotransformations were also tested in HEPES buffer, in order to investigate whether transamination can occur outside of the culture media. Surprisingly, replacing the culture media with HEPES buffer lead to slightly higher conversion in low cell densities. However, that was not the case for concentrations of 150 and 200 mg mL^{-1} WCP (Figure 3.15). These results show that some of the cadaverine produced stays inside the cell, indicating an autonomous nature of this system. The ability of the cells to mediate an ATA reaction in different aqueous media can be exploited in biocascades, by combining with different whole-cell or cell-free systems. Also, the addition of PLP as a supplement was investigated, as it could impact conversion. Biotransformations supplemented with PLP were tested in parallel and showed insignificant differences in conversions. These results demonstrate that *C. glutamicum* naturally produces the co-factor (PLP) required for transamination of **27**.

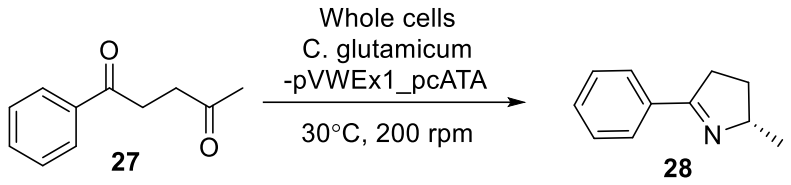

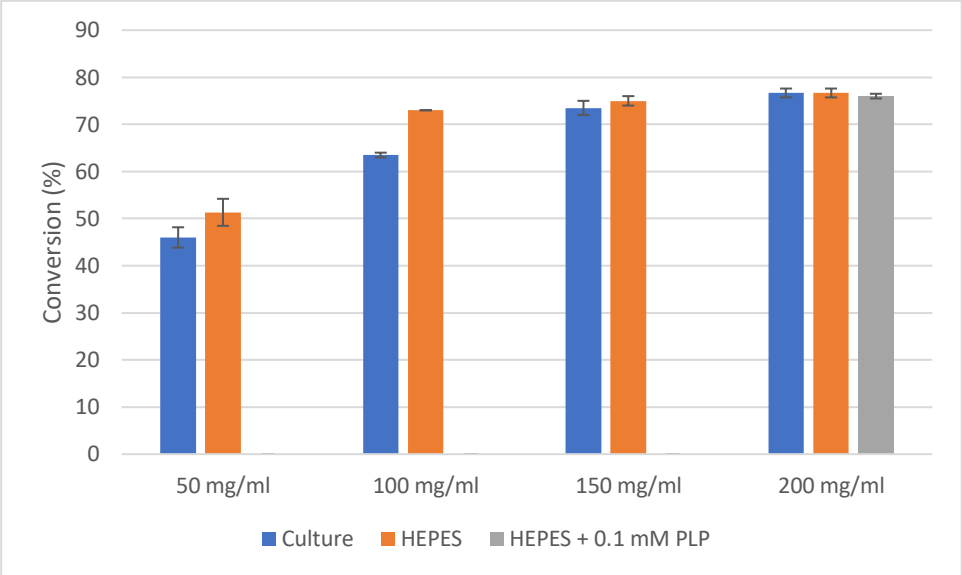

***Figure 3.15**. Conversion (n=3, error bars show std) of **27** from different cell densities and media. Conversions were measured as previously described in section 2.6.5.*

Stability studies were performed, by evaluating the conversion of **27** after 24h (cycle 1), 48h (cycle 2) and 72h (cycle 3). These findings (Figure 3.16) indicate the cells can be used again, with little impact on conversion. A significant drop to 25% is observed thereafter, during the third cycle. Cells were washed (3x2 mL HEPES) between each cycle, with final wash being extracted with EtOAc (1 mL) and analysed on GC-FID, to verify no product is carried forward.

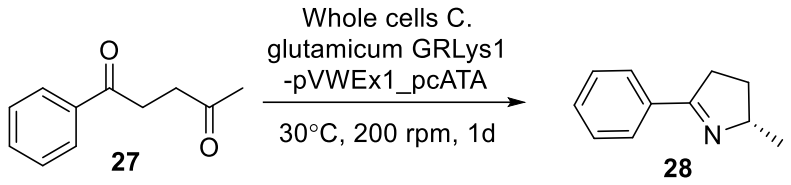

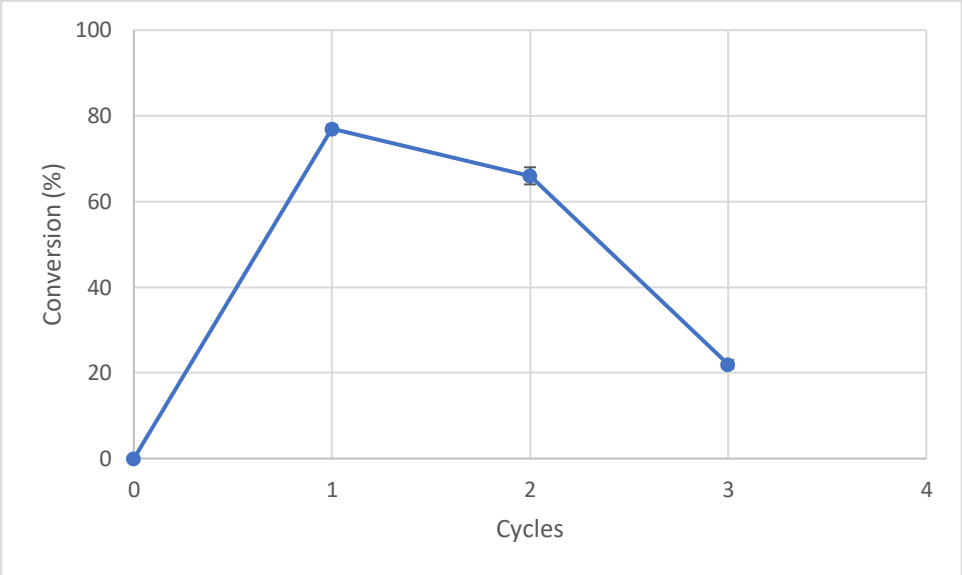

***Figure 3.16**. Results of three consecutive cycles (n=3, std <1%) of the transamination of **27** utilizing 200 mg mL^{-1} wet cell pellets at 30°C, 200 rpm. Conversions were measured as previously described in section 2.6.5.*

A greater-scale reaction of 130 mg (5 mM in DMSO) of **27** was carried out utilizing 150 mg mL^{-1} WCP resuspended in HEPES buffer (see section 3.8.14). A moderate conversion of 61% was observed after 24h on GC-FID, with a minor increase to 67% after 48h. Compound (*S*)-**28** was isolated in 42% yield. The absolute configuration was determined by measuring the optical rotation of (*S*)-**28**.[179,204]

3.7 Conclusion and future work

In conclusion, five (*S*)-selective ATAs capable of converting carbonyl-containing substrates with 'smart' amine donors, in low enzymatic loads, were identified and used for the development of novel whole-cell biocatalysts. Side reactions (HEWT) or complications with expression (3HMU) in *C. glutamicum* cells hampered the use of two ATAs. The former

could potentially be tackled with metabolic engineering, creating a more versatile system for the production of primary amines.

Three putrescine ATAs (Pc, Pf and Pp) were successfully transformed and utilized for the whole-cell transamination of a model ketone substrate. New strains with enhanced ATA production were developed and the reaction conditions were optimized for the conversion of the model substrate to its corresponding imine with good yield and high enantioselectivity. This is the first report of a whole-cell system mediating ATA reaction in a self-sufficient manner. There is tremendous potential for this system, as more enzymes can be co-expressed and facilitate biocascades. Also, the ability of whole-cells to remain active in different media offer great flexibility, expanding its application.

3.8 Experimental

General Methods and Materials

All chemicals were of analytical grade purity and obtained from Sigma Aldrich (München, Germany), Merck (Darmstadt, Germany), VWR (Hannover, Germany) or Acros (Geel, Belgium). Restriction enzymes, 1kb plus protein marker and phusion polymerase were bought from Thermo Fischer Scientific (Waltham, MA, US), Coomassie brilliant blue G-250 stain was purchased from Bio-Rad (Hercules, CA, USA), T4 ligase and NEBuilder® HiFi DNA assembly were purchased from New England Biolabs (Ipswich, MA, USA), oligos and sequencing services were purchased from Eurofins Genomics (Ebersberg, Germany). *Escherichia coli* DH5α and BL21 (DE3) cells were purchased from New England Biolabs (Ipswich, MA, USA).

3.8.1 Sterile conditions

All glassware, plastics and solutions used for culturing were autoclaved for 30 mins at 121˚C prior to use. All bacterial work was performed next to a Bunsen burner flame with all surfaces wiped with methylated spirits.

3.8.2 Media and agar preparation

3.8.2.1 Preparation of Luria-Bertani media

Luria-Bertani (LB) media was prepared by dissolving 5 g yeast extract, 10 g tryptone and 10 g sodium chloride in distilled water to a final volume of 1000 mL and sterilized by autoclave.

3.8.2.2 Preparation of mCGXII media

A standard protocol was followed for the preparation of mCGXII media in 1 L final volume as described in the literature.[182] In detail, an aqueous solution containing 20 g ammonium sulfate, 1 g dipotassium phosphate, 1 g monopotassium phosphate, 250 mg magnesium sulfate heptahydrate and 42 g 3-(N-morpholino) propanesulfonic acid (MOPS) in 700 mL distilled water was prepared. The pH of the mixture was adjusted to 7.5 using aqueous potassium hydroxide (1M) and the solution was brought to 778 mL final volume with distilled water followed by sterilization by autoclave. To this, filter sterilized aqueous solutions of glucose (200 mL of 20% w/v), urea (5g in 20 mL), trace elements (1 mL of 1000x stock) and biotin (1 mL of 0.02% w/v) were added prior to use for culturing. The trace element 1000x stock solution contains 1 g calcium chloride, 1 g iron sulfate heptahydrate, 1 g manganese sulfate monohydrate, 1g zinc chloride heptahydrate, 20 mg copper sulfate 2 mg nickel chloride hexahydrate dissolved in 100 mL distilled water.

3.8.2.2 Preparation of LB agar

LB agar was prepared by dissolving 8.75 g of LB agar powder (Lennox) into a 250 mL of distilled water. The solution was autoclaved and allowed to cool to 50˚C, followed by addition of appropriate antibiotic stock prior to pouring onto plates.

3.8.3 Preparation of chemo- and electro- competent cells

3.8.3.1 Chemically-competent E. coli cells

Frozen commercial stock of *E. coli* cells was steaked onto LB agar plate without antibiotic and the plate was incubated at 37˚C overnight. A single colony was picked to inoculate 10 mL starter culture in LB media, incubating at 37˚C, 200 rpm overnight. A 100 mL LB main cultures was inoculated with 1 mL of starter's culture (1% v/v) and incubated at 37˚C, 200 rpm until OD_{600} reached 0.5 – 0.7. The culture was cooled on ice for 20 mins and transferred to 50 mL ice-cold falcon tubes before the centrifugation step. The cells were harvested via centrifugation at 3000 g, 4˚C for 10 mins and the supernatant was decanted away. Pellets were re-suspended in 10 mL ice-cold sterile solution of $MgCl_2$ (100 mM). The cells were harvested by centrifugation at 3000g, 4˚C for 10 mins, the supernatant was removed, the pellets were re-suspended in 20 mL ice-cold $CaCl_2$ solution (100 mM) and incubated on ice for 1 hour. Cells were harvested by centrifugation at 3000 g, 4˚C for 10 mins, the supernatant was removed and the pellets were washed with 10 mL ice-cold sterile solution of $CaCl_2$ (85 mM) containing glycerol (15% v/v). The cells were harvested via centrifugation at 3000 g, 4˚C for 10 mins and the supernatant was decanted away. Pellets were re-suspended in 1 mL ice-cold sterile solution of $CaCl_2$ (85 mM) containing glycerol (15%v/v) and 50 µL suspension was aliquoted in sterile tubes and froze at -80 ˚C.

3.8.3.2 Electro-competent C. glutamicum cells

Frozen glycerol stock of *C. glutamicum* cells were streaked onto LB agar plate supplemented with selection antibiotic (or not, for the wild type) and incubated at 30˚C overnight. A single colony was picked and re-streaked onto a new LB agar plate with selection antibiotic (or not, for the wild type) and incubated at 30˚C overnight. From that plate, several colonies (a lot of biomass is required) were picked to inoculate 15 mL starter culture Brain Heart Infusion media enriched with 5% w/v sorbitol (BHIS), supplemented with selection antibiotic (or not, for the wild type) and incubated at 30˚C, 200 rpm overnight. Two main cultures (25 mL fresh BHIS in 250 mL baffled flask) were inoculated with 5 mL of starter's culture, and incubated at 30˚C, 200 rpm until OD_{600} reached 1.75. Cultures were cooled on ice and transferred to 50 mL ice-cold falcon tubes. Cell were harvested by centrifugation at 3000 g, 4˚C for 10 mins and the supernatant was removed. Pellets were re-suspended in 5 mL ice-cold Tris-glycerol buffer (1 mM Tris·HCl, pH 7.5, 87% v/v glycerol) carefully. To that 15 mL of ice-cold Tris-glycerol buffer were added and the cells were harvested by centrifugation at 3000 g, 4˚C for 10 mins. This step was repeated one more time. The supernatant was removed, the pellets were re-suspended in 1 mL ice-cold glycerol (10% v/v), aliquoted (150 µL) in sterile tubes and froze at -80 ˚C.

3.8.4 Transformation protocols

3.8.4.1 Transformation of chemically-competent E. coli cells

An aliquot (150 µL) of chemically competent *E. coli* cells was thawed on ice. Plasmid DNA (1-150 ng) were added and the suspension was incubated on ice for 30 mins. Cells were heat-shocked at 42˚C for 1 min, cooled on ice for 2 mins before adding 750 µL LB, and incubated at 37˚C shaking at 200 rpm for 1 hour. An aliquot (10-100 µL) of transformed cell suspension was pipetted onto LB agar plate with selection antibiotic and evenly distributed using sterile spreader. Remaining cells were harvested by centrifugation at

3000 g, 20˚C for 10 mins. The supernatant was removed and the pellets were re-suspended in 100 µL LB before plated onto a different plate with selection antibiotic. Both plates were incubated at 37˚C overnight. A single colony was used to inoculate 10 mL LB starter culture supplemented with selection antibiotic and incubated at 37˚C, 200 rpm overnight. An aliquot (750 µL) of the starter culture was mixed with 250 µL glycerol (80% v/v) and stored at -80˚C.

3.8.4.2 Transformation of electro-competent C. glutamicum cells

Electrocompetent *C. glutamicum* cells (150 µL) were thawed on ice. Plasmid DNA (1-10 µg) was added to the cells and incubated on ice for 10 mins. The suspension was transferred into electroporation cuvette and was electroporated at 25 µF, 200 Ω, 2.5 kV. Cell suspension was Immediately transferred in prewarmed BHIS and incubated at 46˚C for 6 mins. The tube was cooled down with running tap-water for 30 secs and the suspension was incubated at 30˚C for 45-60 mins. An aliquot of transformed cell suspension (10-100 µL) was pipetted onto LB agar plate with selection antibiotic and spread using sterile spreader. The remaining cells were harvested by centrifugation at 3000 g, 20˚C for 10 mins. The supernatant was removed, the pellets were re-suspended in 100 µL BHIS and 50 – 100 µL were pipetted onto a different plate with selection antibiotic. Both plates were incubated at 30˚C overnight. A single colony was picked and re-streaked onto a new LB agar plate with selection antibiotic and incubated at 30˚C overnight. From the latter plate, multiple colonies (a lot of biomass) were picked to inoculate 15 mL BHIS starter culture supplemented with selection antibiotic. Culture was incubated at 30˚C, 200 rpm overnight. An aliquot (750 µL) of the starter culture was mixed with 250 µL glycerol (80% v/v) and stored at -80˚C.

3.8.5 Polymerase-chain reaction (PCR) mixing protocol

Reagents in the quantities described in the table below were pipetted into PCR tubes. The resulting mixtures were placed in a thermal cycler and ran according to the program described in A.2.5.

Reagent	Quantity
HiFi buffer (PCRBiosystems)	10 µL
Primer (forward) (10 µM)	2 µL
Primer (reverse) (10 µM)	2 µL
DNA template (roughly 10 ng/ µL)	1 µL
HiFi Polymerase (PCR Biosystems)	0.5 µL
DNAase free H_2O	34.5 µL

3.8.6 Plasmid isolation and restriction digestion with restriction enzyme

Isolation of the plasmid DNA was performed using the GeneJet Plasmid Miniprep Kit from Thermo Fischer Scientific on overnight cultures of cells featuring the plasmid of interest. Isolated DNA was examined by agarose gel electrophoresis (see section 3.8.7). Small scale centrifugation was performed with Eppendorf 5424R microcentrifuge.

Isolated plasmids were digested (when mentioned) using restriction enzymes from New England Biolabs (NEB) following the conditions described in appendix section A.2.6.

3.8.7 Agarose Gel Electrophoresis

Agarose gels (1% w/v) were prepared by dissolving 0.5 g agarose in 50 mL Tris-acetate ethylenediaminetetraacetic acid (EDTA) buffer (40 mM Tris, 20 mM acetic acid, 1 mM EDTA) and bringing suspension to boil, till clear solution. The solution was cooled to 50-60˚C, before adding 5 µL of 10 000x Sybr Safe dye from Thermo Fischer Scientific (Waltham, MA, US) and poured onto a tray. The gel was cooled to solidify for 20-30 mins. Aliquots (5-10 µL) of samples were mixed with 1-2 µL of 6x DNA loading dye (Thermo Fischer Scientific) and loaded onto the gel along with 6 µL of DNA ladder

(Thermo Fischer Scientific). The gels were run at 75 V for 60 mins and visualised using a UV-illuminator in a dark room.

3.8.8 Expression of recombinant protein

3.8.8.1 In E. coli

All ATA genes were codon-optimized and were kindly offered from Prof. Nicholas Turner and his group from University of Manchester, UK, and Prof. Uwe Bornscheuer and his group from University of Greiswald, Germany. In pET-22b, the (*S*)-selective ATAs (3HMU, 3I5T, Vibflu, ChrVio, PcATA, PpATA) and the (*R*)-selective ATAs (AspFum, NeoFis) were cloned. The (*S*)-selective PfATA was cloned in pET-28b and the (*R*)-selective MycVan and AspOry were cloned in pGASTON. Transformed *E. coli* BL21(DE3) cells were cultivated in 500 mL LB medium supplemented with selection antibiotic (100 µg mL^{-1} ampicillin or 50 µg mL^{-1} kanamycin) at 37°C shaking at 200 rpm, starting with 5 mL inoculum of single-colony culture previously grown overnight. The culture was grown till OD_{600} reached 0.5-0.7 and the expression was induced with 1 mM IPTG or (5% w/v) Rhamnose and the cultures were incubated at 20°C (VibFlu, ChrVio, AspFum, AspOry, NeoFis, MycVan) for 20h or 30°C (3HMU and 3I5T) for 6h and then harvested with centrifugation (4000 rpm, 20 mins) and stored at -20°C.

The pellets were thawed, resuspended in lysis buffer containing potassium phosphate buffer (50 mM, pH 7), pyridoxal-5'-phosphate (0.1 mM) and halt™ protease inhibitors cocktails (1X) from Thermo Scientific, and disrupted by sonication at 4°C with 10 cycles of 30s of sonication and 30s of cooling at 40% amplitude, using QSonica model Q55. After centrifugation (24,000 rpm, 4°C, 25 mins) in an Eppendorf 5424R microcentrifuge, the supernatant was clarified via filtration (0.45 µm filter) and either purified (see section 3.8.9) or used as crude, for SDS-PAGE analysis (see section 3.8.10), spectrophotometric enzymatic assay (see section 3.8.11) and biotransformations (see section 3.8.13) on the same day.

3.8.8.2 In C. glutamicum

Multiple colonies of transformed *C. glutamicum* were used to inoculate 25 mL BHIS, supplemented with selection antibiotic (100 µg mL^{-1} spectinomycin and/or 50 µg mL^{-1} kanamycin) and grown at 30°C overnight. Pellets were harvested *via* centrifugation (4000 rpm, 7 mins), washed with minimal medium mCGXII[182] (3x20 mL) and used to inoculate 50 mL main culture with starting OD_{600} of 0.5 (for the NA6 or Wild Type) or 1 (for GRLys1). The cultures were instantly induced with 1 mM IPTG, unless otherwise specified, and incubated at 30°C shaking at 200 rpm. After 24 hours (OD_{600} = 20), pellets were harvested *via* centrifugation (4000 rpm, 7 mins) and either used directly or stored at -20°C.

The pellets were thawed, resuspended in lysis buffer containing potassium phosphate buffer (50 mM, pH 7), 1X cocktail of proteases inhibitors and PLP (0.1 mM) for ATA expression, and disrupted by sonication at 4°C with 20 cycles of 30s of sonication and 30s of cooling at 40% amplitude, using QSonica model Q55. After centrifugation (24,000 rpm, 4°C, 25 mins) in an Eppendorf 5424R microcentrifuge, the supernatant was clarified via filtration (0.45 µm filter) and used for fluorescence (GFP) or MALDI-TOF (3HMU-K292A) analysis or in a spectrophotometric assay (3HMU, HEWT, HEWTx2, pHEWTtx2).

3.8.9 Protein purification

Purification of the ATAs was carried on Akta Pure system (GE, Healthcare, Little Chalford, UK). Clarified extract was loaded into a 5 mL HisTrap column, washed with 10 column volumes of de-gassed phosphate buffer (50 mM, pH 8.0 containing 0.1 mM PLP and 30 mM imidazole) and eluted with de-gassed phosphate buffer (50 mM, pH 8.0 containing 0.1 mM PLP and 300 mM imidazole). Fractions of 5 mL were collected during the elution phase and SDS-PAGE gel was run to identify fractions containing the ATA. The protein solution was concentrated using VivaSpin 20, 50,000 MWCO PES

(Sartorius, Gottingen, Germany) and the imidazole was removed *via* dialysis tubing (Sigma Aldrich). Purified protein was analyzed by SDS-PAGE (found 95% pure) and instantly used for biotransformations.

3.8.10 Protein determination and SDS-PAGE analysis

The concentration of the total protein of clarified and purified extracts was determined spectrophotometrically by UV absorption at 280 nm. The extinction co-efficient of each ATA at 280 nm, measured in water, was estimated by ExPASy ProtoParam tool (www.expasy.org).[205]

Gels for SDS-PAGE analysis were prepared using the reagents described in the table below.

Reagent	Stacking Gel (15%)	Resolving Gel (5%)
H_2O	6.1 mL	4.1 mL
Acrylamide (30% v/v)	1.3 mL	3.3 mL
Tris-HCl (0.5 M, pH 6.8)	2.5 mL	2.5 mL
SDS (10% w/v)	100 µL	100 µl
TEMED	10 µl	10 µl
Ammonium persulfate (10% w/v)	100 µl	32 µl

Protein sample (15 µl) was mixed with 5 µl of 4x protein loading dye and heated at 70˚C for 10 mins, before loading. Electrophoresis was performed at 200V for 45 mins. Gels were stained with Coomassie Brilliant Blue G-250 from Bio-Rad (CA, USA) for 20 mins and de-stained with SDS-PAGE de-stain solution (30% v/v methanol, 10% v/v glacial acetic acid). A broad range of protein marker (10-200 kDa) from Thermo Fischer Scientific was used to determine the relative molecular weight.

3.8.11 Acetophenone assay

A kinetic assay developed from Schatzle *et al.* 2009,[177] was used as a standard enzymatic assay employing pyruvate and *S*-phenylethylamine ((*S*)-PEA) as amine acceptor and donor, respectively. The reactions were carried

out at 25°C in 1 mL HEPES buffer (50 mM, pH 8.0) containing 2.5 mM pyruvate, 2.5 mM (*S*)-PEA and appropriate amount of enzyme. The activity was determined by following the production of acetophenone during the first two minutes of reaction at 245 nm using the spectrophotometer EPOCH2.

3.8.12 Colony based solid-phase ATA assay

Colonies of transformed *E. coli* or *C. glutamicum* were grown at 30°C overnight on LB agar supplemented with selection antibiotic. Under sterile conditions, colonies were transferred onto a cellulose membrane, placed on top of filter papers soaked with 1 mM IPTG (for induction) and incubated at 30°C for 24 hours. Subsequently, the membrane was transferred onto filter papers soaked in a solution of *o*-xylylenediamine (10 mM) and pyruvate (10 mM) and allowed to react at room temperature. ATA activity was detected in the form of colored colonies, after 0.5, 8 and 24 hours.

3.8.13 Analytical scale biotransformations

3.8.13.1 In vitro biotransformations

To a solution of PLP (0.1 mM), ketone substrate (5 mM from a 500 mM stock in DMSO) and amine donor (1,2,3 or 5 equiv.) in phosphate (100 mM, pH 7-8), or HEPES (100 mM, pH 7-8) or Tris buffer (100 mM, pH 9-10), the pH was adjusted, depending on the enzyme used. To this, clarified extract of the ATA (1.5 mg/mL) was added and reactions were incubated at 30°C shaking at 200 rpm in a gyratory incubator. After 24 hours the reactions were basified (pH 12), extracted with EtOAc (750 µL), derivatized with 10 µL triethylamine and 10 µL acetic anhydride and analyzed by GC-FID, following the method that has been previously described in section 2.6.4, and conversions were measured as described in section 2.6.5.

3.8.13.2 In vitro biotransformation with conditioned medium

Cultures of *C. glutamicum* NA6 or GRLys1 were grown as mentioned in 3.8.1 and an aliquot was taken after 24 hours and 48 hours. To 1 mL of one-day or two-day mature culture media, PLP (0.1 mM), 1-phenyl-1,4-pentanedione (5 mM from 500 mM stock in DMSO) and purified ATA extract (1 mg mL^{-1}) were added and the reaction mixture was incubated at 30 °C shaking at 200 rpm. After 24 hours the reactions were basified (pH 12), extracted with EtOAc (750 µL), derivatized with 10 µL triethylamine and 10 µL acetic anhydride and analyzed by GC-FID, following the method that has been previously described in section 2.6.4, and conversions were measured as described in section 2.6.5.

3.8.13.3 Whole cell biotransformations

Transformants of *C. glutamicum* were grown as described in 3.8.1. After 24h the cells were either used directly or harvested *via* centrifugation (4000 rpm, 7 mins) and resuspended in media or HEPES buffer in different concentrations (50, 100, 150 and 200 mg mL^{-1}). To this, 1-phenyl-1,4-pentanedione (5 mM from 500 mM stock in DMSO) was added and the reaction mixture was incubated at 30°C shaking at 200 rpm. After 24 hours the reaction was pelleted *via* centrifugation and the cells were reused, where specified. The supernatant was basified (pH 12), extracted with EtOAc (750 µL), derivatized with 10 µL triethylamine and 10 µL acetic anhydride and analyzed by GC-FID, following the method that has been previously described in section 2.6.4, and conversions were measured as described in section 2.6.5.

3.8.14 Preparative scale biotransformation of **27**

Multiple pre-cultures of 50 mL of *C. glutamicum* GRLys1 with the pVWEx1-*ldcC*-PcATA, in BHIS were prepared. A main culture of 800 mL mCGXII (starting OD_{600} = 1) supplemented with 50 µg mL^{-1} kanamycin was induced

with 1 mM IPTG and incubated at 30°C shaking at 200 rpm. After 24h, the cells were pelleted *via* centrifugation (4000 rpm, 7 mins), washed with mCGXII (3x20 mL) and resuspended in 140 mL HEPES buffer (100 mM, pH 8.0) at a final concentration of 150 mg mL^{-1} WCP. To this, a solution of 1-phenyl-1,4-pentanedione **27** (130 uL, 738 µmol) in 10 mL DMSO was added and the reaction mixture was incubated at 30°C shaking at 200 rpm. After 24h, an aliquot was extracted and analyzed by GC-FID (as described in 3.6.5). The reaction mixture was centrifuged (4000 rpm, 15 mins) and the supernatant was clarified *via* filtration (0.45 µm filter), basified with NaOH (pH 12.0) and extracted with EtOAc (4x50 mL). The combined organic extracts were dried over $MgSO_4$ and the volatiles were removed under reduced pressure. The mixture was purified in silica gel utilizing petrol:dichloromethane (10:90) affording **28** as a light yellow oil (50 mg, 42% yield).

28. (*S*)-5-methyl-2-phenyl-1-pyrroline[179]

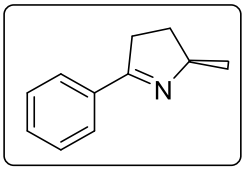

Light yellow liquid (50 mg, 42%) ^{1}H NMR (400 MHz, Chloroform-d) δ 7.84 (dd, J = 7.5, 2.1 Hz, 2H), 7.44 – 7.35 (m, 3H), 4.35 – 4.25 (m, 1H), 3.06 (dddd, J = 16.8, 9.9, 4.8, 2.1 Hz, 1H), 2.89 (dddd, J = 17.0, 9.6, 7.7, 1.8 Hz, 1H), 2.25 (dddd, J = 12.5, 9.8, 7.6, 4.8 Hz, 1H), 1.59 – 1.52 (m, 1H), 1.37 (d, J = 6.8 Hz, 3H). ^{13}C NMR (101 MHz, $CDCl_3$) δ 172.0, 134.5, 130.4, 128.4, 127.7, 68.3, 35.2, 30.6, 22.1. IR (ART cm^{-1}) 2961, 2925. MS (EI) m/z: calculated C11H14N $[M+H]^+$ 160.1121; found: 160.1137. $[a]_D^{25} = -108.4$ (c 2.0, $CHCl_3$ lit: [179]). Data consistent with the literature.[179]

4: Overall conclusion and future work

Chiral amines are important building blocks in a variety of pharmaceutical compounds and natural products and hence their synthesis is of great importance to both industry and the academic community.[26] There is growing interest in the use of more sustainable methods for the synthesis of chiral amines, and amine transaminase (ATA) biocatalysts offer an attractive alternative to more traditional chemical synthesis or catalysis.[50-52] Despite their potential, the widespread use of these enzymes has been hampered for a number of reasons, including difficulties associated with displacing the challenging reaction equilibrium towards product formation.[50-52] As a result, recent endeavors to overcome this problem have led to the development of various novel methodologies, including displacing the equilibrium *via* the use of 'smart' amine donors, such as *o*-xylylenediamine[130] and cadaverine.[131, 200, 201] The application of 'smart' amine donors in ATA reactions is relatively new, therefore one of the aims of this PhD project, described in **chapter 2**, was the development of a facile route for chiral amine production utilizing these donors with commercially available ATAs._The approach was successfully used to synthesize chiral amines that are difficult to isolate or synthesize using more traditional chemical approaches. A rapid *o*-xylylenediamine assay, [130] combined with the use of lower-cost cadaverine for scale-up, was employed for the production of chiral amines on a multi-milligram scale (up to X mgs). The use of readily available reagents and enzymes makes this approach accessible to the wider research community and helps expand the existing variety of chiral amines commercially available.

Additionally, the application of *o*-xylylenediamine for high-throughput screening is reinforced, as more than four hundred compounds were assayed in this study. Color change indicative of activity, is observed within hours, without requiring additional analysis. It was showed that

commercially available ATA256 performs better with small (MW <200) carbonyl substrates and poorly with larger (MW >200) structures and identified the maximum molecular weight range accepted within the active site of ATA256. Researchers can utilize this screen to rapidly examine the carbonyl substrate scope of any ATA, while also extracting experimental information relating to the space available in the active site. However, the results should be carefully examined, as false positive color change was observed for low conversions. These findings (**chapter 2**) agree with previous reports in the literature[130] indicating that further optimization is required to make the screen more reliable.

With the aim of broadening the application of smart diamine donors, **chapter 3** sought to develop a self-sufficient whole-cell system for ATA reactions, where the catalysts, donor and coenzyme are supplied by the engineered host cell, *C. glutamicum*. A panel of wild-type ATAs were screened against various diamines and carbonyl substrates and othe results matched previously reported observations[201] when high amounts of purified ATAs were used. Diamines produced from *C. glutamicum* were successfully used for the transamination of a model ketone substrate. This organism has been metabolically engineered to grow in defined minimal media and produce cadaverine[156] or putrescine,[154] which further reduces the operational cost of ATA catalysis. The methodology has enormous potential for the production of high-value chiral amines in engineered *C. glutamicum*, but further studies with a variety of carbonyl substrates and ATAs at different concentrations are required to assess the scope of this approach.

An interesting aspect of **chapter 3** were the difficulties encountered with the expression of the widely used ATA, 3HMU, in *C. glutamicum*. The ATA was codon optimized for expression in the organism and tests with inactive mutants indicated potential problems at a transcriptional level. Further

studies on an RNA level could shed light as to whether there is an internal signal for transcriptional termination. This problem was observed only for 3HMU, as the rest of the ATAs were successfully expressed in *C. glutamicum*. One of the ATAs (HEWT) tested does not accept ketone substrates and thus a model aldehyde was employed. The alcohol side-product was predominantly formed, which can be attributed to endogenous ADH activity. In this study, the host cell, *C. glutamicum*, expresses a number of endogenous ADHs[190-194] and AldDHs,[195,196] which can act on the aldehyde substrate and hamper the ATA reaction. Silencing the genes for ADH and AldDH expression could help overcome this problem, but the viability of the new strains could also be compromised. Future experiments could focus on metabolic engineering and the generation of a modified host cell for the transamination of aldehydes.

The self-sufficient whole-cell system was successfully developed with three putrescine ATAs (PcATA, PfATA and PpATA) [200, 201] for the transamination of a model ketone substrate (chapter 3). New strains with enhanced ATA production were generated and the reaction conditions optimized for the conversion of a model substrate to its corresponding imine with 42% isolated yield. This represents a cost-effective way of synthesizing chiral products, as both biocatalyst, diamine substrate and coenzyme are produced by the bacterial host growing in defined minimal media. Future studies will focus on testing a wider range of substrates and increasing the concentration of carbonyl employed, in order to broaden the utility of this system. Potential problems with poor diffusion of ketones and chiral amines through the membrane can be overcome by restructuring the ATA as a membrane protein and catalyze the reaction on the surface of the bacteria. This could also help overcome problems associated with the intracellular pH, as the ATAs used in this study are less active at neutral pH, thus limiting their capabilities within the cell. It could be possible to maintain physiological pH while the bacteria are growing and then switch to a more suitable pH for the ATA biotransformation. The whole-cell system

presented in chapter 3 utilizes a single vector (pVWEx1), but additional enzymes could be co-expressed using a compatible vector (pEKEx3) to facilitate enzymatic cascades.

A. Appendix

A.1 Supplementary material to 'Application of smart amine donors for the production and commercialization of chiral amines'

Table A.1.1. *Conversions of ketones* ***1-13*** *using ATA256*

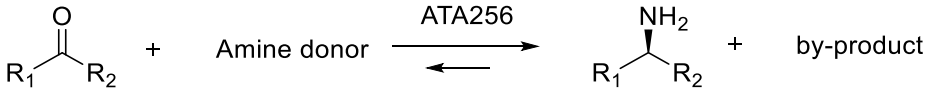

ketone	R_1	R_2	Conversion (%)			
			1 eq Cad.	3 eq Cad.	1 eq IPA	3 eq IPA
1	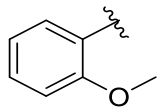	Me	79	98	43	71
2	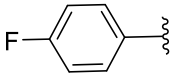	Et	39	33	27	35
3	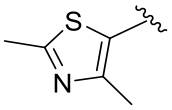	Me	n.d.	n.d.	n.d.	n.d.
4	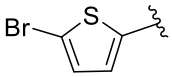	Me	43	42	7	7
5	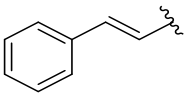	Me	19	29	10	18
6	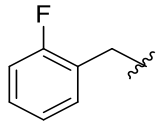	Me	77	92	29	26
7	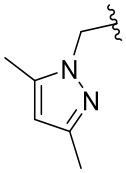	Me	n.d.	n.d.	n.d.	n.d.
8	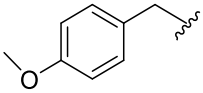	Me	79	99	44	72
9	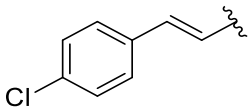	Me	n.d.	n.d.	n.d.	n.d.

A.2 Supplementary material to 'development of self-sufficient whole-cell biocatalyst for chiral amine synthesis'

A.2.1 Activity measurement through acetophenone assay

The acetophenone assay was first described by Schätzle et al. 2009, as a spectrophotometric assay for the rapid characterization of ω-TAs.[177] It is based on the conversion of S-PEA to acetophenone, utilizing pyruvate as amine acceptor. The formation of acetophenone over time is monitored by detecting its absorbance at 245 nm over time with high sensitivity (ε = 12 $mM^{-1}cm^{-1}$) [177]. The rate of the absorbance is converted to concentration of acetophenone, following the Beer-Lambert law shown below:

$$A = \varepsilon * l * C$$

A: absorption

ε: extinction co-efficient factor (equals to 12 $mM^{-1}cm^{-1}$ for acetophenone)[177]

l: pathlength (equals to 1 cm in this case)

C: concentration of acetophenone

Over time, the above equation is written as:

$$\frac{dA}{dt} = \varepsilon * l * \frac{dC}{dt}$$

The linear increase of absorbance over time is measured during the assay, i.e. the dA/dt with units $(min)^{-1}$. Thus, the concentration of acetophenone produced over time (dC/dt) can be calculated by the equation:

$$\frac{dC}{dt} = \frac{\frac{dA}{dt}}{\varepsilon * l}$$

The amount of acetophenone (µmoles) produced over time can be calculated by incorporating the volume:

$$\frac{dn}{dt} = \left(\frac{dC}{dt}\right) * V * DF$$

dn/dt: µmoles acetophenone over time

V: volume of reaction (equals to 1 mL in this study)

DF: dilution factor [DF = (volume of reaction/ volume of enzymatic extract added)]

One unit of activity is defined as the amount of enzyme required to produce 1 µmol acetophenone in 1 minute and thus is calculated from the equation:

$$specific\ activity = \frac{\frac{dn}{dt}}{amount\ in\ mg\ of\ enzyme\ in\ 1\ mL\ extract}$$

A.2.2 Estimation of the amount of HEWT (mg) in clarified extract

Cerioli *et al*. 2015, have already characterized HEWT with reported specific activity of 2.96 U per mg of purified HEWT measure by the acetophenone assay.[189]Thus, it is safe to assume that:

1 mg of purified HEWT has activity equal to 2.96 U

To optimize the expression of HEWT, the amount of HEWT produced from a 20 mL culture of *C. glutamicum* was estimated. *C. glutamicum* cultures were prepared as previously described (see section 3.8.8). The total amount of protein and activity of the clarified extract were determined as described in section 3.8.10 and 3.8.11, respectively. Assuming the activity is generated solely due to the overexpressed ATA, an immediate correlation between the amount of HEWT and activity can be drawn. For clarity, an example is described below;

A 20 mL culture of *C. glutamicum* induced with 1 mM IPTG, afforded 3 mL of clarified extract. The concentration of the total protein in this extract was found 0.121 mg/mL with a relative activity of 0.014 U per 1 mL of clarified extract. The relative activity is divided by the concentration of total protein:

$$Activity\ of\ extract\ \left(\frac{U}{mg\ total\ protein}\right) = \frac{relative\ activity\ \left(\frac{U}{mL}\right)}{concentration\ (\frac{mg}{mL})}$$

In this example, this would be: Activity = (0.014/0.121) = 0.115 U per mg of total protein. Meaning, 1 mg of total protein (from the clarified extract) affords 0.115 U.

It is known that 1 mg of pure HEWT afford 2.96 U.

Assuming the activity observed in the clarified extract stems only from HEWT overproduced, then:

$$mg\ HEWT\ (in\ extract) = \frac{Activity\ of\ extract\ (\frac{U}{mg})}{HEWT\ specific\ activity\ (\frac{U}{mg})} * 1\ mg$$

In this example; The amount of HEWT in 1 mL of clarified extract equals to (0.115/2.96)*1 = 0.039 mg HEWT.

A.2.3 Statistical analysis

The statistical analysis of results from experiments focused on optimizing the production of HEWT and yield of whole cell system are described below.

A.2.3.1 Analysis of variants (ANOVA) on experiments focused on increasing production of transaminase HEWT

Null hypothesis (1): Increase of IPTG concentration will lead in increased production of HEWT.

a) On wild-type *C. glutamicum* overexpressing HEWT from pEKEx3 vector at different IPTG concentrations.

Table A.2.3.1.1. a) *The amount (mg) of HEWT produced from wild-type C. glutamicum harboring the insert in pEKEx3 vector, induced with different IPTG concentration and incubated at 30˚C for 16h, and* ***b)*** *the results from the ANOVA analysis*.

a) Samples

Replicate	mg HEWT with IPTG conc.		
	0.1 mM	1 mM	5 mM
1	0.002957	0.00319	0.006584
2	0.012279	0.009065	0.012799
3	0.010676	0.008655	0.010672

b) ANOVA results

Source of Variation	*SS*	*df*	*MS*	*F*	*P-value*	*F crit*
Between Groups	1.4E-05	2	6.99E-06	0.460	0.652	5.143
Within Groups	9.12E-05	6	1.52E-05			
Total	0.0001	8				

b) On *C. glutamicum* NA6 overexpressing HEWT from pEKEx3 vector at different IPTG concentrations.

Table A.2.3.1.2. a) *The amount (mg) of HEWT produced from C. glutamicum NA6 harboring the insert in pEKEx3 vector, induced with different IPTG concentration and incubated at 30˚C for 16h, and* ***b)*** *the results from the ANOVA analysis.*

a) Sample

Replicate	mg HEWT with IPTG conc.		
	0.1 mM	1 mM	5 mM
1	0.003455	0.005886	0.00568
2	0.006227	0.008487	0.009451
3	0.009821	0.012899	0.012061

b) ANOVA results

Source of Variation	*SS*	*df*	*MS*	*F*	*P-value*	*F crit*
Between Groups	1.33E-05	2	6.64E-06	0.602	0.578	5.143
Within Groups	6.61E-05	6	1.1E-05			
Total	7.94E-05	8				

c) On *C. glutamicum* GRLys1 overexpressing HEWT from pEKEx3 vector at different IPTG concentrations.

Table A.2.3.1.3. a) *The amount (mg) of HEWT produced from C. glutamicum GRLys1 harboring the insert in pEKEx3 vector, induced with different IPTG concentration and incubated at 30˚C for 16h, and* ***b)*** *the results from the ANOVA analysis.*

a) Samples

Replicate	mg HEWT with IPTG conc.		
	0.1 mM	1 mM	5 mM
1	0.006875	0.002545	0.009317
2	0.011455	0.013774	0.014175
3	0.00898	0.014553	0.013207

b) ANOVA results

Source of Variation	*SS*	*df*	*MS*	*F*	*P-value*	*F crit*
Between Groups	1.5E-05	2	7.49E-06	0.394	0.691	5.143
Within Groups	0.000114	6	1.9E-05			
Total	0.000129	8				

A table with a summary of all samples and ANOVA results is presented below.

Table A.2.3.1.4. *A summary of the amounts (mg) of HEWT produced from the different strains of C. glutamicum induced with different IPTG concentration and incubated at 30˚C for 16h, and the corresponding P-values derived from statistical analysis.*

Strain	Replicate	mg HEWT with IPTG conc.			*P-value*
		0.1 mM	1 mM	5 mM	
WT	1	0.002957	0.00319	0.006584	0.652
	2	0.012279	0.009065	0.012799	
	3	0.010676	0.008655	0.010672	
NA6	1	0.003455	0.005886	0.00568	0.578
	2	0.006227	0.008487	0.009451	
	3	0.009821	0.012899	0.012061	
GRLys1	1	0.006875	0.002545	0.009317	0.691
	2	0.011455	0.013774	0.014175	
	3	0.00898	0.014553	0.013207	

The null hypothesis (1) is rejected, since the P-value in all cases is higher than 0.05. Thus, increasing the IPTG concentration does not lead to statistically significant increase in HEWT production.

<u>Null hypothesis (2)</u>: Increase of incubation time of IPTG-induced cultures at 30 ˚C will lead in increased production of HEWT.

a) On Wild-type *C. glutamicum* overexpressing HEWT from pEKEx3 vector and 1 mM IPTG, incubated at 30˚C for 16h or 32h.

Table A.2.3.1.5. a) *The amount (mg) of HEWT produced from wild-type C. glutamicum harboring the insert in pEKEx3 vector, induced with 1 mM IPTG and incubated for different time lengths at 30˚C, and* ***b)*** *the results from the ANOVA analysis.*

a) Samples

Replicate	mg HEWT after expressing for	
	16h	32h
1	0.00319	0.003014
2	0.009065	0.001318
3	0.008655	0.004292

b) ANOVA results

Source of Variation	*SS*	*df*	*MS*	*F*	*P-value*	*F crit*
Between Groups	2.52E-05	1	2.52E-05	3.875	0.120	7.709
Within Groups	2.6E-05	4	6.49E-06			
Total	5.11E-05	5				

b) On *C. glutamicum* NA6 overexpressing HEWT from pEKEx3 vector and 1 mM IPTG, incubated at 30˚C for 16h or 32h.

Table A.2.3.1.6. a) *The amount (mg) of HEWT produced from C. glutamicum NA6 harboring the insert in pEKEx3 vector, induced with 1 mM IPTG and incubated for different time lengths at 30˚C, and* ***b)*** *the results from the ANOVA analysis.*

a) Samples

Replicate	mg HEWT after expressing for	
	16h	32h
1	0.005886	0.002669
2	0.008487	0.000971
3	0.012899	0.002722

b) ANOVA results

Source of Variation	*SS*	*df*	*MS*	*F*	*P-value*	*F crit*
Between Groups	7.29E-05	1	7.29E-05	10.745	0.031	7.709
Within Groups	2.71E-05	4	6.78E-06			
Total	1E-04	5				

From the table above, the *P-value* is lower than 0.05, thus deemed significant. In this case, a Bonferroni post-hoc analysis is required, where a new threshold for significant *P-value* is set following the equation below.

$$a' = a/n$$

α': Bonferroni-corrected p-value
α = 0.05
n: number of tests performed (i.e. number of groups comparing)

In the above experiment two groups (16h and 32h of induction) were examined and so, the new threshold is:

$$a' = \frac{0.05}{2} = 0.025$$

The *P-value* from the ANOVA analysis is higher than 0.025, and so it is not significantly important.

c) On *C. glutamicum* GRLys1 overexpressing HEWT from pEKEx3 vector and 1 mM IPTG, incubated at 30˚C for 16h or 32h.

Table A.2.3.1.7. a) *The amount (mg) of HEWT produced from C. glutamicum GRLys1 harboring the insert in pEKEx3 vector, induced with 1 mM IPTG and incubated for different time lengths at 30˚C, and* ***b)*** *the results from the ANOVA analysis.*

a) Samples

Replicate	mg HEWT after expressing for	
	16h	32h
1	0.002545	0.015494
2	0.013774	0.001225
3	0.014553	0.003564

b) ANOVA results

Source of Variation	*SS*	*df*	*MS*	*F*	*P-value*	*F crit*
Between Groups	1.87E-05	1	1.87E-05	0.360	0.581	7.709
Within Groups	0.000207	4	5.19E-05			
Total	0.000226	5				

A table with a summary of all samples and ANOVA results is presented below.

Table A.2.3.1.8. *A summary of the amounts (mg) of HEWT produced from the different strains of C. glutamicum induced 1 mM IPTG and incubated at 30˚C for 16h or 32h, and the corresponding P-values derived from statistical analysis.*

Strain	Replicate	mg HEWT after expressing for		*P-value*
		16h	32h	
WT	1	0.00319	0.003014	0.120
	2	0.009065	0.001318	
	3	0.008655	0.004292	
NA6	1	0.005886	0.002669	0.031
	2	0.008487	0.000971	
	3	0.012899	0.002722	
GRLys1	1	0.002545	0.015494	0.581
	2	0.013774	0.001225	
	3	0.014553	0.003564	

After a Bonferroni post-hoc analysis, the null hypothesis (2) is rejected, thus expression of HEWT for longer incubation times does not lead to significant increase in HEWT production.

Null hypothesis (3): Incorporating a second copy of the gene in the plasmid, will lead in increased production of HEWT.

a) On wild-type *C. glutamicum* expressing HEWT from pEKEx3 with either one or two copies of the gene, including or not a second copy of the promoter and terminator sequence.

Table A.2.3.1.9. a) *The amount (mg) of HEWT produced from wild-type C. glutamicum harboring one or two copies of the insert in pEKEx3 vector, induced with 1 mM IPTG and incubated at 30˚C for 16h, and* ***b)*** *the results from the ANOVA analysis.*

a) Samples

Replicate	mg of HEWT from gene insert		
	HEWT	HEWTx2	pHEWTtx2
1	0.00319	0.024177	0.039
2	0.009065	0.019	0.044
3	0.008655	0.022	0.037

b) ANOVA results

Source of Variation	*SS*	*df*	*MS*	*F*	P-value	*F crit*
Between Groups	0.001643	2	0.000821	80.740	4.6E-05	5.143
Within Groups	6.1E-05	6	1.02E-05			
Total	0.0017	8				

From the table above, the *P-value* is well below 0.05, thus deemed significant. In this case, a Bonferroni post-hoc analysis is required, where a new threshold for significant *P-value* is set. In the above experiment 3 groups were examined (HEWT, HEWTx2, pHEWTtx2) and so, the new threshold is:

$$a' = \frac{0.05}{3} = 0.0167$$

The *P-value* from the ANOVA analysis is below 0.0167, thus the groups compared are significantly different, and so the null hypothesis is confirmed.

b) On *C. glutamicum* NA6 strains expressing HEWT from pEKEx3 with either one or two copies of the gene, including or not a second copy of the promoter and terminator sequence.

Table A.2.3.1.10. a) *The amount (mg) of HEWT produced from C. glutamicum NA6 harboring one or two copies of the insert in pEKEx3 vector, induced with 1 mM IPTG and incubated at 30˚C for 16h, and* ***b)*** *the results from the ANOVA analysis.*

a) Samples

Replicate	mg of HEWT from gene insert		
	HEWT	HEWTx2	pHEWTtx2
1	0.005886	0.027804	0.037618
2	0.008487	0.032	0.0428
3	0.012899	0.026	0.034

b) ANOVA results

Source of Variation	*SS*	*df*	*MS*	*F*	P-value	*F crit*
Between Groups	0.001315	2	0.0006	47.419	0.0002	5.143
Within Groups	8.32E-05	6	1.39E-05			
Total	0.001399	8				

From the table above, the *P-value* is well below 0.05, thus deemed significant. In this case, a Bonferroni post-hoc analysis is required, where a new threshold for significant *P-value* is set. In the above experiment 3

groups were examined (HEWT, HEWTx2, pHEWTtx2) and so, the new threshold is:

$$a' = \frac{0.05}{3} = 0.0167$$

The *P-value* from the ANOVA analysis is below 0.0167, thus the groups compared are significantly different, and so the null hypothesis is confirmed.

c) On *C. glutamicum* GRLys1 strains expressing HEWT from pEKEx3 vector with either one or two copies of the gene, including or not a second copy of the promoter and terminator sequence.

Table A.2.3.1.11. a) *The amount (mg) of HEWT produced from C. glutamicum GRLys1 harboring one or two copies of the insert in pEKEx3 vector, induced with 1 mM IPTG and incubated at 30˚C for 16h, and* ***b)*** *the results from the ANOVA analysis.*

a) Samples

Replicate	mg of HEWT from gene insert		
	HEWT	HEWTx2	pHEWTtx2
1	0.002545	0.015	0.019368
2	0.013774	0.0187	0.021
3	0.014553	0.013	0.017

b) ANOVA results

Source of Variation	*SS*	*df*	*MS*	*F*	P-value	*F crit*
Between Groups	0.000118	2	5.92E-05	3.088	0.120	5.143
Within Groups	0.000115	6	1.92E-05			
Total	0.000234	8				

A table with a summary of all samples and ANOVA results is presented below.

Table A.2.3.1.12. *A summary of the amounts (mg) of HEWT produced from the different strains of C. glutamicum harboring one or two copies of the insert in pEKEx3, induced 1 mM IPTG and incubated at 30˚C for 16h, and the corresponding P-values derived from statistical analysis.*

Strain	Replicate	mg HEWT from gene insert			*P-value*
		HEWT	HEWTx2	pHEWTtx2	
WT	1	0.00319	0.024177	0.039	4.6E-05
	2	0.009065	0.019	0.044	
	3	0.008655	0.022	0.037	
NA6	1	0.005886	0.027804	0.037618	0.0002
	2	0.008487	0.032	0.0428	
	3	0.012899	0.026	0.034	
GRLys1	1	0.002545	0.015	0.019368	0.120
	2	0.013774	0.0187	0.021	
	3	0.014553	0.013	0.017	

After a Bonferroni post-hoc analysis, the null hypothesis (3) is confirmed for wild-type and NA6 *C. glutamicum* strains, thus using two copies of HEWT in pEKEx3 vector leads to statistically significant increase in HEWT production.

A.2.3.2 Analysis of variants (ANOVA) on experiments focusing on increasing yield of whole cell system

Null hypothesis (4): Increased amounts of transaminase (from incorporating a second copy or using a high copy number plasmid) will lead to increased yield

a) On *C. glutamicum* NA6 strains expressing pcATA from pEKEx3 with either one or two copies of the gene, or pVWEx1 with a single copy of the gene.

Table A.2.3.2.1. a) *The conversion (%) of* ***27*** *to* ***28*** *utilizing whole cells of C. glutamicum NA6 expressing pcATA from pEKEx3 with a single or two copies of the insert, or from pVWEx3 with a single copy, and* ***b)*** *the results from the ANOVA analysis.*

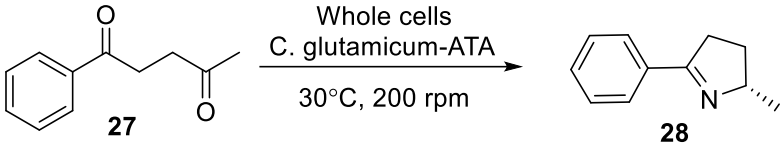

a) Samples

Replicate	Conversion (%) with plasmid		
	pEKEx3-pcATA	pEKEx3-pcATAx2	pVWEx1-pcATA
1	9	22	11
2	11	22	7
3	7	22	4

b) ANOVA results

Source of Variation	*SS*	*df*	*MS*	*F*	P-value	*F crit*
Between Groups	386.8889	2	193.4444	35.531	0.00047	5.1432
Within Groups	32.66667	6	5.444444			
Total	419.5556	8				

From the table above, the *P-value* is well below 0.05, thus deemed significant. In this case, a Bonferroni post-hoc analysis is required, where a new threshold for significant *P-value* is set. In the above experiment 3 groups are examined (pEKEx3-HEWT, pEKEx3-HEWTx2, pVWEx1-HEWT) and so, the new threshold is:

$$a' = \frac{0.05}{3} = 0.0167$$

The *P-value* from the ANOVA analysis is below 0.0167, thus the groups compared are significantly different, and so the null hypothesis is confirmed.

b) On *C. glutamicum* GRLys1 strains expressing pcATA from pEKEx3 with either one or two copies of the gene, or pVWEx1 with a single copy of the gene.

Table A.2.3.2.2. a) *The conversion (%) of* ***27*** *to* ***28*** *utilizing whole cells of C. glutamicum GRLys1 expressing pcATA from pEKEx3 with a single or two copies of the insert, or from pVWEx3 with a single copy, and* ***b)*** *the results from the ANOVA analysis.*

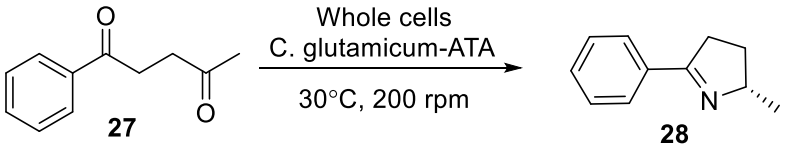

a) Samples

Replicate	Conversion (%) with plasmid		
	pEKEx3-pcATA	pEKEx3-pcATAx2	pVWEx1--pcATA
1	12	14	31
2	18	17	41
3	7	10	35

b) ANOVA results

Source of Variation	*SS*	*df*	*MS*	*F*	P-value	*F crit*
Between Groups	1030.222	2	515.111	22.725	0.0016	5.143
Within Groups	136	6	22.667			
Total	1166.222	8				

From the table above, the *P-value* is well below 0.05, thus deemed significant In this case, a Bonferroni post-hoc analysis is required, where a new threshold for significant *P-value* is set. In the above experiment 3 groups are examined (pEKEx3-HEWT, pEKEx3-HEWTx2, pVWEx1-HEWT) and so, the new threshold is:

$$a' = \frac{0.05}{3} = 0.0167$$

The *P-value* from the ANOVA analysis is below 0.0167, thus the groups compared are significantly different, and so the null hypothesis is confirmed.

Table A.2.3.2.3. *A summary of conversion (%) of* ***27*** *to* ***28*** *utilizing whole cells of C. glutamicum GRLys1 or NA6, expressing pcATA from pEKEx3 with a single or two copies of the insert, or from pVWEx3 with a single copy, and the corresponding P-values derived from statistical analysis.*

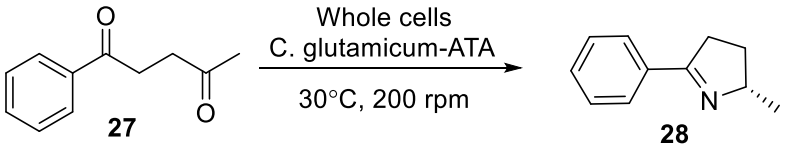

Strain	Replicate	Conversion (%) with plasmid			*P-value*
		pEKEx3-pcATA	pEKEx3-pcATAx2	pVWEx1-pcATA	
NA6	1	9	22	11	0.000472
	2	11	22	7	
	3	7	22	4	
GRLys1	1	12	14	31	0.001586
	2	18	17	41	
	3	7	10	35	

After a Bonferroni post-hoc analysis, the null hypothesis (4) is confirmed for *C. glutamicum NA6 and GRLys1* strains, thus increasing the amount of transaminase with double copy (HEWTx2) or high copy-number plasmid (pVWEx1) leads to statistically significant increase in yield (%).

<u>Null hypothesis (5):</u> Increased cell density will lead to increased yield

Table A.2.3.2.4. a) *The conversion (%) of* ***27*** *to* ***28*** *utilizing different cell density (mg/mL) whole cells of C. glutamicum GRLys1 expressing pcATA from pVWEx3 with a single copy, and* ***b)*** *the results from the ANOVA analysis.*

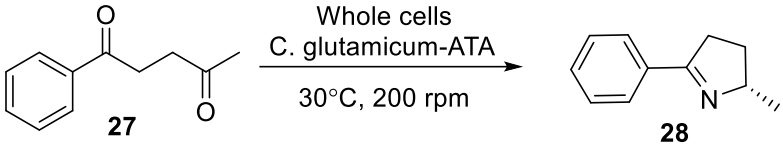

a) Samples

Replicate	Conversion (%) with cell density			
	50 mg/mL	100 mg/mL	150 mg/mL	200 mg/mL
1	49	64	75	76
2	45	63	72	76
3	44			78

b) ANOVA results

Source of Variation	*SS*	*df*	*MS*	*F*	*P-value*	*F crit*
Between Groups	1633.93	3	544.644	150.825	4.88E-06	4.757
Within Groups	21.667	6	3.611			
Total	1655.6	9				

From the table above, the *P-value* is well below 0.05, thus deemed significant. In this case, a Bonferroni post-hoc analysis is required, where a new threshold for significant *P-value* is set. In the above experiment 4 groups are examined (cell densities: 50, 100, 150 and 200 mg/mL) and so, the new threshold is:

$$a' = \frac{0.05}{4} = 0.0125$$

The *P-value* from the ANOVA analysis is below 0.0125, thus the groups compared are significantly different, and so the null hypothesis is confirmed.

A.2.4 Supplementary data

Table A.2.4.1. *Conversions of ketone* ***28*** *utilizing clarified extract of (R) or (S) ATAs.*

Selectivity	ATA	Conversion (%)			
		cadaverine	Putrescine	o-xylylene diamine	IPA
S	ChrVio	2	8	7	10
	3I5T	10	14	7	6
	VibFlu	n.d.	n.d.	6	2
	3HMU	19	21	20	19
R	MycVan	n.d.	n.d.	5	n.d.
	AspFum	n.d.	n.d.	n.d.	n.d.
	NeoFis	n.d.	n.d.	n.d.	n.d.

Table A.2.4.2. *Estimation of HEWT (in mg) in clarified extract of C. glutamicum strains cultivated in different expression conditions. Best results are highlighted in red (and presented in thesis).*

Strain	Insert(s)	Conditions	Average Amount of HEWT (mg)	StDev
Wild type	HEWT	0.1 mM IPTG/ 1 o.n.	0,009	0,004069
		1 mM IPTG/1 o.n.	0,007	0,002678
		5 mM IPTG/1 o.n.	0,010	0,002579
		0.1 mM IPTG/2 o.n.	0,006	0,00563
		1 mM IPTG/2 o.n.	0,003	0,001218
		5 mM IPTG/2 o.n.	0,002	0,000862
	HEWTx2	1 mM IPTG/1 o.n.	0,024	0,002
		1 mM IPTG/2 o.n.	0,002	0,001
	pHEWTtx2	1 mM IPTG/1 o.n.	0,040	0,004
		1 mM IPTG/2 o.n.	0,005	0,001
NA6	HEWT	0.1 mM IPTG/1 o.n.	0,007	0,003
		1 mM IPTG/1 o.n.	0,009	0,003
		5 mM IPTG/1 o.n.	0,009	0,003
		0.1 mM IPTG/2 o.n.	0,001	0,000
		1 mM IPTG/2 o.n.	0,002	0,001
		5 mM IPTG/2 o.n.	0,003	0,001
	HEWTx2	1 mM IPTG/1 o.n.	0,028	0,003
		1 mM IPTG/2 o.n.	0,004	0,001
	pHEWTtx2	1 mM IPTG/1 o.n.	0,038	0,004
		1 mM IPTG/2 o.n.	0,003	0,000
GRLys1	HEWT	0.1 mM IPTG/1 o.n.	0,009	0,002
		1 mM IPTG/1 o.n.	0,010	0,005
		5 mM IPTG/1 o.n.	0,012	0,002
		0.1 mM IPTG/2 o.n.	0,002	0,001
		1 mM IPTG/2 o.n.	0,007	0,006
		5 mM IPTG/2 o.n.	0,007	0,005
	HEWTx2	1 mM IPTG/1 o.n.	0,015	0,002
		1 mM IPTG/2 o.n.	0,001	0,000
	pHEWTtx2	1 mM IPTG/1 o.n.	0,019	0,002
		1 mM IPTG/2 o.n.	0,001	0,000

Table A.2.4.3. *Conversions of ketone* ***32*** *utilizing clarified extract of putrescine ATAs (Pc, Pf or Pp).*

Biocatalyst	Conversion			
	1 eq. Putrescine	3 eq. Putrescine	1 eq. Cadaverine	3 eq. Cadaverine
PcATA	20	41	43	75
PfATA	28	31	54	60
PpATA	24	49	53	66

Table A.2.4.4. *Conversions of ketone* ***32*** *from NA6 and GRLys1 strains with PcATA or PcATAx2 insert.*

Strain	Insert	Conversion (%)	
		1d	**2d**
NA6	PcATA	9	12
	PcATAx2	22	32
GRLys1	PcATA	12	17
	PcATAx2	14	20

Table A.2.4.5. *Conversions of ketone* ***32*** *from different cell densities of GRLys1-pVWEx1-ldcC-PcATA in different media. N/A: not available*

Cell density	Conversion (%)		
	Media culture	HEPES buffer	HEPES buffer + 0.1 mM PLP
50 mg/mL	46	51	N/A
100 mg/mL	64	73	N/A
150 mg/mL	74	75	N/A
200 mg/mL	77	77	76

Table A.2.4.6. *Conversion of* ***32*** *utilizing 100 mg mL^{-1} wet cell pellets of C. glutamicum GRLys1-pVWEx1-ldcC-PcATA in three consecutive cycles.*

Cycle	**Conversion (%)**
1	77
2	66
3	22

Table A.2.4.7. *Strains used in this study.*

Strain	Relevant characteristic	reference or source
E. coli DH5a	F- thi-1 endA1 hsdR17 (r m) supE44 DlacU169 (F80lacZDM15) recA1 gyrA96 relA1	New Englands Biolabs
E. coli BL21	F^- *ompT gal dcm lon* $hsdS_B(r_B^- m_B^-)$ λ(DE3 [*lacI lacUV5-T7p07 ind1 sam7 nin5*]) $[malB^+]_{K-12}(\lambda^S)$	New Englands Biolabs
C. Glutamicum ATCC 13032 (Wild type)	Wild type strains naturally overproducing L-lysine	American Type Culture Collection
C. Glutamicum GRLys1	WT carrying the pVWEx1-*ldcC* plasmid	this study
C. glutamicum NA2	in frame deletion of ArgR and argF, L-ornithine overproducing strain, derived from C. glutamicim ATCC13032; auxotrophic for L-arginine, replacement of start codon GTG to TTG for chromosomal odhA, carrying plamid pVWEx1-*speC*	[1]
C. glutamicum NA6	NA2, with chromosomal deletion of snaA, carrying pVWEx1-*speC*-gapA-pyc-argBA49V/M54V-argF21 instead of pVWEx1-*speC*	[1]

Table A.2.4.8. Plasmids used in this study.

Plasmid	Relevant characteristic	Reference or source
pET-22b	Amp-r; E. coli vector (PT7 lacI, pBR322-Ori)	lab stock
pET-22b-3HMU	derived from pET-22b, for regulated expression of 3HMU from S. pomeroyi	[2]
pET-22b-3I5T	derived from pET-22b, for regulated expression of 3I5T from R. sphaeroides KD131	[2]
pET-22b-ChrVio	derived from pET-22b, for regulated expression of ChrVio from C. violaceum	[3]
pET-22b-Vibflu	derived from pET-22b, for regulated expression of Vibflu from V. fluvialis	[4]

pET-22b-PcATA	derived from pET-22b, for regulated expression of PcATA from P. chlororaphis subsp. Aureofaceins	[5]
pET-22b-PpATA	derived from pET-22b, for regulated expression of PpATA from P. putida	[5]
pET-22b-AspFum	derived from pET-22b, for regulated expression of AspFum from A. fumigatus	[2]
pET-22b-NeoFis	derived from pET-22b, for regulated expression of NeoFis from N. fischeri	[2]
pET-28b	Km-r; E. coli vector (PT7 lacI, pBR322-Ori)	Lab stock
pET-28b-PfATA	derived from pET-28b, for regulated expression of PfATA from P. fluorescens	[5]
pRSET B	Amp-r; E. coli vector (PT7 lacI, pBR322-Ori)	[6]
pHEWT	derived from pHES-PUC, for regulated expression of HEWT from H. elongata	[6]
pGASTON	Amp-r; E. coli vector (Prha, pBR322-Ori)	[7]
pGASTON-MycVan	derived from pGASTON, for regulated expression of MycVan from M. vanbaalenii	[7]
pGASTON-AspORy	derived from pGASTON, for regulated expression of AspOry from A. oryzae	[8]
pEKEx3	*Spec*-r; C. glutamicum/E. coli (Ptac lacIq, pBL1 ori)	[9]
pEKEx3-3HMU	derived from pEKEx3, for regulated expressions of 3HMU from S. pomeroyi	this study
pEKEx3-GFP	derived from pEKEx3, for regulated expressions of GFP from A. victoria	this study
pEKEx3-3HMUK292A	derived from pEKEx3, for regulated expressions of 3HMU from S. pomeroyi, with catalytic lysine (K292) mutated to alanine	this study
pEKEx3-HEWT	derived from pEKEx3, for regulated expression of HEWT from H. elongata	this study
pEKEx3-pHEWTtx2	derived from pEKEx3, for regulated expression of double insert of HEWT from H. elongata under two separate pTac	this study
pEKEx3-HEWTx2	derived from pEKEx3, for regulated expression of double insert of HEWT from H. elongata	this study
pEKEx3-PcATA	derived from pEKEx3, for regulated expression of PcATA from P. chlororaphis subsp. Aureofaceins	this study

pEKEx3-PcATAx2	derived from pEKEx3, for regulated expression of double insert of PcATA from P. chlororaphis subsp. Aureofaceins	this study
pEKEx3-PfATA	derived from pEKEx3b, for regulated expression of PfATA from P. fluorescens	this study
pEKEx3-PpATA	derived from pEKEx3, for regulated expression of PpATA from P. putida	this study
pVWEx1	Km-r; C.glutamicum/E.coli shuttle vector (Ptac lacIQ, pCG ori)	[10]
pVWEx1-*ldcC*	derived from pVWEx1, for regulated expression of *ldcC* from E. coli MG1655	this study
pVWEx1-*speC*	derived from pVWEx1, for regulated expression of *speC* from E. coli MG1655	this study
pVWEx1-*speC*-gapA-pyc-argBA49V/M54V-argF21	derived from pVWEx1 for the regulated expression of argBA49B/M54V, pyc and gapA from C. glutamicum, *speC* from E. coli MG1655 and leaky expression of argF	[1]
pVWEx1-*ldcC*-PcATA	derived from pVWEx1, for regulated expression of *ldcC* from E. coli MG1655 and PcATA from P. chlororaphis subsp. Aureofaceins	this study
pVWEx1-*ldcC*-PfATA	derived from pVWEx1, for regulated expression of *ldcC* from E. coli MG1655 and PfATA from P. fluorescens	this study
pVWEx1-*ldcC*-PpATA	derived from pVWEx1, for regulated expression of *ldcC* from E. coli MG1655 and PpATA from P. putida	this study
pVWEx1-*speC*-PcATA	derived from pVWEx1, for regulated expression of *speC* from E. coli MG1655 and PcATA from P. chlororaphis subsp. Aureofaceins	this study
pVWEx1-*speC*-PfATA	derived from pVWEx1, for regulated expression of *speC* from E. coli MG1655 and PfATA from P. fluorescens	this study
pVWEx1-*speC*-PpATA	derived from pVWEx1, for regulated expression of *speC* from E. coli MG1655 and PpATA from P. putida	this study

Table A.2.4.9. *Primers used in this study.*

Primer Name	Sequence	Restr. site	Purpose
SG1_F	GCCTGCAGTCGACC*GAAAGGAGG ACAACC***ATG**AGCCTGGCGACCATTAC G	SalI	Cloning of 3HMU
SG2_R	GGTTCTAGAGGAGCTCGAATTCGG ATCCTTATTAGTGG	EcoRI	Cloning of 3HMU
SG3_F	GGTGTCGACC*GAAAGGAGGACAA CC***ATG**AGTAAAGGCGAAGAACTTTTC AC	SalI	Cloning GFP
SG4_R	GGTGGTGAATTCTTATTTGTATAGT TCATCCATGCCATGTGTAATC	EcoRi	Cloning GFP
SG5_F	CATATTATGACGATCGCAGCAGGT CTGAGTTCC	-	mutate K292A
SG6_R	GGAACTCAGACCTGCTGCGATCGT CATAATATG	-	mutate K292A
SG7_F	CTTGCATGCCTGCA*GAAAGGAGGT CGACC***ATG**CGGGGTTCTCATCATCAT		Cloning HEWT
SG8_R	CGAGCTCGGTACCCGGGGATCCAA TTCTCATGCGGTTGGCTCCTC		Cloning HEWT
SG9_F	GCCAAGCTTGCATGCCTGCA*GAAA GGAGGTCGACC***ATG**C	SalI	HiFi assembly (pEKEx3, HEWT twice)
SG10_R	CCACCGGTGGTGGTCTCATGCGGT TGGCTCCTC	-	HiFi assembly (pEKEx3, HEWT twice)
SG11_F	AACCGCATGAGACCACCACCGGTGGT GGTC*GAAAGGAGGTCGACC***ATG**C	SalI	HiFi assembly (pEKEx3, HEWT twice)
SG12_R	CTGTAAAACGACGGCCAGTGTCATGC GGTTGGCTCCTC	EcoRI	HiFi assembly (pEKEx3, HEWT twice)
SG13_F	TGCAGAAAGGAGGGTTGACAATTAAT CATCGG	-	HiFi assembly (pEKEx3,prom -HEWT-term twice)
SG14_R	CCACCGGTGGTGGTCCAAAAGAGTTT GTAGAAACG	-	HiFi assembly (pEKEx3,prom -HEWT-term twice)

SG15_F	AACTCTTTTGGACCACCACCGGTGG TGGTCGTTGACAATTAATCATCGG	-	HiFi assembly (pEKEx3,pro m-HEWT-term twice)
SG16_R	CTGTAAAACGACGGCCAGTGCAAAA GAGTTTGTAGAAACG	EcoRI	HiFi assembly (pEKEx3,pro m-HEWT-term twice)
SG17_F	GGTGTCGACC*GAAAGGAGGACAAC C***ATG**ATCAGCAACAATCCGCAAACC	SalI	Cloning pcATA
SG18_R	GGTGGTGAATTCGCCGGATCTCAGT GGTG	EcoRI	Cloning pcATA
SG19_F	GGTGTCGACC*GAAAGGAGGACAAC C***ATG**GGCAGCAGCCATCATC	SalI	Cloning pfATA & ppATA
SG20_R	GGTGGTGAATTCTTAGCCTTGCAAC GCACTGAGC	EcoRI	Cloning pfATA
SG21_R	GGTGGTGAATTCGCTACCGAATCGC CTCAAGG	EcoRI	Cloning ppATA
SG22_F	CAAGCTTGCATGCCTGCAGGTCGAC C*GAAAGGAGGACAAC*	SalI	HiFi assembly (pEKEx3, pcATA twice)
SG23_R	CGAACCACCGGTGGTTCATAGGTGG TGGTGGTG	-	HiFi assembly (pEKEx3, pcATA twice)
SG24_F	CCACCTATGAACCACCGGTGGTTCG ACC*GAAAGGAGGACAAC*	-	HiFi assembly (pEKEx3, pcATA twice)
SG25_R	CTGTAAAACGACGGCCAGTGTCATA GGTGGTGGTGGTG	EcoRI	HiFi assembly (pEKEx3, pcATA twice)
SG26_F	CCTGCAGGTCGACTCTAGAGGATTC C*GAAAGGAGGCCCTTCAG***ATG**AACA TCA TTGCCATTATGGG	SalI	HiFi assembly (pVWEx1-*ldcC*-pATA) - amplify *ldcC*
SG27_R	CATGGTTGTCCTCCTTTCGTTATCCCG CCATTTTTAGGAC	-	HiFi assembly (pVWEx1-*ldcC*-pATA) - amplify *ldcC*
SG28_F	CCTGCAGGTCGACTCTAGA*GAAAGG AGGCCCTTCAG***ATG**AAATCAATGAA TATTGCCGC	SalI	HiFi assembly (pVWEx1-*speC*-pATA) - amplify *speC*
SG29_R	CATGGTTGTCCTCCTTTCGTTACTTCA ACACATAACCGTACAAC	-	HiFi assembly (pVWEx1-*speC*-pATA) - amplify *speC*

SG30_F	TAAC*GAAAGGAGGACAACC***ATG**ATCAG	-	HiFi assembly (pVWEx1-*ldcC/speC*-pATA) - amplify pcATA
SG31_R	ATTCGAGCTCGGTACCCGGGGATCTCAGCCCTGTAATGCACTCAACGTCAG	-	HiFi assembly (pVWEx1-*ldcC*-pcATA) - amplify pcATA
SG32_F	TAAC*GAAAGGAGGACAACC***ATG**ACCCGCAATAACCCGCAAAC	-	HiFi assembly (pVWEx1-*ldcC/speC*-pATA) - amplify pfATA
SG33_R	ATTCGAGCTCGGTACCCGGGGATCTTAGCCTTGCAACGCACTGAGC	-	HiFi assembly (pVWEx1-*ldcC*-pfATA) - amplify pfATA
SG34_F	TAAC*GAAAGGAGGACAACC***ATG**AGCACCAACAACCCGCAAAC	-	HiFi assembly (pVWEx1-*ldcC/speC*-pATA) - amplify ppATA
SG35_R	ATTCGAGCTCGGTACCCGGGGATCCTACCGAATCGCCTCAAGGGTC	-	HiFi assembly (pVWEx1-*ldcC*-pfATA) - amplify ppATA

Restriction sites are underlined, start codons are bold and ribosomal binding sides including spacer are italicized

A.2.5 Polymerase Chain Reaction (PCR) conditions

Phusion polymerase from Thermo Fischer Scientific was used for all PCRs and the supplier's protocol was followed for the preparation of the PCR mixtures.

Table A.2.5.1. *PCR conditions for amplifying 3HMU insert with SG1_F and SG2_R primers.*

Stage	Temperature (˚C)	time	cycles
initial denaturation	98	2 mins	-
denaturation	98	10 sec	10
Annealing*	72	30 sec	
elongation	72	1 min	
denaturation	98	10 sec	20
annealing	62	30 sec	
elongation	72	1 min	
final elongation	72	2 mins	-

*Every cycle the annealing temperature drops by 1˚C

Table A.2.5.2. *PCR conditions for amplifying GFP insert with SG3_F and SG4_R primers.*

Stage	Temperature (˚C)	time	cycles
initial denaturation	98	2 mins	-
denaturation	98	10 sec	12
Annealing*	72	30 sec	
elongation	72	1 min	
denaturation	98	1 min	20
annealing	50	30 sec	
elongation	72	1 min	
final elongation	72	2 min	-

*Every cycle the annealing temperature drops by 2˚C

Table A.2.5.3. *PCR conditions for site-directed mutagenesis of 3HMU_K292A;* ***a)*** *amplification of 3HMU_K292A in two fragments using SG5_F with SG2_R and SG1_F with SG6_R primers,* ***b)*** *conditions of overlapping PCR using SG1_F and SG2_R to afford the whole 3HMU_K292A insert.*

a)

Stage	Temperature (˚C)	time	cycles
initial denaturation	95	1 min	-
denaturation	95	15 sec	30
annealing	60	15 sec	
elongation	72	30 sec	
final elongation	72	2 mins	-

b)

Stage	Temperature (˚C)	time	cycles
initial denaturation	95	1 min	-
denaturation	95	15 sec	30
annealing	60	15 sec	
elongation	72	1 min	
final elongation	72	2 mins	-

Table A.2.5.4. *PCR conditions for amplifying HEWT insert with SG7_F and SG8_R primers.*

Stage	Temperature (˚C)	time	cycles
initial denaturation	98	30 sec	-
denaturation	98	10 sec	12
Annealing*	72	30 sec	
elongation	72	1 min	
denaturation	98	1 min	25
annealing	50	30 sec	
elongation	72	1 min	
final elongation	72	2 min	-

*Every cycle the annealing temperature drops by 1˚C

Table A.2.5.5. *PCR conditions for amplifying two copies of HEWT insert with SG9_F, SG10_R and SG11_F. SG12_R pairs of primers. Same conditions applied amplifying two copies of pcATA with its pairs of primers.*

Stage	Temperature (˚C)	time	cycles
initial denaturation	95	1 min	-
denaturation	95	15 sec	30
annealing	55	15 sec	
elongation	72	1 min	
final elongation	72	2 mins	-

Table A.2.5.6. *PCR conditions for amplifying two copies of promoter-HEWT insert-terminator with SG13_F, SG14_R and SG15_F, SG16_R pairs of primers.*

Stage	Temperature (˚C)	time	cycles
initial denaturation	95	1 min	-
denaturation	95	15 sec	30
annealing	50	15 sec	
elongation	72	2 min	
final elongation	72	3 mins	-

Table A.2.5.7. *PCR conditions for amplifying pcATA insert with SG17_F and SG18_R primers. Same conditions applied for amplification of pf and pp ATA with their pair of primers.*

Stage	Temperature (˚C)	time	cycles
initial denaturation	95	1 min	-
denaturation	95	15 sec	30
annealing	58	15 sec	
elongation	72	1 min	
final elongation	72	2 mins	-

Table A.2.5.8. *PCR conditions for amplifying ldcC insert with SG26_F and SG27_R primers. Same conditions applied for amplification of speC insert with its pair of primers.*

Stage	Temperature (˚C)	time	cycles
initial denaturation	95	1 min	-
denaturation	95	15 sec	30
annealing	55	15 sec	
elongation	72	1.5 mins	
final elongation	72	3 mins	-

Table A.2.5.9. *PCR conditions for amplifying pcATA insert with SG30_F and SG31_R primers. Same conditions applied for amplification of pf and pp ATA inserts with SG32_F, SG33_R and SG34_F, SG35_R, respectively.*

Stage	Temperature (˚C)	time	cycles
initial denaturation	95	1 min	-
denaturation	95	15 sec	30
annealing	60	15 sec	
elongation	72	1.5 mins	
final elongation	72	3 mins	-

A.2.6 Restriction enzyme conditions

Restriction enzymes EcoRI-HF and SalI-HF from New England Biolabs were used for all digestions and the supplier's protocol was followed as described in tables A.2.6.1 and A.2.6.2.

Table A.2.6.1. Reagents mixing protocol for double digestion.

Reagent	Quantity
10x CutSmart buffer (NEB)	5 µL
Plasmid DNA (200-400 ng/uL)	2 µL
EcoRI-HF (NEB)	1 µL
SalI-HF (NEB)	1 µL
DNAase free H_2O	41 µL

Table A.2.6.2. Conditions used for restriction digest of plasmids using the restriction enzymes EcoRI and SalI.

Stage	Temperature (˚C)	time
Restriction digest	37	30 mins
Heat inactivation	70	20 mins

A.2.7 Gas Chromatography (GC) traces

Herein, representative GC-chromatographs showing the traces from compounds and their respective products are showed.

1. 2-methoxy-acetophenone

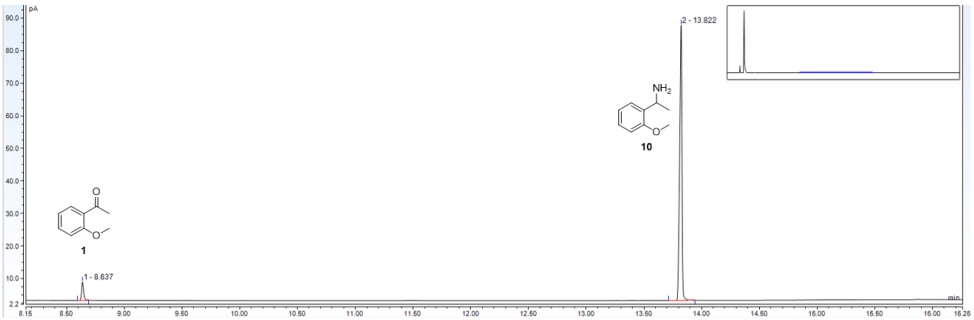

2. 4-fluoropropiophenone

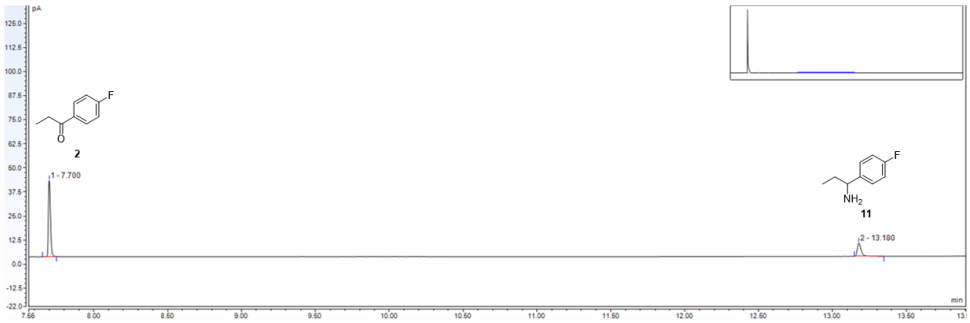

4. 2-acetyl-5-bromothiophene

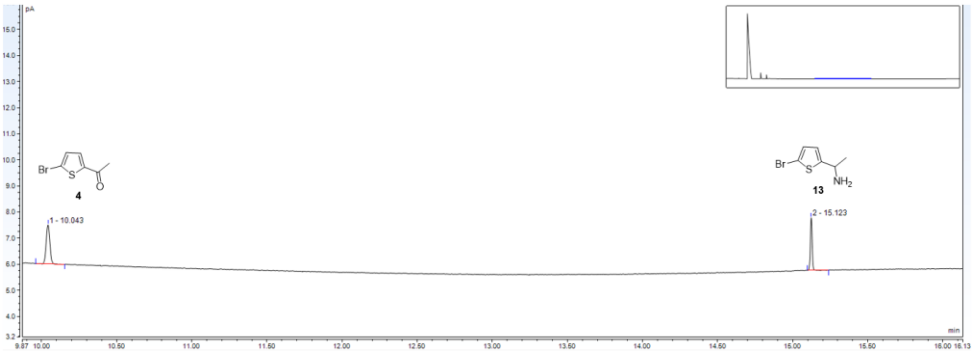

5. 4-phenyl-3-buten-2-one

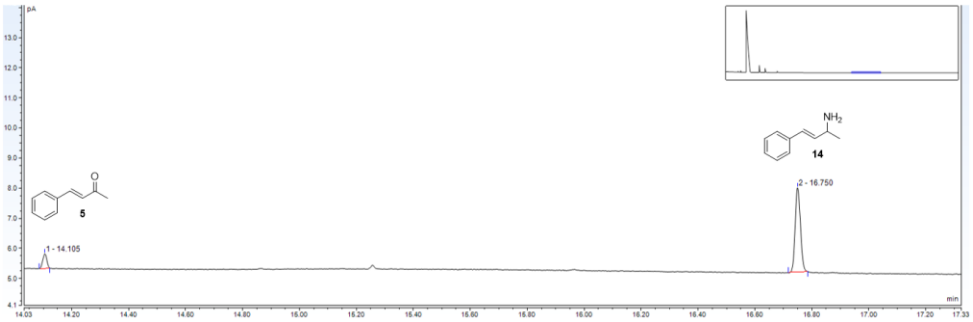

6. 2-fluorophenyl acetone

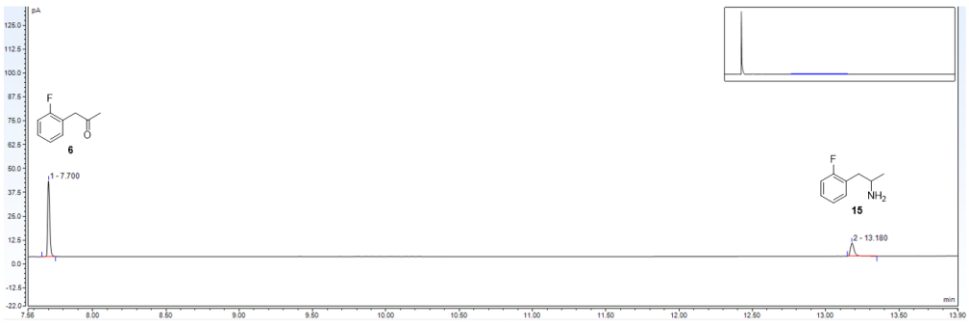

8. 4-methoxyphenyl acetone

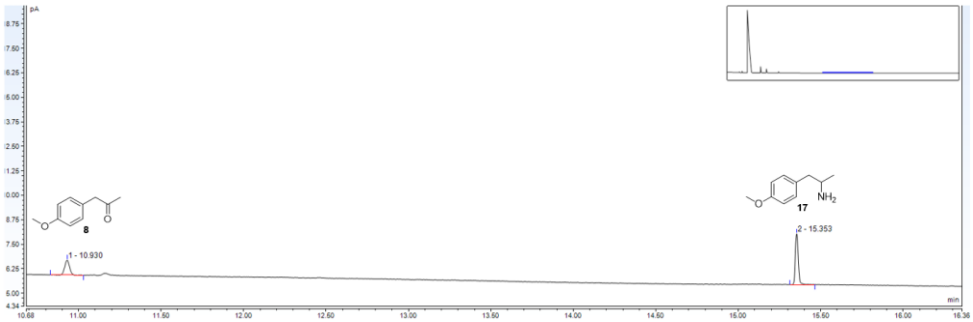

23. 4-phenyl-2-butanone

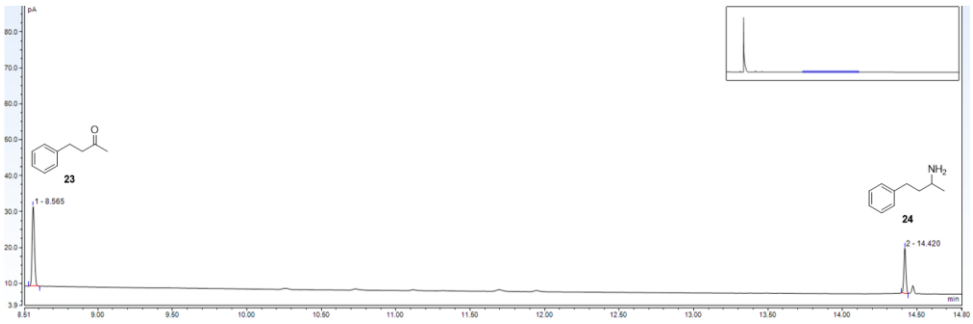

25. Acetophenone

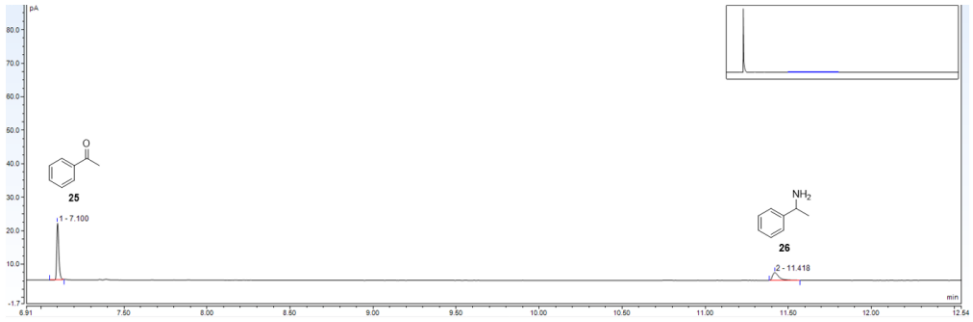

27. 4-phenyl-2-pentanedione

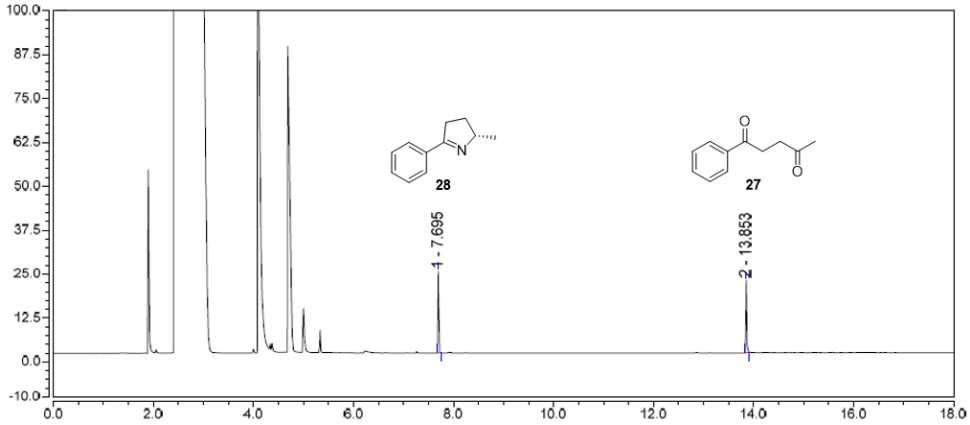

29. Benzaldehyde

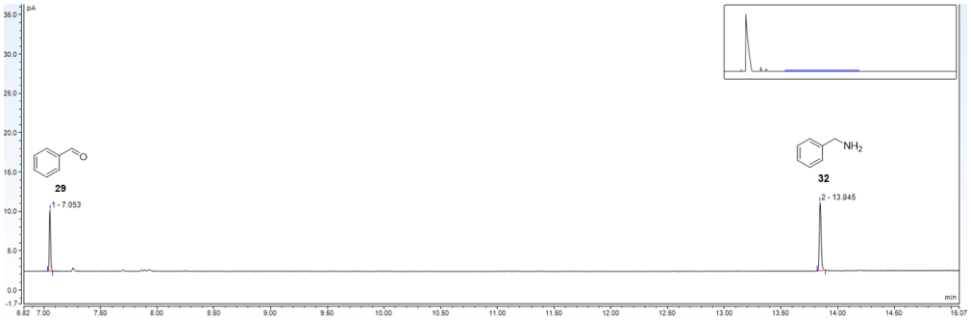

39. 2-fluorophenylacetophenone

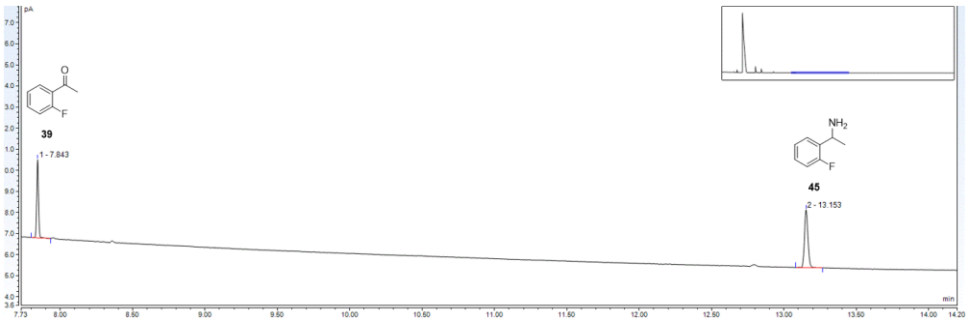

40. 4-fluorophenylacetone

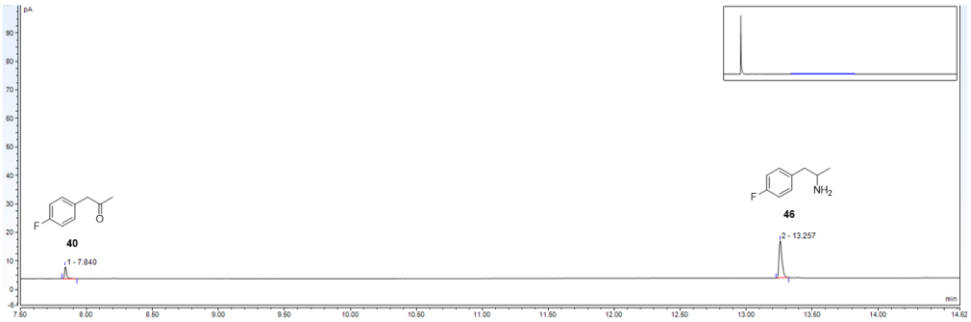

41. E-non-3-ene-2-dione

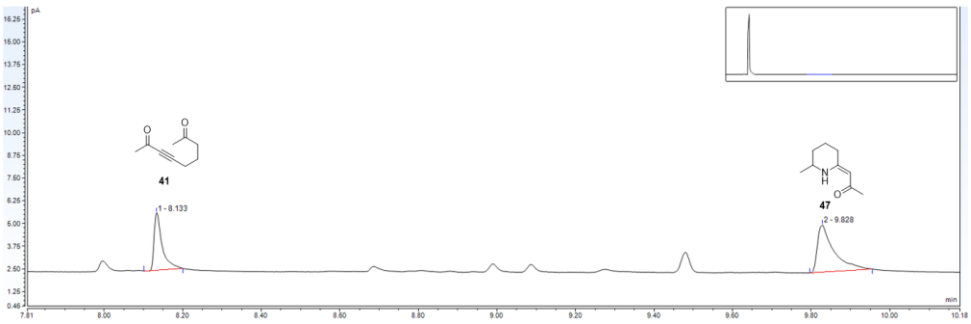

Note: Smaller peaks at the baseline were present in the starting material standards as well. They do not seem to interact, as the area of these peaks does not change.

References

[1] Clayden, J., Greeves, N., Warren, S. **2012**. *Organic Chemistry.* 2nd ed. Oxford: Oxford University Press.

[2] S. Borman, *Chem. Eng. News* **2001**, *42*, 5.

[3] L. A. Nguyen, H. He, C. Pham-Huy, *Int. J. Biomed. Sci.* **2006**, *2*, 85-100.

[4] F. Jamali, R. Mehvar, F. M. Pasutto, *J. Pharm. Sci.* **1989**, *78*, 695–715.

[5] A. Marzo, E. Heftmann, *J. Biochem. Biophys. Methods* **2002**, *54*, 57–70.

[6] N. M. Davies, X. W. Teng, B. *Adv. Pharm.* **2003**, *1*, 242-252.

[7] G. Pifferi, E. Perucca, *Eur. J. Drug Metab. Pharmacokinet.* **1995**, *20*, 15–25.

[8] J. Leffingwell, *Spec Chem*, **2011**.

[9] R. Eccles, *J. Pharm. Pharmacol.* **1994**, *46*, 618–630.

[10] H. Okugawa, R. Ueda, K. Matsumoto, K. Kawanishi, A. Kato, *Phytomedicine* **1995**, *2*, 119–126.

[11] A. Bommareddy, S. Brozena, J. Steigerwalt, T. Landis, S. Hughes, E. Mabry, A. Knopp, A. L. VanWert, C. Dwivedi, *Nat. Prod. Res.* **2019**, *33*, 527–543.

[12] A. Krotz, G. Helmchen, *Liebigs Ann. der Chemie* **1994**, *1994*, 601–609.

[13] P. Ettmayer, M. Hübner, B. Andreas, R. Brigitte, G. Hubert, *Bioorganic Med. Chem. Lett.* **1994**, *4*, 2851–2856.

[14] N. J. Turner, *Curr. Opin. Chem. Biol.* **2010**, *14*, 115–121.

[15] Y. Yang, L. hui Zhang, B. xian Yang, J. kui Tian, L. Zhang, *J. Cell. Mol. Med.* **2015**, *19*, 1055–1064.

[16] D. Koszelewski, I. Lavandera, D. Clay, D. Rozzell, W. Kroutil, *Adv. Synth. Catal.* **2008**, *350*, 2761–2766.

[17] Nugent, T. C. **2010**. *Chiral Amine Synthesis*. NJ:Wiley.

[18] O. Onomura, Y. Kouchi, F. Iwasaki, Y. Matsumura, *Tetrahedron Lett.* **2006**,

47, 3751–3754.

[19] F. Iwasaki, O. Onomura, K. Mishima, T. Kanematsu, T. Maki, Y. Matsumura, *Tetrahedron Lett.* **2001**, *42*, 2525–2527.

[20] Z. Wang, M. Cheng, P. Wu, S. Wei, J. Sun, *Org. Lett.* **2006**, *8*, 3045–3048.

[21] Z. Wang, X. Ye, S. Wei, P. Wu, A. Zhang, J. Sun, *Org. Lett.* **2006**, *8*, 999–1001.

[22] Z. Wang, S. Wei, C. Wang, J. Sun, *Tetrahedron Asymmetry* **2007**, *18*, 705–709.

[23] P. Wu, Z. Wang, M. Cheng, L. Zhou, J. Sun, *Tetrahedron* **2008**, *64*, 11304–11312.

[24] M. R. Axet, F. Amoroso, G. Bottari, A. D'Amora, E. Zangrando, F. Faraone, D. Drommi, M. Saporita, C. Carfagna, P. Natanti, et al., *Organometallics* **2009**, *28*, 4464–4474.

[25] D. S. Bhalerao, A. K. R. Arkala, Y. V. Madhavi, M. Nagaraju, S. R. Gade, U. K. S. Kumar, R. Bandichhor, V. H. Dahanukar, *Org. Process Res. Dev.* **2015**, *19*, 1559–1567.

[26] M. E. Welsch, S. A. Snyder, B. R. Stockwell, *Curr. Opin. Chem. Biol.* **2010**, *14*, 347–361.

[27] D. J. Tocco, F. A. DeLuna, A. E. W. Duncan, T. C. Vassil, E. H. Ulm, *Drug Metab. Dispos.* **1982**, *10*, 15–19.

[28] M. Akif, D. Georgiadis, A. Mahajan, V. Dive, E. D. Sturrock, R. E. Isaac, K. R. Acharya, *J. Mol. Biol.* **2010**, *400*, 502–517.

[29] G. Zhu, X. Zhang, *J. Org. Chem.* **1998**, *63*, 9590–9593.

[30] M. J. Burk, Y. Ming Wang, J. R. Lee, *J. Am. Chem. Soc.* **1996**, *118*, 5142-5143.

[31] R. Noyori, M. Ohta, M. Kitamura, *J. Am. Chem. Soc.* **1986**, *108*, 7177–7119.

[32] W. Hu, M. Yan, C. P. Lau, S. M. Yang, A. S. C. A. Chan, Y. Jiang, A. Mi,

Tetrahedron Lett. **1999**, *40*, 973–976.

[33] W. Tang, X. Zhang, *Angew. Chem. Int. Ed.* **2002**, *41*, 1612-1614.

[34] H. B. Kagan, T.-P. Dang, *J. Am. Chem. Soc.* **1972**, *94*, 6429–6433.

[35] F. Y. Zhang, C. C. Pai, A. S. C. Chan, *J. Am. Chem. Soc.* **1998**, *120*, 5808–5809.

[36] Z. Zhang, G. Zhu, Q. Jiang, D. Xiao, X. Zhang, *J. Org. Chem.* **1999**, *64*, 1774–1775.

[37] H.-U. Blaser, H.-P. Buser, H.-P. Jalett, B. Pugin, F. Spindler, *Synlett* **1999**, *1999*, 867–868.

[38] D. Menche, F. Arikan, J. Li, S. Rudolph, *Org. Lett.* **2007**, *9*, 267–270.

[39] T. C. Nugent, R. Seemayer, *Org. Process Res. Dev.* **2006**, *10*, 142–148.

[40] M. Kawatsura, J. F. Hartwig, *J. Am. Chem. Soc.* **2000**, *122*, 9546–9547.

[41] O. Löber, M. Kawatsura, J. F. Hartwig, *J. Am. Chem. Soc.* **2001**, *123*, 4366–4367.

[42] F. Pohlki, I. Bytschkov, H. Siebeneicher, A. Heutling, W. A. König, S. Doye, *European J. Org. Chem.* **2004**, 1967–1972.

[43] D. V. Gribkov, K. C. Hultzsch, F. Hampel, *J. Am. Chem. Soc.* **2006**, *128*, 3748–3759.

[44] R. P. Reddy, H. M. L. Davies, *Org. Lett.* **2006**, *8*, 5013–5016.

[45] D. N. Zalatan, J. Du Bois, *J. Am. Chem. Soc.* **2008**, *130*, 9220–9221.

[46] C. G. Espino, J. Du Bois, *Angew. Chem. Int. Ed.* **2001**, *40*, 598-600.

[47] D. J. C. Constable, P. J. Dunn, J. D. Hayler, G. R. Humphrey, J. L. Leazer, R. J. Linderman, K. Lorenz, J. Manley, B. A. Pearlman, A. Wells, A. Zaks, T. Y. Zhang *Green Chem.* **2007**, *9*, 411–420.

[48] P. J. Dunn, *Chem. Soc. Rev.* **2012**, *41*, 1452–1461.

[49] L. Chrast, R. Chaloupkova, J. Damborsky, *FEMS Microbiol. Lett.* **2018**, *365*,

1–7.

[50] M. Breuer, K. Ditrich, T. Habicher, B. Hauer, M. Keßeler, R. Stürmer, T. Zelinski, *Angew. Chem. Int. Ed.* **2004**, *43*, 788–824.

[51] A. Gomm, E. O'Reilly, *Curr. Opin. Chem. Biol.* **2018**, *43*, 106–112.

[52] D. Ghislieri, N. J. Turner, *Top. Catal.* **2014**, *57*, 284–300.

[53] K.-E. Jaeger, M. T. Reetz, *trends Biotechnol.* **1998**, *16*, 396–403.

[54] G. A. Aleku, S. P. France, H. Man, J. Mangas-Sanchez, S. L. Montgomery, M. Sharma, F. Leipold, S. Hussain, G. Grogan, N. J. Turner, *Nat. Chem.* **2017**, *9*, 961–969.

[55] N. Itoh, C. Yachi, T. Kudome, *J. Mol. Catal. - B Enzym.* **2000**, *10*, 281–290.

[56] F. Balkenhohl, K. Ditrich, B. Hauer, W. Ladner, *J. für Prakt. Chemie/Chemiker-Zeitung* **2005**, *339*, 381–384.

[57] C. J. Dunsmore, R. Carr, T. Fleming, N. J. Turner, *J. Am. Chem. Soc.* **2006**, *128*, 2224–2225.

[58] H. Li, P. Williams, J. Micklefield, J. M. Gardiner, G. Stephens, *Tetrahedron* **2004**, *60*, 753–758.

[59] A. S. Bommarius, M. Schwarm, K. Stingl, M. Kottenhahn, K. Huthmacher, K. Drauz, *Tetrahedron: Asymmetry* **1995**, *6*, 2851–2888.

[60] S.-Y. Wu, R. Takeya, M. Eto, C. Tomizawa, *J. Pestic. Sci.* **2011**, *12*, 221–227.

[61] A. Schöll, L. Kilian, Y. Zou, J. Ziroff, S. Hame, F. Reinert, E. Umbach, R. H. Fink, *Science* **2010**, *329*, 303–305.

[62] N. M. Shaw, K. T. Robins, A. Kiener, *Adv. Synth. Catal.* **2003**, *345*, 425–435.

[63] S. Shimizu, M. Kataoka, K. Kita, *J. Mol. Catal. - B Enzym.* **1998**, *5*, 321–325.

[64] K. M. Draths, D. R. Knop, J. W. Frost, *J. Am. Chem. Soc.* **1999**, *121*, 1603–1604.

[65] K. Li, J. W. Frost, *J. Am. Chem. Soc.* **1998**, *120*, 10545–10546.

[66] A. Schmid, A. Kollmer, R. G. Mathys, B. Witholt, *Extremophiles* **1998**, *2*, 249–256.

[67] H. Sakurai, S. Ogawa *Chem. Pharm. Bull.* **1979**, *27*, 2171-2176.

[68] T. Ishige, K. Honda, S. Shimizu, *Curr. Opin. Chem. Biol.* **2005**, *9*, 174–180.

[69] L. P. Williams, S. D. Bull, M. J. Danson, **2010**, 2405.

[70] A. Brugging, E. C. Roos, E. De Vroom, *Org. Process Res. Dev.* **1998**, *2*, 128–133.

[71] A. Liese, M. V. Fihlo, *Curr. Opin. Biotechnol*, **1999**, *10*, *595-603*.

[72] M. Wada, M. Kataoka, H. Kawabata, Y. Yasohara, N. Kizaki, J. Hasegawa, S. Shimizu, *Biosci. Biotechnol. Biochem.* **1998**, *62*, 280–285.

[73] R. Grifanti, I. Gal, G. Carpani, C. Pratesi, G. Frascotti, G. Grandit, *Microbiol.* **1998**, *144*, 947–954.

[74] J. Schneider, K. Niermann, V. F. Wendisch, *J. Biotechnol.* **2011**, *154*, 191–198.

[75] V. F. Wendisch, M. Bott, B. J. Eikmanns, *Curr. Opin. Microbiol.* **2006**, *9*, 268–274.

[76] M. Schrewe, M. K. Julsing, B. Bühler, A. Schmid, *Chem. Soc. Rev.* **2013**, *42*, 6346–6377.

[77] J. Wachtmeister, D. Rother, *Curr. Opin. Biotechnol.* **2016**, *42*, 169–177.

[78] D. J. Pollard, J. M. Woodley, *Trends Biotechnol.* **2007**, *25*, 66–73.

[79] A. V. Presečki, D. Vasić-Rački, *Biotechnol. Lett.* **2005**, *27*, 1835–1839.

[80] F. Leipold, S. Hussain, D. Ghislieri, N. J. Turner, *ChemCatChem* **2013**, *5*, 3505–3508.

[81] P. Both, H. Busch, P. P. Kelly, F. G. Mutti, N. J. Turner, S. L. Flitsch, *Angew. Chem. Int. Ed.* **2016**, *55*, 1511–1513.

[82] A. V. Presečki, B. Zelić, D. Vasić-Rački, *Enzyme Microb. Technol.* **2007**, *41*, 605–612.

[83] H. Gröger, F. Chamouleau, N. Orologas, C. Rollmann, K. Drauz, W. Hummel, A. Weckbecker, O. May, *Angew. Chem. Int. Ed.* **2006**, *45*, 5677–5681.

[84] D. Kuhn, M. A. Kholiq, E. Heinzle, B. Bühler, A. Schmid, *Green Chem.* **2010**, *12*, 815–827.

[85] B. Bühler, A. Schmid, *J. Biotechnol.* **2004**, *113*, 183–210.

[86] H. Fukuda, S. Hama, S. Tamalampudi, H. Noda, *Trends Biotechnol.* **2008**, *26*, 668–673.

[87] C. Wandrey, A. Liese, D. Kihumbu, *Org. Process Res. Dev.* **2000**, *4*, 286–290.

[88] P. Giesbrecht, J. Wecke, B. Reinicke, *Int. Rev. Cytol.* **1976**, *44*, 225–318.

[89] W. B. Ober, *N. Y. State J. Med.* **1970**, *70*, 986–992.

[90] J. M. Klenk, B. A. Nebel, J. L. Porter, J. K. Kulig, S. A. Hussain, S. M. Richter, M. Tavanti, N. J. Turner, M. A. Hayes, B. Hauer, S. Flitsch., *Biotechnol. J.* **2017**, *12*, 1600520.

[91] A. Schmid, J. S. Dordick, B. Hauer, A. Kiener, M. Wubbolts, B. Witholt, *Nature* **2001**, *409*, 258-268.

[92] M. Cánovas, T. Torroglosa, J. L. Iborra, *Enzyme Microb. Technol.* **2005**, *37*, 300–308.

[93] F. Rundbäck, M. Fidanoska, P. Adlercreutz, *J. Biotechnol.* **2012**, *157*, 154–158.

[94] P. Zajkoska, M. Rebroš, M. Rosenberg, *Appl. Microbiol. Biotechnol.* **2013**, *97*, 1441–1455.

[95] C. Grant, D. Deszcz, Y. C. Wei, R. J. Martínez-Torres, P. Morris, T. Folliard, R. Sreenivasan, J. Ward, P. Dalby, J. M. Woodley, *Sci. Rep.* **2014**, *4*, 1–9.

[96] C. Parker, W. O. Barnell, J. L. Snoep, L. O. Ingram, T. Conway, *Mol. Microbiol.* **1995**, *15*, 795–802.

[97] P. Weisser, R. Kramer, H. Sahm, G. A. Sprenger, *J. Bacteriol.* **1995**, *177*,

3351–3354.

[98] T. Mogi, H. Yamamoto, T. Nakao, I. Yamato, Y. Anraku, *Mol. Gen. Genet.* **1986**, *202*, 35–41.

[99] H. Nikaido, *Microbiol. Mol. Biol. Rev.* **1996**, *67*, 29–47.

[100] T. Shibasaki, H. Mori, A. Ozaki, *Biosci. Biotechnol. Biochem.* **2000**, *64*, 746–750.

[101] M. V. H. Moura, G. P. Da Silva, A. C. De Oliveira Machado, F. A. G. Torres, D. M. G. Freire, R. V. Almeida, *PLoS One* **2015**, *10*, 1–12.

[102] F. W. Ströhle, E. Kranen, J. Schrader, R. Maas, D. Holtmann, *Biotechnol. Bioeng.* **2016**, *113*, 1225–1233.

[103] J. S. Shin, B. G. Kim, *Biotechnol. Bioeng.* **1997**, *55*, 348–358.

[104] H. Pfruender, M. Amidjojo, U. Kragl, D. Weuster-Botz, *Angew. Chem. Int. Ed.* **2004**, *43*, 4529–4531.

[105] Carrea, G. and Riva, S. **2008**. Organic synthesis with Enzymes in non-aqueous media. NJ:Wiley.

[106] S. Wu, Z. Li, *ChemCatChem* **2018**, *10*, 2164–2178.

[107] F. Steffen-Munsberg, C. Vickers, H. Kohls, H. Land, H. Mallin, A. Nobili, L. Skalden, T. van den Bergh, H. J. Joosten, P. Berglund, M. Höhne, U. T. Bornscheuer, *Biotechnol. Adv.* **2015**, *33*, 566–604.

[108] D. Schiroli, A. Peracchi, *Biochim. Biophys. Acta - Proteins Proteomics* **2015**, *1854*, 1200–1211.

[109] R. Percudani, A. Peracchi, *BMC Bioinformatics* **2009**, *10*, 273.

[110] J. N. Jansonius, *Curr. Opin. Struct. Biol.* ***1998***, *8*, 759-769**.**

[111] N. V. Grishin, M. A. Phillips, E. J. Goldsmith, *Protein Sci.* **1995**, *4*, 1291–1304.

[112] K. Soda, T. Yoshimura, N. Esaki, *Chem. Rec.* **2001**, *1*, 373–384.

[113] G. Schneider, H. Käck, Y. Lindqvist, *Structure* **2000**, *8*, 1-6.

[114] M. Höhne, S. Schätzle, H. Jochens, K. Robins, U. T. Bornscheuer, *Nat. Chem. Biol.* **2010**, *6*, 807–813.

[115] C. Rausch, A. Lerchner, A. Schiefner, A. Skerra, *Proteins Struct. Funct. Bioinforma.* **2013**, *81*, 774–787.

[116] M. S. Malik, E. S. Park, J. S. Shin, *Appl. Microbiol. Biotechnol.* **2012**, *94*, 1163–1171.

[117] Y. C. Shin, H. Yun, H. H. Park, *Sci. Rep.* **2018**, *8*, 1-9.

[118] J. M. Berg, J. L. Tymoczko, L. Stryer, *Biochemistry, 5th Edition*, **2002**.

[119] K. E. Cassimjee, B. Manta, F. Himo, *Org. Biomol. Chem.* **2015**, *13*, 8453–8464.

[120] S. Mathew, H. Yun, *ACS Catal.* **2012**, *2*, 993–1001.

[121] T. Pavkov-Keller, G. A. Strohmeier, M. Diepold, W. Peeters, N. Smeets, M. Schürmann, K. Gruber, H. Schwab, K. Steiner, *Sci. Rep.* **2016**, *6*, 1-12.

[122] P. A. F. Lehmann, *Trends Pharmacol. Sci.* **1986**, *7*, 281–285.

[123] H. Yun, B. Y. Hwang, J. H. Lee, B. G. Kim, *Appl. Environ. Microbiol.* **2005**, *71*, 4220–4224.

[124] D. Koszelewski, D. Clay, K. Faber, W. Kroutil, *J. Mol. Catal. B Enzym.* **2009**, *60*, 191–194.

[125] D. Koszelewski, D. Pressnitz, D. Clay, W. Kroutil, *Org. Lett.* **2009**, *11*, 4810–4812.

[126] J. S. Shin, B. G. Kim, *Biotechnol. Bioeng.* **1999**, *65*, 206–211.

[127] M. Höhne, S. Kühl, K. Robins, U. T. Bornscheuer, *ChemBioChem* **2008**, *9*, 363–365.

[128] H. YUN, B.-G. KIM, *Biosci. Biotechnol. Biochem.* **2008**, *72*, 3030–3033.

[129] I. G. Fotheringham, N. Grinter, D. P. Pantaleone, R. F. Senkpeil, P. P. Taylor, *Bioorganic Med. Chem.* **1999**, *7*, 2209–2213.

[130] A. P. Green, N. J. Turner, E. O'Reilly, *Angew. Chem. Int. Ed.* **2014**, *53*,

10714–10717.

[131] A. Gomm, W. Lewis, A. P. Green, E. O'Reilly, *Chem. A Eur. J.* **2016**, *22*, 12692–12695.

[132] F. Guo, P. Berglund, *Green Chem.* **2017**, *19*, 333–360.

[133] D. Baud, N. Ladkau, T. S. Moody, J. M. Ward, H. C. Hailes, *Chem. Commun.* **2015**, *51*, 17225–17228.

[134] M. D. Truppo, J. D. Rozzell, J. C. Moore, N. J. Turner, *Org. Biomol. Chem.* **2009**, *7*, 395–398.

[135] The sequence for ATA256 can be found in the following patent. Crowe et al. Chemical processes for preparing spiroindolones and intermediates therof. US Patent US **2015**/0045562 A1, filed 22 March 2013 and issued 12 February 2015.

[136] More information on ATA 256 is provided from Codexis website at https://www.codexis-estore.com/protocols [accessed 29/06/2020]**.**

[137] Á. Mourelle-Insua, M. López-Iglesias, V. Gotor, V. Gotor-Fernández, *J. Org. Chem.* **2016**, *81*, 9765–9774.

[138] D. Monti, M. C. Forchin, M. Crotti, F. Parmeggiani, F. G. Gatti, E. Brenna, S. Riva, *ChemCatChem* **2015**, *7*, 3106–3109.

[139] A. Gomm, S. Grigoriou, C. Peel, J. Ryan, N. Mujtaba, T. Clarke, E. Kulcinskaja, E. O'Reilly, *European J. Org. Chem.* **2018**, *2018*, 5282–5284.

[140] Volume calculated with Molinspiration https://www.molinspiration.com/ the tool implemented in virtual computational chemistry laboratories (VCCLAB), http://www.vcclab.org/ [both accessed: 29/06/2020].

[141] C. B. Kelly, M. A. Mercadante, N. E. Leadbeater, *Chem. Commun.* **2013**, *49*, 11133–11148.

[142] J. Gonzalez-Sabin, V. Gotor, F. Rebolledo, *Tetrahedron* **2002**, *13*, 1315–1320.

[143] F. Campos, M. P. Bosch, A. Guerrero, *Tetrahedron Asymmetry* **2000**, *11*,

2705–2717.

[144] D. Brenna, M. Pirola, L. Raimondi, A. J. Burke, M. Benaglia, *Bioorganic Med. Chem.* **2017**, *25*, 6242–6247.

[145] W. Ou, S. Espinosa, H. J. Meléndez, S. M. Farré, J. L. Alvarez, V. Torres, I. Martínez, K. M. Santiago, M. Ortiz-Marciales, *J. Org. Chem.* **2013**, *78*, 5314–5327.

[146] T. C. Nugent, D. E. Negru, M. El-Shazly, D. Hu, A. Sadiq, A. Bibi, M. N. Umar, *Adv. Synth. Catal.* **2011**, *353*, 2085–2092.

[147] X. Dai, T. Nakai, J. A. C. Romero, G. C. Fu, *Angew. Chem. Int. Ed.* **2007**, *46*, 4367–4369.

[148] M. Atobe, N. Yamazaki, C. Kibayashi, *J. Org. Chem.* **2004**, *69*, 5595–5607.

[149] L. Muñoz, A. M. Rodriguez, G. Rosell, M. P. Bosch, A. Guerrero, *Org. Biomol. Chem.* **2011**, *9*, 8171–8177.

[150] T. R. Hoye, C. S. Jeffrey, F. Shao, *Nat. Protoc.* **2007**, *2*, 2451–2458.

[151] T. R. Hoye, M. K. Renner, *J. Org. Chem.* **1996**, *61*, 2056–2064.

[152] G. R. Sullivan, J. A. Dale, H. S. Mosher, *J. Org. Chem.* **1973**, *38*, 2143–2147.

[153] S. E. Payer, J. H. Schrittwieser, W. Kroutil, *European J. Org. Chem.* **2017**, *2017*, 2553–2559.

[154] A. Q. D. Nguyen, J. Schneider, G. K. Reddy, V. F. Wendisch, *Metabolites* **2015**, *5*, 211–231.

[155] J. Schneider, D. Eberhardt, V. F. Wendisch, *Appl. Microbiol. Biotechnol.* **2012**, *95*, 169–178.

[156] T. Mimitsuka, H. Sawai, M. Hatsu, K. Yamada, *Biosci. Biotechnol. Biochem.* **2007**, *71*, 2130–2135.

[157] Y. H. Oh, K. H. Kang, M. J. Kwon, J. W. Choi, J. C. Joo, S. H. Lee, Y. H. Yang, B. K. Song, I. K. Kim, K. H. Yoon, et al., *J. Ind. Microbiol. Biotechnol.* **2015**, *42*, 1481–1491.

[158] N. Ikeda, M. Miyamoto, N. Adachi, M. Nakano, T. Tanaka, A. Kondo, *AMB Express* **2013**, *3*, 1–7.

[159] Z. G. Qian, X. X. Xia, S. Y. Lee, *Biotechnol. Bioeng.* **2011**, *108*, 93–103.

[160] J. Kalinowski, B. Bathe, D. Bartels, N. Bischoff, M. Bott, A. Burkovski, N. Dusch, L. Eggeling, B. J. Eikmanns, L. Gaigalat, et al., *J. Biotechnol.* **2003**, *104*, 5–25.

[161] J. Y. Kim, Y. A. Lee, C. Wittmann, J. B. Park, *Biotechnol. Bioeng.* **2013**, *110*, 2846–2855.

[162] E. Y. Hong, M. Cha, H. Yun, B. G. Kim, *J. Mol. Catal. B Enzym.* **2010**, *66*, 228–233.

[163] P. G. Peters-Wendisch, B. Schiel, V. F. Wendisch, E. Katsoulidis, B. Möckel, H. Sahm, B. J. Eikmanns, *J. Mol. Microbiol. Biotechnol.* **2001**, *3*, 295–300.

[164] S. Klatte, E. Lorenz, V. F. Wendisch, *Bioengineered* **2013**, *5*, 56-62.

[165] D. Siebert, V. F. Wendisch, *Biotechnol. Biofuels* **2015**, *8*, 1–13.

[166] J. Schneider, V. F. Wendisch, *Appl. Microbiol. Biotechnol.* **2010**, *88*, 859–868.

[167] H. Mallin, M. Höhne, U. T. Bornscheuer, *J. Biotechnol.* **2014**, *191*, 32–37.

[168] S. Schätzle, F. Steffen-Munsberg, A. Thontowi, M. Höhne, K. Robins, U. T. Bornscheuer, *Adv. Synth. Catal.* **2011**, *353*, 2439–2445.

[169] D. Koszelewski, M. Göritzer, D. Clay, B. Seisser, W. Kroutil, *ChemCatChem* **2010**, *2*, 73–77.

[170] M. S. Humble, K. E. Cassimjee, M. Hãkansson, Y. R. Kimbung, B. Walse, V. Abedi, H. J. Federsel, P. Berglund, D. T. Logan, *FEBS J.* **2012**, *279*, 779–792.

[171] K. E. Cassimjee, M. S. Humble, V. Miceli, C. G. Colomina, P. Berglund, *ACS Catal.* **2011**, *1*, 1051–1055.

[172] U. Kaulmann, K. Smithies, M. E. B. Smith, H. C. Hailes, J. M. Ward, *Enzyme Microb. Technol.* **2007**, *41*, 628–637.

[173] M. Genz, C. Vickers, T. van den Bergh, H. J. Joosten, M. Dörr, M. Höhne, U. T. Bornscheuer, *Int. J. Mol. Sci.* **2015**, *16*, 26953–26963.

[174] K. S. Midelfort, R. Kumar, S. Han, M. J. Karmilowicz, K. McConnell, D. K. Gehlhaar, A. Mistry, J. S. Chang, M. Anderson, A. Villalobos, J. Minshull, S. Govindarajan, J. W. Wong, *Protein Eng. Des. Sel.* **2013**, *26*, 25–33.

[175] J. S. Shin, H. Yun, J. W. Jang, I. Park, B. G. Kim, *Appl. Microbiol. Biotechnol.* **2003**, *61*, 463–471.

[176] F. Steffen-Munsberg, C. Vickers, A. Thontowi, S. Schätzle, T. Tumlirsch, M. SvedendahlHumble, H. Land, P. Berglund, U. T. Bornscheuer, M. Höhne, *ChemCatChem* **2013**, *5*, 150–153.

[177] S. Schätzle, M. Höhne, E. Redestad, K. Robins, U. T. Bornscheuer, *Anal. Chem.* **2009**, *81*, 8244–8248.

[178] D. Schiroli, A. Peracchi, *Biochim. Biophys. Acta - Proteins Proteomics* **2015**, *1854*, 1200–1211.

[179] E. O'Reilly, C. Iglesias, D. Ghislieri, J. Hopwood, J. L. Galman, R. C. Lloyd, N. J. Turner, *Angew. Chem. Int. Ed.* **2014**, *53*, 2447–2450.

[180] M. Hartmann, D. Kim, F. Bernsdorff, Z. Ajami-Rashidi, N. Scholten, S. Schreiber, T. Zeier, S. Schuck, V. Reichel-Deland, J. Zeier, *Plant Physiol.* **2017**, *174*, 124–153.

[181] D. B. Hope, K. C. Horncastle, R. T. Aplin, *Biochem. J.* **1967**, *105*, 663–667.

[182] M. Baumgart, S. Unthan, C. Rückert, J. Sivalingam, A. Grünberger, J. Kalinowski, M. Bott, S. Noack, J. Frunzke, *Appl. Environ. Microbiol.* **2013**, *79*, 6006–6015.

[183] B. J. Eikmanns, E. Kleinertz, W. Liebl, H. Sahm, *Gene* **1991**, *102*, 93–98.

[184] H. Morise, O. Shimomura, F. H. Johnson, J. Winant, *Biochemistry* **1974**, *13*, 2656–2662.

[185] C. W. Cody, C. Harv, **1979**, *31*, 615.

[186] B. P. Cormack, R. H. Valdivia, S. Falkow, *Gene* **1996**, *173*, 33–38.

[187] Link to online platform http://gcua.schoedl.de/seqoverall_v2.html [accessed: 29/07/2020].

[188] Codon usage table was imported from: http://www.kazusa.or.jp/codon/cgi-bin/showcodon.cgi?species=196627&aa=1&style=N. [accessed: 29/072020]

[189] L. Cerioli, M. Planchestainer, J. Cassidy, D. Tessaro, F. Paradisi, *J. Mol. Catal. B Enzym.* **2015**, *120*, 141–150.

[190] H. Il Kim, J. Y. Nam, J. Y. Cho, C. S. Lee, Y. J. Park, *J. Microbiol.* **2013**, *51*, 877–880.

[191] A. Arndt, B. J. Eikmanns, *J. Bacteriol.* **2007**, *189*, 7408–7416.

[192] A. Kotrbova-Kozak, P. Kotrba, M. Inui, J. Sajdok, H. Yukawa, *Appl. Microbiol. Biotechnol.* **2007**, *76*, 1347–1356.

[193] S. Witthoff, A. Mühlroth, J. Marienhagen, M. Bott, *Appl. Environ. Microbiol.* **2013**, *79*, 6974–6983.

[194] A. Fanous, W. Weiss, A. Görg, F. Jacob, H. Parlar, *Proteomics* **2008**, *8*, 4976–4986.

[195] L. Lessmeier, M. Hoefener, V. F. Wendisch, *Microbiol.* **2013**, *159*, 2651–2662.

[196] L. Du, L. Ma, F. Qi, X. Zheng, C. Jiang, A. Lifi, X. Wan, S. J. Liu, S. Li, *J. Biol. Chem.* **2016**, *291*, 6583–6594.

[197] L. J. Hepworth, S. P. France, S. Hussain, P. Both, N. J. Turner, S. L. Flitsch, *ACS Catal.* **2017**, *7*, 2920–2925.

[198] K. T. Elliott, L. E. Cuff, E. L. Neidle, *Future Microbiol.* **2013**, *8*, 887–899.

[199] F. A. Kondrashov, *Proc. R. Soc. B Biol. Sci.* **2012**, *279*, 5048–5057.

[200] C. D. Lu, Y. Itoh, Y. Nakada, Y. Jiang, *J. Bacteriol.* **2002**, *184*, 3765–3773.

[201] J. L. Galman, I. Slabu, N. J. Weise, C. Iglesias, F. Parmeggiani, R. C. Lloyd, N.

J. Turner, *Green Chem.* **2017**, *19*, 361–366.

[202] Liebl, W. **2005**. '*Corynebacterium Taxonomy'. Handbook of Corynebacterium glutamicum*. Eggeling, L. and Bott, M. Boca Raton:T & F group.

[203] I. Wilmut, *Nature* **1997**, *385*, 810–813.

[204] D. S. Wang, Z. S. Ye, Q. A. Chen, Y. G. Zhou, C. Bin Yu, H. J. Fan, Y. Duan, *J. Am. Chem. Soc.* **2011**, *133*, 8866–8869.

[205] E. Gasteiger, A. Gattiker, C. Hoogland, I. Ivanyi, R. D. Appel, A. Bairoch, *Nucleic Acids Res.* **2003**, *31*, 3784–3788.